

**High resolution genetic and physical mapping of a major powdery mildew
resistance locus in barley**

Dissertation

to obtain the Ph.D. degree

in the Ph.D. Program for Agricultural Sciences in Göttingen (PAG)

at the Faculty of Agricultural Sciences,

Georg-August-University Göttingen, Germany

presented by

Parastoo Hoseinzadeh

born in 18.09.1982, Tehran

Göttingen, 06.07.2018

D7

1. Name of supervisor: Prof. Dr. Nils Stein

2. Name of co-supervisor: Dr. Christian Möllers

Date of dissertation: 6th July 2018

Acknowledgement

I would like to express my sincere appreciation to my supervisor Prof. Dr. Nils Stein for giving me the opportunity to work in the DURESTrit consortium (Financed by German Research Foundation, DFG) and integrating me into the international barley research community. I am grateful for his excellent supervision, constructive criticism, support and valuable suggestions during this study.

I would like to express the deepest appreciation to my second supervisor Dr. Christian Möllers for continuous and generous support, dedicated help, advice and encouragement. He was the one that I could always count on his support during my MSc. and Ph.D. studies.

Similar, profound gratitude goes to Dr. Patrick Schweizer (Previous leader of Pathogen Stress Genomics group and the DURESTrit consortium) who was a truly dedicated mentor. I am particularly indebted to Patrick for his constant support and valuable guidance. He kindly allowed me to continue his work and provided me all the required material, scientific background information and generously hosted me in his laboratory.

I would like to express my appreciation to Dr. Andreas Börner for accepting to evaluate this thesis and for his kind support.

A special thank goes to Dr. Martin Mascher for excellent support and collaboration in 'Exome capture sequencing data analysis. His constant guidance and suggestions contributed significantly to my sequencing analysis.

I would like to acknowledge Dr. Axel Himmelbach for organizing the sequencing lab work and for his valuable and constructive suggestions during the sequencing planning.

My heartfelt gratitude goes to Prof. Dr. Wolfgang Link, who has made a deep impression on me. His scientific inputs and friendly nature has always made me feel at ease with him.

It gives me great pleasure to express my sincere thanks and gratitude to my colleagues who I consider as my friends, Dr. Helen Pidon, Dr. Matthias Jost, Dr. Ruonan Zuo and Dr. Naser Poursarebani. They were always willing to help me and supported me a lot. Without their

precious support, excellent scientific discussions, insightful advices and encouragement, it would not be possible to accomplish this research.

I am also very grateful to Dr. Dimitar Kostadinov Douchkov, Dr. Daniela Nowara and Dr. Jeyaraman Rajaraman from Pathogen Stress Genomics group for their kind technical lab support and helpful scientific discussions.

My sincere thanks goes to Dr. Rients Niks, Dr. Yajun Wang and Cynara Romero for their excellent scientific collaboration in Vada BAC library sequencing and sharing their valuable knowledge with me.

I would like to thank all my colleagues in Genomics of Genetic Resources, Genome Diversity and Plant Architecture groups, for their scientific supports as well as providing a friendly and positive atmosphere. Special thanks to Dr. Mark Timothy Wallace for providing support in ‘PacBio sequencing’ and ‘English proof reading of my thesis. I would like to also thank Dr. Sudharsan Padmarasu, Dr. Sandip Kale, Dr. Mingjiu Li and Dr. Ronny Brandt who never hesitated to help and share their knowledge with me during my study. I deeply acknowledge Manuela Knauff, Manuela Kretschmann and Beate Kamm for their excellent technical assistance. I am also very grateful to Susanne König for her wonderful work in sequencing service. I would like to thank Mary Ziems for admirable assistance in greenhouse and lab work. In addition, I would kindly like to acknowledge all the team of gardeners specially Kathrin Gramel-Eikenroth, Saskia Appenroth, Kathrin Tiemann, Marina Amthor, Daniela Feldmann, Claudia Voigt and all the others for their outstanding efforts in conducting the greenhouse experiments.

I would like to express my deepest appreciation to Dr. Britt Leps for her constant support and kind efforts that made my daily life convenient in Gatersleben.

I would like to thoroughly appreciate the support of PhD students, Post-docs, technical assistants and other employees who somehow helped me during the course of my PhD studies at IPK.

A special thanks to my love, my true friend and my beloved husband, Ershad. Words cannot express how grateful and happy I am to have Ershad in my life.

Finally, but by no means least, my warm, deepest and heartfelt thanks goes to my mother, father and sisters for their unbelievable supports. They are the most important people in my world.

Dedicated

To

‘Patrick Schweizer’

Abbreviation

ASL	Above sea level
ARC	Apaf-1, R proteins and CED-4
ATP	Adenosine triphosphate
Avr	Avirulence
BAC	Bacterial artificial chromosome
Bgh	<i>Blumeria graminis</i> f. sp. <i>hordei</i>
BR	Broad range
BSA	Bulked segregant analysis
CAM	Chloramphenicol
CAPS	Cleaved amplified polymorphic sequence
CAS9	CRISPR-associated protein 9
CC	Coiled-coil
CC-NBS-LRR	Coiled coil-nucleotide-binding site-leucine-rich repeat
4C	Circularized chromosome conformation capture
CIM	Composite interval mapping
CNV	Copy number variation
CRISPR	Clustered regularly interspaced short palindromic repeat
CTAB	Cetyl-trimethylammonium bromide-based
DArT	Diversity arrays technology
DH	Doubled haploid
DLA	Detached leaf assay
DMSO	Dimethyl sulfoxide
DNA	Deoxyribonucleic acid
dNTP	Deoxynucleotide
dpi	Days post inoculation
dsDNA	Double stranded DNA
eQTL	Expression quantitative trait locus
EtBr	Ethidium bromide
ETI	Effector triggered immunity
EST	Expressed sequence tags
GBS	Genotyping by sequencing
GTP	Guanosine triphosphate
GC-content	Guanine-cytosine content
GWAS	Genome wide association
HC	High-confidence
Hi-C	Chromosome conformation capture
hpi	Hours post inoculation
HS	High sensitivity
HTS	High-throughput sequencing
ITMI	International <i>Triticeae</i> Mapping Initiative

LBA	Solid lysogeny broth medium
LC	Low-confidence
LOD	Logarithm of odds
LRR	Leucine rich repeat
MAF	Minor allele frequency
MAMP	Microbe-associated molecular pattern
MAPK	Mitogen-activated protein kinase
MAS	Marker assisted selection
T _m	Melting temperature
<i>Mla</i>	Mildew resistance locus A
<i>MLLa</i>	Mildew resistance locus derived from <i>Hordeum laevigatum</i>
<i>mlo</i>	Mildew resistance locus O
MTP	Minimum tiling path
NBS	Nucleotide binding site
NGS	Next-generation sequencing
NIL	Near isogenic line
NLR or NBS-LRR	Nucleotide binding site leucine rich repeat
PacBio	Pacific Biosciences
PAMP	Pathogen-associated molecular pattern
PAV	Presence/absence variation
PCR	Polymerase chain reaction
POPSEQ	Population sequencing
PRR	Pattern recognition receptor
PTI	PAMP-triggered immunity
QTL	Quantitative trait locus
R gene	Resistance gene
RFLP	Restriction fragment length polymorphism
RGA	Resistance gene analog
RHL	Residual heterozygous line
RIL	Recombinant inbred line
RLCK	Receptor-like cytoplasmic kinase
RLK	Receptor like kinase
RLP	Receptor like protein
RNA	Ribonucleic acid
RNAi	RNA interference
ROS	Reactive oxygen species
RSTK	Receptor-like serine / threonine kinase
RT	Room temperature
SIM	Interval mapping
SMRT	Single-molecule sequencing chemistry with real time detection
SNP	Single nucleotide polymorphism

SP	Signal peptide
SSR	Simple sequence repeat
STS	Sequence-tagged site
SV	Structural variation
TACCA	Targeted chromosome-based cloning
TALE	Transcription activator-like effector
TIGS	Transient induced gene silencing
TIR	Toll and interleukin-1 receptor
TLA	Targeted locus amplification
TM-LRR	Transmembrane leucine rich repeat
WES	Whole exome sequencing
WGS	Whole genome sequencing

Table of Contents

Abstract	XVII
1 Introduction	1
1.1 General introduction	1
1.2 Powdery mildew	3
1.3 Genetic basis of powdery mildew resistance in barley.....	5
1.4 Mechanisms underlying plant resistance to pathogens.....	7
1.5 Structure of disease resistance gene analogs in plants	10
1.6 Plant disease assessment and phenotype scoring	12
1.7 From QTL mapping toward map-based cloning	14
1.8 Barley genomic infrastructure	19
1.9 The aims of this study.....	21
2 Materials and methods.....	22
2.1 Plant material	22
2.2 Phenotyping and experimental design	22
2.3 Preparation of genomic DNA	23
2.3.1 Cetyltrimethyl Ammonium Bromide (CTAB)-based DNA isolation	23
2.3.2 Guanidine thiocyanate-based DNA isolation	24
2.4 Assessment of genomic DNA quality and quantity.....	24
2.4.1 Genomic DNA Quality through gel electrophoresis	24
2.4.2 Genomic DNA Quantity through Qubit Fluorometer	25
2.4.3 Genomic DNA Quantity through Picogreen	25
2.5 Marker development and primer design.....	26
2.6 Polymerase chain reaction (PCR).....	27
2.7 Purification of PCR products for cycle-sequencing	27
2.8 Sequencing and data analysis	28

2.8.1	Sanger sequencing of PCR amplicon	28
2.8.2	Genotyping by Sequencing (GBS).....	28
2.8.3	Exome capture sequencing.....	29
2.9	Genetic linkage analysis	31
2.10	Physical mapping and BAC library screening.....	32
2.10.1	Identification of positive BAC pools	32
2.10.2	BAC monoclonal isolation	32
2.10.3	BAC clone sequencing	33
2.11	Statistics of the phenotypic analysis.....	34
2.12	QTL analysis.....	35
3	Results	36
3.1	Low resolution mapping identified a major locus for seedling stage resistance to barley powdery mildew on chromosome 2H	36
3.1.1	Phenotypic data analysis	36
3.1.2	Genotyping of the RIL population	39
3.1.3	QTL mapping for powdery mildew resistance.....	42
3.2	Overlap of the mildew resistance locus with previously identified mildew resistance QTL	45
3.3	High resolution genetic mapping of the 2HL resistance locus	47
3.4	<i>In silico</i> based candidate gene identification at the <i>MILa-H</i> locus.....	56
3.5	Re-sequencing of potential candidate genes in ‘HOR2573’ identified potentially causative mutations	65
3.6	Physical map construction for the <i>MILa-H</i> locus in a powdery mildew resistant haplotype	69
4	Discussion.....	72
4.1	Fine mapping allowed to map the <i>MILa-H</i> locus in a 850 kb interval	73
4.2	A gene encoding LRR-RLK protein is the best candidate gene in the <i>MILa-H</i> interval.....	74
4.3	Is another gene present in the <i>MILa-H</i> interval?	77

4.4	Genetic mapping and its successors: advanced tools for defining the gene location	82
4.5	Can the durability of <i>MILa-H</i> be increased by allele or gene pyramiding?	85
5	Outlook	88
6	Summary	90
7	References	92
8	Appendix Tables	116
9	Erklärungen	133

Table of Figures

Figure 1: Asexual life cycle of <i>B. graminis</i> f. sp. <i>hordei</i>	4
Figure 2: Schematic representation of the plant immune system.....	9
Figure 3: Schematic overview of common structures of four major plant R proteins.	12
Figure 4: Schematic representation of the basic process of genotyping by sequencing and exome capture enrichment assays.	18
Figure 5: Schematic illustration for the quantitative classification of barley susceptibility against powdery mildew according to symptom severity.	36
Figure 6: Distribution of powdery mildew disease severity of ‘HOR2573 × Morex’ population through three independent phenotyping experiments.	37
Figure 7: Performance evaluation of phenotyping scoring.	38
Figure 8: Genetic linkage map of F2S5 ‘HOR2573 x Morex’ composed of 1,394 GBS-derived SNPs markers on seven barley linkage groups.	41
Figure 9: Results of the QTL mapping analysis of F2S5 population ‘HOR2573 × Morex’ in each phenotyping experiment (environment).	43
Figure 10: Schematic illustration for qualitative scoring of susceptibility to powdery mildew in barley based on DLA.....	44
Figure 11: Physical position of the powdery mildew resistance <i>MILa-H</i> locus originated from ‘HOR2573’ and quantitative resistance locus <i>MILa</i> derived from ‘Vada’ on the barley reference genome.	46
Figure 12: High resolution mapping of the powdery mildew resistance locus <i>MILa-H</i>	55
Figure 13: <i>In silico</i> characterization of the <i>MILa-H</i> locus interval	64

Figure 14: Characterization of the four potential candidate genes in the *MILa-H* interval through re-sequencing in the resistant parent ‘HOR2573’68

Figure 15: Schematic illustration of the physical map construction for the *MILa-H* interval in ‘Vada’ draft assembly.71

Figure 16: Schematic illustration of the structural variation within the *MILa-H* locus interval between resistant (Vada) and susceptible (Morex) haplotype.....81

Table of Tables

Table 1: Variance component and significance across experiments.....	37
Table 2: Number of detected SNPs derived from GBS before and after filtration in two levels of read coverage.....	39
Table 3: Summary of the genetic linkage map constructed based on 1,394 SNP markers derived from GBS in the barley RIL population.....	40
Table 4: Summary of QTL found for <i>Bgh</i> resistance in F2S5 generation of ‘HOR2573 x Morex’ population.....	42
Table 5: List of flanking and co-segregating DNA markers with the <i>MILa</i> locus in ‘L94 × Vada’ population.....	46
Table 6: Observed phenotypic variation among eight biological replicates for RHLs 145, 567, 836 in response to powdery mildew (infected leaf area %) through three independent phenotyping experiments.	48
Table 7: Allele coverage of heterozygous variants at the QTL interval for three RHLs 145, 567 and 836.....	49
Table 8: Phenotypic segregation pattern of each residual heterozygous sub family for resistance to the powdery mildew isolate.	51
Table 9: List of CAPS markers used for initial high resolution mapping.....	51
Table 10: List of CAPS markers derived from GBS and exome capture data used to narrow down the target interval.....	53
Table 11: List of markers derived from GBS and exome capture data used in Sanger sequencing to narrow down the target interval.	54
Table 12: Summary of the overlapping BAC clones with flanking and co segregating markers information in the <i>MILa-H</i> interval.....	58

Table 13: Manual annotation of four resistance gene models within the *MILa-H* interval compared to the barley automated gene annotation.60

Table 14: List of orthologous loci in rice, bread wheat and tausch's goatgrass for the four resistance gene models in the *MILa-H* interval60

Table 15: Manual annotation of the three other HC genes models within the *MILa-H* interval compared to the barley automated gene annotation.63

Table 16: List of orthologous loci in closest crop model species to the three predicted gene models in the *MILa-H* interval63

Table 17: Summary of sequence analysis of four disease resistance homologs within target interval from ‘HOR2573’ (resistance parent).67

Table 18: Summary of sequence comparison result between draft ‘Vada’ assemblies and the markers PCR amplicon.....70

Table of Appendix

Appendix 1: List of the identified resistant barley accessions, available in Gatersleben genebank, to seven modern, highly virulent powdery mildew isolates.....	116
Appendix 2: Summary of QTL found for <i>Bgh</i> resistance in F2 generation of ‘HOR2573 x Morex’ population.....	118
Appendix 3: List of the gene located in the confidence interval of the detected major single QTL flanked by M238 and M252	119
Appendix 4: Summary of BAC clones spanning the <i>MIL-H</i> interval	124

Abstract

Barley powdery mildew caused by *Blumeria graminis* f. sp. *hordei* (*Bgh*) is a foliar disease with potentially severe impact on yield and malt quality. The cultivated barley lines and landraces have proven to be valuable sources of powdery mildew resistance. The identification of new powdery mildew resistance genes and / or introducing novel alleles of known genes from barley germplasm resources have significantly contributed to the progress in barley resistance breeding. This study describes the high resolution mapping of a resistance locus, named '*MILa-H*' derived from an Ethiopian spring barley accession 'HOR2573', conferring resistance to seven modern highly virulent European and Israeli isolates. Using the progeny of three identified residual heterozygous lines (RHLs) from an F2S5 recombinant inbred line (RIL) population and the state-of-the-art high throughput DNA sequencing assays as well as recently developed barley web-based genetic resources, the resistance interval was narrowed down from originally 3.5 Mbp to a 850 kb interval. The result revealed that the *MILa-H* interval contains four potential candidate genes belonging to disease resistance gene family according to barley reference genome sequence cv. 'Morex'. Among these four, a receptor like kinase is considered as the strongest candidate gene for *MILa-H*. Interestingly, this interval was co-localizing with a previously mapped QTL from *Hordeum laevigatum* on the basis of *Laevigatum*-QTL flanking and co-segregating markers, suggesting these two intervals possibly harbor the same gene with different alleles or otherwise different genes. In this regard, a BAC library carrying the *MILa* locus was utilized to reconstruct the physical map of the *MILa-H* region based on a resistance haplotype as 'Morex' is the reference genome for barley physical map and may be lacking the gene of interest. The identified co-segregating markers in this study should be useful for marker-assisted selection in barley breeding employing crosses between resistant genotypes with a resistance interval on the distal portion of chromosome 2HL, and susceptible genotypes. In addition, the final identification of candidate gene will positively contribute to barley resistance breeding programs.

1 Introduction

1.1 General introduction

Cultivated barley (*Hordeum vulgare* ssp. *vulgare* L.), the domesticated form of *H. vulgare* ssp. *spontaneum* K. Koch, is one of the oldest crops in the world (Weiss and Zohary, 2011). Archaeological remains of barley grains found at various sites in the Fertile Crescent indicate that the domestication of barley was dated back to 10,000 years before the present (cal BP) (Zohary et al., 2012). The genetic data supported by prehistoric archaeobotanical information present the barley's migration from Fertile Crescent into the horn of Africa, Europe and Tibetan Plateau in the Far East (Badr et al., 2000; Allaby, 2015).

Barley can be found in highly diverse environments, comprising extremes of latitude and altitude where other crops cannot be adapted (Dawson et al., 2015). Due to its huge environmental adaptability, many types of barley are grown throughout the world (Newman and Newman, 2008). Barley is a short season and early-maturing cereal crop with high yield potential. It is cultivated in both high-input and highly productive agricultural systems as well as in subsistence and low-input systems. Its cultivation requires simple agronomic management practices in comparison to other crops (Dawson et al., 2015). Furthermore, the low diploid chromosome number ($2n=14$) and ease of crossing, make barley a favorable biological model for researchers (Saisho and Takeda, 2011). Predominantly, lessons taken from barley are particularly applicable to other cereal crops, especially to other members of the *Triticeae* family, including hexaploid bread wheat (*Triticum aestivum* L.), one of the world's most substantial food sources.

The prevalent use of barley is as a source of feed and forage for livestock, and as source for food and beverages for humans (Ullrich, 2010a; Newton et al., 2011). In terms of crop production, it is ranked fourth among other cereal crops after rice (*Oryza sativa* L.), wheat (*Triticum aestivum* L.) and maize (*Zea mays* L.). According to FAO reports on global trade of barley and barley products, more than 20 million tons of barley grains have been exported and imported annually worldwide, accounting for about US\$3 billion per year. The value of malt export and imports has grown significantly from an average of US\$1.35 billion in the year 2000 to about US\$2.0 billion in 2005, which is a 48% increase in the value of global barley malt trade (Ullrich, 2010b).

Despite its global value, the respective barley cultivation area has declined from 68 million ha in 1995 to less than 50 million ha in 2014. This decline roots in the high yielding capacity of new cultivars, compensating for reduced acreages (<http://www.fao.org/faostat/en/#data>, FAO Statistical annual book 2014). Nevertheless, losses due to pests and diseases in cereals continue to pose a substantial threat to agricultural food and feed production and make significant influences on economic decisions as well as practical developments. To overcome these problems, agricultural production requires high-yielding crops withstanding crop diseases. Barley with its wide environmental adaptation range, wide variety of users and different end uses is considered as a promising model for research investigations in this area (Newton et al., 2011).

A cost effective and environmentally sustainable strategy to mitigate the damage and losses caused by plant pathogens is to deploy plant varieties possessing genetic resistance (Johnston et al., 2013). Over the last decades, concerns about risk of yield loss have been raised owing to the genetic uniformity of modern cultivars. The intensive selection in modern plant breeding programs for many years, led to crop genetic erosion through the gradual “masking out” of alleles desired for resilient and sustainable production (McCouch et al., 2013). This is in contrast with high genetic variation of landraces observed between and within the populations. In fact, landraces represent a domesticated and locally adapted varieties developed over time by farmers, through adaptation to natural environment (Villa et al., 2005). Compared to landraces, the modern barley cultivars have been selectively improved by breeders for particular characteristics, derived through line breeding leading to highly inbred, homozygous and homogenous plant material. This reduced genetic base in modern crop cultivars makes them susceptible to disease epidemics. The comparatively high level of genetic variation in landraces is one of their advantages to further improved cultivars. Even though landraces’ yield may not be as high, their stability in face of adverse conditions is typically high (van de Wouw et al., 2010). Ethiopia is a most probable center for barley secondary domestication with high variability in climatic and edaphic conditions. Over 90% of the barley cultivated in Ethiopia, is represented by local landraces. These local barley landraces are cultivated from 1400 to over 4000 meters above sea level (a.s.l.). Hence, the cultivated barley has fairly well adapted to a wide range of microclimatic regimes throughout the country (Asfaw, 2000). Furthermore, its biannual cultivation has likely caused most of the structure of variation in these landraces (Hadado et al., 2009). Thus, they are a

precious source of genes that potentially can impact important agronomic traits, such as high lysine content and protein quality (Munck et al., 1970), malting and brewing quality (Lance and Nilan, 1980) disease (e.g. barley yellow dwarf virus, powdery mildew, scald, net blotch and loose smut) and pest resistance (Wiberg, 1974; Zhang et al., 1987; Jørgensen, 1992; Alemayehu, 1995; Yitbarek et al., 1998).

Considering the above-mentioned reasons, unlocking genetic diversity in genebank collections is of prime importance for future sustainable crop production (McCouch et al., 2013). This indicates the allelic variation of genes which are originally found in the wild relatives and landraces but lost gradually during domestication and breeding, could be recovered by taking the advantage of the genetic resources.

In this study, the high resolution mapping of a powdery mildew resistance locus derived from an Ethiopian landrace ‘HOR2573’ is described. The identification of this locus was achieved through applying novel sequencing-based strategies and taking advantage of the improved barley genomic resources. The main concepts of plant disease resistance and barley genomic infrastructure used for characterization of resistance genes (R genes) will be introduced in the following sections.

1.2 Powdery mildew

Powdery mildew fungi infect more than 9,500 different plant species, leading to a huge yield loss in agricultural production (Inuma et al., 2007). Powdery mildew caused by *Blumeria graminis* f. sp. *hordei* (*Bgh*) is a serious foliar disease of barley with worldwide importance (Glawe, 2008). The relatively cool and humid climate of Europe fosters the spread of powdery mildew, making it the most prevalent European barley disease (Jørgensen and Wolfe, 1994). Yield losses of up to 30%, as well as reduced grain quality have often been reported (Corrion and Day, 2001; Czembor, 2002). *Bgh* belongs to the Ascomycota, the largest phylum of the kingdom Fungi. It is an obligate biotrophic fungus growing only on the living host. It has a specialized feeding structure, called the haustorium, secreting effector proteins that can suppress or modulate the host’s defense responses (Both et al., 2005).

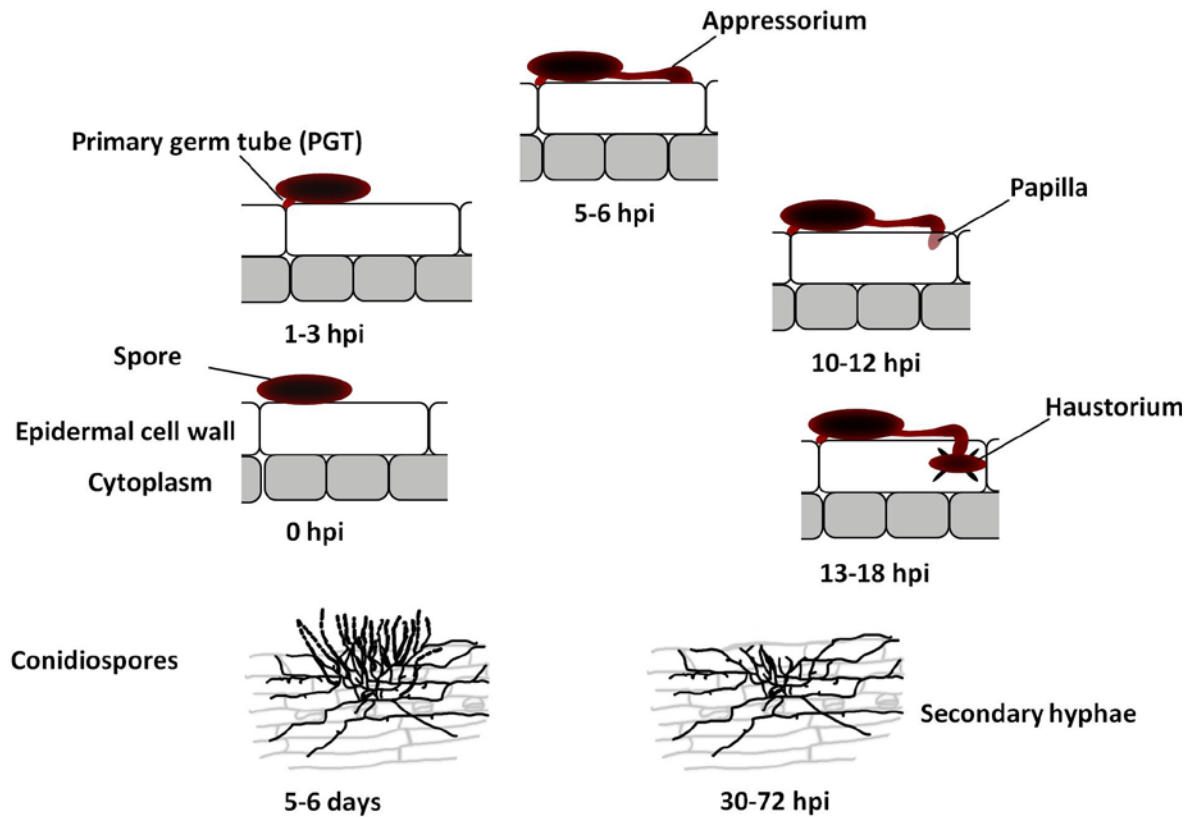


Figure 1: Asexual life cycle of *B. graminis* f. sp. *hordei*.

The pre-penetration stages start from ungerminated conidia (0 hour after inoculation (hpi)) up to development of primary germ tubes (1-2 hpi) followed by appressorium (5-6 hpi) and papilla formation (10-12 hpi). The post-penetration stages are initiated by the formation of the haustorium (13-18 hpi), the development of hyphae on the surface of the leaf (30-72 hpi) and production of abundant conidia (5-6 days). The figures for secondary hyphae and conidiospores were taken from (Both et al., 2005).

B. graminis is an obligate biotrophic fungus, feeds on living tissue exclusively, thus, it requires its host to stay alive (Figure 1). The infection process begins following the contact of an asexual spore, the conidium, with the leaf surface and production of an extracellular matrix (Carver et al., 1999; Mohler et al., 2011). This matrix serves to attach the fungus to the surface and helps to obtain signal cues (Meguro et al., 2001). The initial primary germ tube emerges within the first hour post inoculation (hpi). The tube senses the nature of the surface and transmits a signal to germinate (Kinane et al., 2000; Ellinger et al., 2013). Soon after, a second germ tube appears

from the conidium. The conidium tip grows and forms a dome-shaped penetration structure known as the appressorium which can easily be recognized after 8 hpi (Nielsen et al., 2000; Glawe, 2008). After 15 hpi, a penetration peg is formed underneath the appressorium, generating high internal turgor pressure through the accumulation of compatible solutes. This facilitates mechanical penetration into the plant cell wall (Pryce-jones et al., 1999), leading to haustorium formation. The haustorium is a feeding structure that delivers nutrients from the plant to the fungus, enabling it to multiply quickly on the leaf surface and produce secondary hyphae. The fungal colony can usually be seen by the naked eye on the leaf surface after 3 days post inoculation (dpi). Subsequently, the colony initiates to create conidiophores, which produce large number of conidia. These are airborne and will distribute easily *via* wind over hundreds of kilometers (Both et al., 2005; Glawe, 2008). The successfully invaded barley plant shows typical symptoms of white powdery pustules on the leaf surface. The infected plant reroutes its nutrients into the fungus, which proliferates and disperses very rapidly.

1.3 Genetic basis of powdery mildew resistance in barley

Host resistance to powdery mildew in barley has been characterized by two independent types: (1) hypersensitive resistance and (2) quantitative or partial resistance. Hypersensitive resistance is controlled by a single major gene in a race-specific manner (Flor, 1971), which often is lacking durability (Parlevliet, 2002). In contrast, quantitative or partial resistance is not based on hypersensitivity; it is conditioned by the presence of a number of genes with small effects on the final resistance phenotype which is characterized by an increased latency period and / or reduced infection frequency (Simmonds, 1991; Jørgensen and Wolfe, 1994; Keane, 2012). The latter type of resistance is considered to be more durable compared to the single major gene-dependent and hypersensitive type (Simmonds, 1991; Jørgensen and Wolfe, 1994; Parlevliet, 2002; Kou and Wang, 2010). However, the polygenic nature of partial resistance is more difficult to be managed in breeding programs compared to major effect genes. The breeding of cultivars is facilitated if large effect genes conferring resistance can be identified and combined through marker assisted gene pyramiding. This requires markers that are closely linked to the resistance genes. In this approach, single major R genes can potentially be combined with less expense and fewer technical difficulties compared to combining small effect genes (Poland et al., 2009; Fukuoka et al., 2015).

Until now, some of the previously identified powdery mildew resistance loci in barley have been exploited by plant breeders in developing resistant cultivars. In barley, all seven chromosomes harbor important powdery mildew resistance loci and still, novel genes are continually being allocated to its chromosomes (Řepková et al., 2006). Jørgensen and Wolfe (1994) summarized race-specific powdery mildew resistance loci based on their position on barley chromosomes; *Mla*, *Mlat*, *Mlk*, *Mlnn*, *MlGa*, *Mlra* are located on chromosome 1H, *MILa* on 2H, *mlo*, *Mlg* on 4H and *Mlh* on 6H. Two years later, Schönfeld et al. (1996) reported two genes (*mlt* and *Mlf*) on chromosome 7H and one (*Mlj*) on chromosome 5H. In addition, two genes (*Rar1* and *Rar2*) required for the function of many *Mla* resistance genes and some unlinked R genes (Schulze-Lefert and Vogel, 2000) were mapped on chromosome 2H (Lahaye et al., 1998).

Among all reported barley powdery mildew resistance genes, dominant gene *Mla* (*mildew resistance locus A*) and recessive gene *mlo* (*mildew resistance locus O*) are maybe the most effective and thus most widely deployed loci in barley breeding programs. The latter, originally identified in Ethiopian landraces (Jørgensen, 1992) is derived from a natural gene silencing event and acts at a basal level to resist *Bgh* through inhibition of fungal penetration (Eckardt, 2002). This gene exhibits a broad-spectrum resistance phenotype which was reconfirmed in mutant plants (Büschges et al., 1997). For more than three decades, it protected European barley cultivars against yield losses caused by *Bgh*. However, the barley cultivars with *mlo*-based resistance might suffer from enhanced susceptibility to necrotrophic and hemibiotrophic pathogens such as *Ramularia collo-cygni*, *Magnaporthe oryzae*, and *Cochliobolus sativus* (Brown and Rant, 2013). The spontaneous necrotic spots on leaves can be observed in seedling and adult plants even in the absence of infection (Wolter et al., 1993; Martienssen, 1997), introducing a yield penalty. For full expression of *mlo*-based resistance, two genes (*Ror1* and *Ror2*) are required, which were mapped to the centromeric region of the long arm of chromosome 1H (Freialdenhoven et al., 1996).

In contrast to *mlo*, *Mla* is one of the genetically most thoroughly characterized nucleotide-binding site and leucine-rich repeat genes (NBS-LRRs) that shows race-specific resistance to *Bgh* (Wei et al., 1999). It comprises 32 known variants forming an allelic series in diverse germplasm (Kinizios et al., 1995). The *Mla*-conferred resistant phenotype is highly diverse, ranging from immunity with a rapid hypersensitive response to a late response, allowing the development of

some fungal mycelium (Boyd et al., 1995). Some of these alleles (e.g. *Mla6*, *Mla12* etc.) have been introduced from wild (*H. spontaneum*) into cultivated barley by plant breeders (Jørgensen and Wolfe, 1994; Moscou et al., 2011; Seeholzer et al., 2010).

In general, other powdery mildew resistance genes have been identified in both barley landraces and wild crop relatives; however, they are not as diverse as compared to the *Mla* locus. Therefore, plant breeders continuously look for new monogenic as well as polygenic resistance sources derived from diverse barley germplasm in order to increase the flexibility for barley resistance breeding, specifically for the option of resistance gene pyramiding.

1.4 Mechanisms underlying plant resistance to pathogens

Once the pathogen is able to evade the multiple layers of host defenses, diseases symptoms often develop. Still, plants possess two effective mechanisms based on either perception (I) or loss of susceptibility (II) to respond to potentially hazardous pathogens *via* regulated pre- and post-invasion defense responses in order to diminish the damages imposed by harmful agents. There are sophisticated and dynamic interactions between a pathogen and its host (Figure 2). The former mechanism can be subdivided into: perception through receptor-like proteins / kinases (RLPs / RLKs); nucleotide binding site (NBS) and leucine rich repeat (LRR) protein products encoded by many R genes (NBS-LRR) and Executor genes (Kourelis and Hoorn, 2018).

The first line of pre-formed and inducible defense responses which offer protection against a pathogen is basal resistance (also called innate immunity). Basal resistance can be triggered as plant cells recognize microbe / pathogen-associated molecular patterns (MAMPs / PAMPs). These molecular patterns are conserved features of most microbes / pathogens that may have different forms, including double-stranded RNA, specific sequences of DNA common to microbes, peptides derived from bacterial flagellum proteins, and chitin (which makes up the cell wall of fungi). The recognition of each molecular pattern is performed *via* a class of proteins located on the transmembrane, known as pattern recognition receptors (PRRs). Thus, this type of perception is also called cell surface perception, which can occur directly (sub-mechanism 1) or indirectly (sub-mechanism 2) (Kourelis and Hoorn, 2018), leading to a set of biochemical and transcriptional responses (Jones and Dangl, 2006). For instance, bacterial flagellin, *flg22*, is

perceived directly by the RLK *FLAGELLIN-SENSITIVE2 (FLS2)* in *Arabidopsis* (Gómez-Gómez and Boller, 2000) whereas tomato *Cf-2*, a RLP introgressed from a wild tomato species into cultivated tomato (Dixon et al., 1996) requires *Rcr3*, a secreted tomato cysteine protease to be able to confer resistance against the tomato leaf mold fungus *Cladosporium fulvum* (Dixon et al., 2000; Luderer Rianne et al., 2002). The recognition of pathogen invasion outside of the plant cell and transferring this information through activated signaling pathways trigger innate immune responses which is called “PAMP-triggered immunity” (PTI) (Nürnberger et al., 2004; Zipfel and Felix, 2005; Jones and Dangl, 2006). The activation of PTI results in a series of immune responses such as deposition of callose, reactive oxygen species production (ROS), transcriptional induction of defense genes and mitogen-activated protein kinase (MAPK) cascades activation (Tena et al., 2011). This usually stops the progress of infection before the microbe gains a hold in the plant.

Many pathogens might suppress the PTI components either by interfering with recognition at the plasma membrane or by effector proteins known as avirulence (Avr) proteins, delivered inside the plant cell. This interference process is initiated by the secretion of Avr proteins by the secretory system of pathogen cells. Effector proteins most likely change resistance signaling or manifestation of resistance responses. Indeed, the effector proteins target receptor-like cytoplasmic kinases (RLCKs) to suppress PTI. RLCK belongs to the RLK super family, located in the cytoplasm and lacking the extracellular domain (Yamaguchi et al., 2013). In response, plants have evolved a second line of defense termed effector triggered immunity (ETI) in which the effector molecules are recognized in the plant directly or indirectly through resistance genes (R genes). The indirect recognition occurs through an additional host component, so called guard (the R gene product) that targets the effectors (the guardee). The direct (sub-mechanism 3) and indirect (sub-mechanism 4) interactions of plant R proteins and pathogen-derived molecules will result in a hypersensitive response and rapid cell death around the site of infection (Chisholm et al., 2006; Schwessinger and Zipfel, 2008; Zipfel, 2014). Most R genes that protect plants against pathogens by direct recognition of the effectors encode intracellular proteins with NBS and LRR domains (Marone et al., 2013).

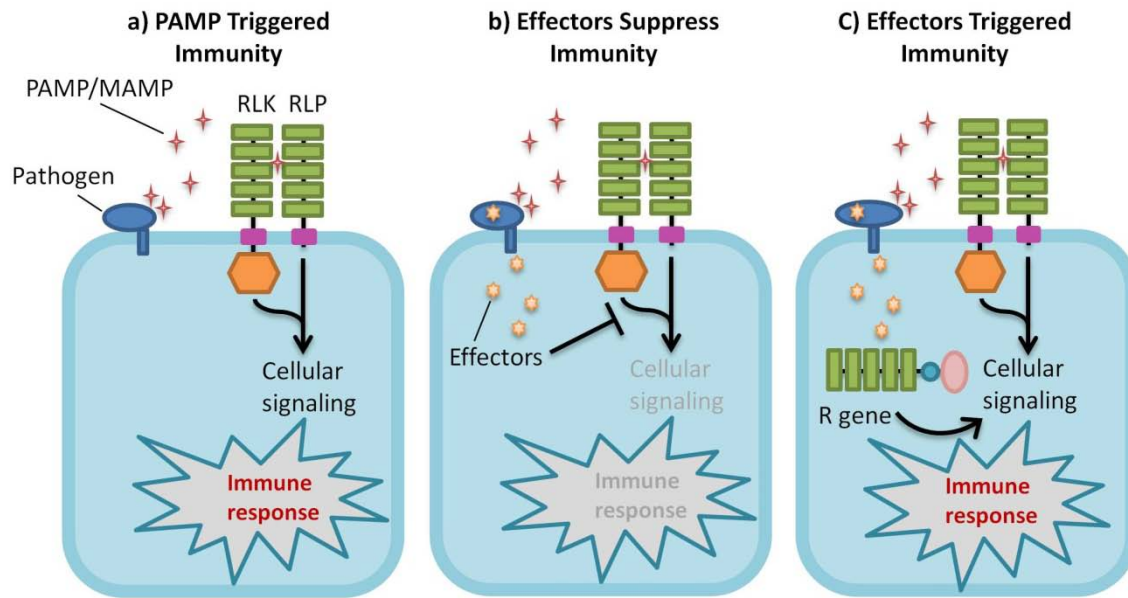


Figure 2: Schematic representation of the plant immune system.

a) Recognition of pathogen /microbe-associated molecular patterns (PAMP /MAMP) by pattern recognition receptor proteins (RLK /RKP) promptly triggering basal immunity. b) Pathogen delivers effector proteins inside host cytoplasm, targeting multiple host proteins to suppress basal immune responses c) Plant resistance proteins (represented by CC-NB-LRR and TIR-NB-LRR; R genes) recognize effector activity and restore resistance through effector-triggered immune responses (with small modifications from Pieterse et al. (2009)).

The fundamental difference between PTI and ETI is the degree of specificity. In fact, ETI shows a highly-specific, gene-for-gene defense response. The high specificity makes this pathway less durable than PTI and more targeted against an individual pathogen.

The perception can occur through executor genes which are a specific group of R genes activated by pathogen transcription activator-like effectors (TALEs) (sub-mechanism 5). This group of R gene confers resistance against only *Xanthomonas* strains. Once the pathogen invades, the transcription of main susceptibility factors in the host is changed though binding of pathogen TALEs to particular DNA sequences. The executor genes trap these TALEs through mimicking

the promoter regions of these susceptibility factors, thus, the TALEs promote transcription of immunity genes instead of susceptibility factors (Hoorn and Kamoun, 2008).

The immunity mechanism through loss-of-susceptibility is divided into: active loss-of-susceptibility, losing interaction with host targets and host reprogramming. The active loss-of-susceptibility mechanism can occur against many pathogens, in which the R genes interrupt the pathogen's main activity (Kourelis and Hoorn, 2018). A second common mechanism is that the host susceptibility factor will lose the interaction with the pathogen effector, such as recessive R genes against viruses (potyviruses) decrease susceptibility by such a loss of interaction during virus infection (Lellis et al., 2002). Loss of susceptibility *via* host reprogramming is the result of mutations causing deregulation of component(s) in cellular pathways. This strategy usually directs durable resistance against a broad range of pathogens such as recessive loss-of-function *mlo*. Indeed, MLO encodes a particular protein acting as a negative regulator of cell death in response to both abiotic and biotic stress (Piffanelli et al., 2002). As a result the loss-of-function alleles in MLO are associated with spontaneous cell death. Hence, the loss of a general cell death suppressor confers durable resistance to powdery mildew (Jørgensen, 1992).

1.5 Structure of disease resistance gene analogs in plants

Resistance gene analogs (RGAs) in plants have conserved domains and motifs that play specific roles in disease resistance (Sekhwal et al., 2015). This facilitates their identification in sequenced genomes using bioinformatic approaches (Ameline-Torregrosa et al., 2008; Arya et al., 2014). RGAs can be classified into two groups: 1) transmembrane leucine rich repeats (TM-LRRs) and 2) NBS-LRRs.

TM-LRRs can be subdivided into two classes: RLKs and RLPs (Hammond-Kosack and Jones, 1997). RLKs and RLPs are considered to be main components of the first line of defense in plants. They recognize conserved molecules characteristic of many microbes or so called “microbial elicitors”. The interactions between receptor and elicitor usually take place in the extracellular space. RLKs / RLPs are present at the plasma membrane and perceive signature molecules from either the invading pathogen or damaged plant tissue. PAMP / MAMP recognition by pattern recognition receptors serves as an early warning system for the presence of

a wide range of potential pathogens (Chisholm et al., 2006; Zipfel, 2014). The structure of RLK and RLP proteins is similar to (1) a signal peptide (SP) at the start point of the N-terminus; (2) the LRRs as extracellular domains for microbial pattern perception; (3) a transmembrane helix domain which anchors RLP and RLK in the plasma membrane. Both RLPs and RLKs are PRRs that detect elicitors such as nucleic acids, proteins, lipids, and carbohydrates. The only structural difference between RLPs and RLKs is that RLPs are lacking an intracellular kinase domain; hence RLPs are incapable of independently transducing the perceived signal into a downstream cascade (López-Larrea, 2012).

The NBS-LRR gene family is a well-known family of RGAs. There are two classes of NBS-LRR genes distinguished according to the features of their N-terminal structure. The TIR-NBS-LRR class includes an N-terminal domain with homology to Toll and interleukin-1 receptor (TIR), whereas the non-TIR class mainly contains a coiled-coil (CC) domain. The TIR-NBS-LRR proteins are not present in cereal species, suggesting that the TIR-NBS-LRR were few in early angiosperm ancestors and might have been lost in the cereal lineage (McHale et al., 2006). Their most striking structural feature is a highly irregular and variable LRR domain at the N-terminal region that is responsible for protein-protein interactions (Jones and Jones, 1997; Meyers et al., 1999; Takken and Govere, 2012; Marone et al., 2013).

In addition, nucleotide-binding (NB) site is a conserved region in R proteins, probably critical for adenosine / guanosine triphosphate (ATP / GTP) binding (Saraste et al., 1990), however, how or which of these nucleotides (ATP / GTP) bind to the NB site is still unknown. This site is part of a larger domain which is similar to some eukaryotic cell death effectors like Apaf-1, R proteins, and Ced-4 (ARC). This enlarged region is called NB-ARC (Biezen and Jones, 1998). Due to the high analogy with Apaf-1 and Ced4 functions in regulating programmed cell death, this domain in NBS-LRR genes might fulfill the same function as an intra-molecular signal transducer (Van der Biezen and Jones, 1998; Takken and Govere, 2012). This domain is divided into ARC1 and ARC2 subdomains. Within domains and subdomains of TIR-NBS-LRR and CC-NBS-LRR, a variety of conserved motifs are present. For instance, the pentapeptide EDVID motif or the so called “CCD” is identified in the CC domain. Likewise, there are four motifs TIR1, TIR2, TIR3 and TIR4 within the TIR domain besides several motifs within the NBS domain (Bent, 1996;

Ellis et al., 2000; Takken and Joosten, 2000; Sekhwal et al., 2015). The common structure and various motifs of four main R proteins are illustrated in Figure 3.

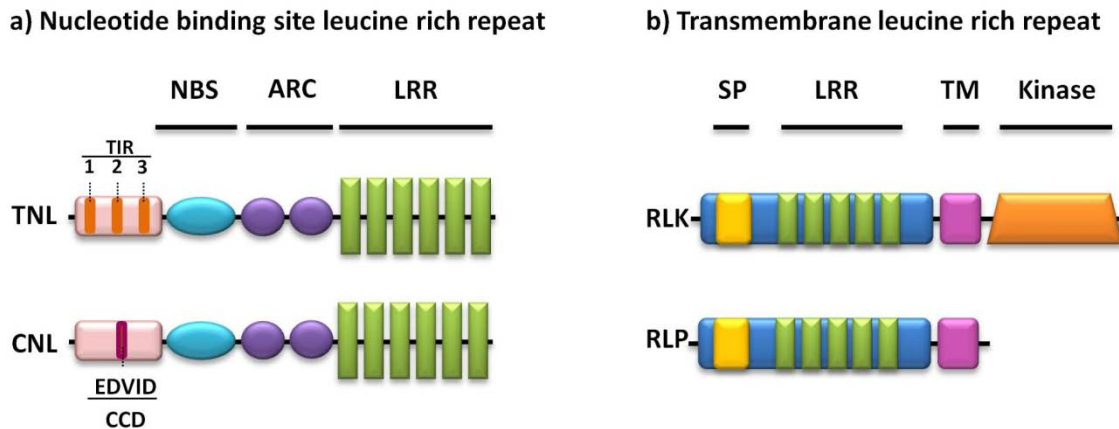


Figure 3: Schematic overview of common structures of four major plant R proteins.

Motifs are represented as colored boxes and labeled under the domain names. The drawn scale for each domain and motif is only for ease of visualization. Only highly conserved motifs are depicted. a) Typical domain dissection for TIR-NBS-LRR and CC-NBS-LRR proteins b) Domain structures for RLKs and RLPs. TIR: Toll / interleukin-1 receptor; NB: nucleotide-binding site; ARC: abbreviated from Apaf-1, R proteins and CED-4; CC: coiled-coil; SP: signal peptide; TM: transmembrane; LRR: leucine-rich repeats (with small modifications from Sekhwal et al. (2015)).

1.6 Plant disease assessment and phenotype scoring

The disease severity in plants is typically measured based on quantitative scales that are defined based on quantitative difference in fungal growth between resistant and susceptible genotypes. It is measured through either visual observation of the fungal infection sites or by progress of disease symptoms (Kranz and Rotem, 1988). Given that a resistant phenotype can be controlled either by a single or multiple genes, using a sensitive and non-subjective quantitative approach for initial evaluation of the disease severity is recommended. Additionally, this approach is convertible to subjective qualitative method, meaning that in the subjective method, plants with $\leq 20\text{-}30\%$ infection area are classified as resistant, if not, considered as susceptible (Ayliffe et al., 2013). In principle, the process of counting infection sites per leaf area and the evaluation of

infected region by naked eye are undeniably labor-intensive and absolutely demand technical training (Kranz, 2012), however, this approach is considered as a primary move toward an accurate crop disease assessment. The following two examples shall explain this in greater detail: Friesen and Faris (2004) studied genomic regions harboring QTL (quantitative trait locus) for resistance to tan spot, a fungal foliar disease of wheat, caused by *Pyrenophora tritici-repentis* (*Ptr*). The quantitative disease evaluation of the International *Triticeae* Mapping Initiative (ITMI) mapping population consisting of 104 recombinant inbred lines (RILs), was performed at the seedling stage according to 1–5 scale described by Lamari and Bernier (1989). The QTL analysis of the population led into identification of a single major QTL conferring resistance against wheat tan spot. Later on, the disease severity was re-scored as either parental type and treated as a marker to determine linkage to existing markers. This resulted into 1:1 segregation ratio at $P < 0.05$, consistent with Mendelian pattern for a single gene, implying that the identified QTL was governed by a single dominant gene accounting for 69% of the phenotypic variation. Another study was conducted in sugarcane on an F_2 bi-parental population consisting of 227 individuals derived from a cross between a yellow spot-resistant variety, M 134/75, and a susceptible parent, R570. The population was phenotyped using a 1-4 scale according to Ricaud (1974). QTL analysis identified a single QTL for yellow spot (*Mycovellosiella koepkei*) disease resistance in this sugarcane population. Following re-scoring of the disease severity as either parental type, the X^2 test (at 98% confidence level) of the observed segregation pattern for yellow spot disease showed a putatively monogenic dominant inheritance for the trait with a 3 (resistant):1(susceptible) ratio (Aljanabi et al., 2007).

More recently, for disease symptoms quantification, image-scanning methodologies have been used to solve the problem of lacking access to plant phenotyping capabilities. The imaging techniques provide a more precise phenotype of infected plants by quantitative assessment of disease symptoms and host responses through a less laborious and high-throughput data production approach compared to human raters (Seiffert and Schweizer, 2005; Pethybridge and Nelson, 2015).

1.7 From QTL mapping toward map-based cloning

As noted earlier, the quantitative evaluation of resistance to powdery mildew in mapping populations may result into the identification of either a single resistance locus with large effect or several QTL (having both minor and major QTL), thus, QTL mapping can be used as a tool to explain the genetic basis of disease resistance trait using phenotypic data.

A QTL analysis of quantitative powdery mildew resistance on a doubled haploid (DH) population derived from 'Igri × Danilo' using 67 RFLP loci determined a single major QTL in both field testing with natural infection and on detached primary leaves (Backes et al., 1996). Schiff et al. (2001) studied the natural genetic diversity of disease resistance against powdery mildew in *Arabidopsis thaliana*. In a QTL analysis of a RIL population derived from a cross between Warschau-1 (resistant parent) and Columbia-0 (susceptible parent) two powdery mildew disease resistance loci were identified, one with a major effect and one with a minor effect on disease resistance, in total explaining 65% of the variation in resistance.

Traits that are inherited according to Mendelian laws can be allocated in the genome by means of genetic mapping (single locus or QTL). Indeed, it not only indicates whether the transmitted phenotype from the parent to a progeny is linked to a single or multiple genes but it also specifies the chromosomal region(s) carrying the responsible gene(s). For instance, previous QTL mapping studies conducted on barley powdery mildew resistance have suggested that the telomeric region of barley chromosome 2HL represents an important genomic region for mildew resistance. Von Korff et al. (2005) detected a strong QTL localized to a 7.0 cM interval on 2HL, where the exotic allele derived from *H. spontaneum* reduced powdery mildew severity by 51.5%. The location of this QTL corresponded to a previously reported quantitative locus conferring resistance to *Bgh*, identified at seedling stage in an RI population (Backes et al., 2003). This RI population was derived from a cross between the cultivar 'Vada' carrying *MILa* (*mildew resistance locus* derived from *H. laevigatum*) and the wild barley accession 1B-87. The identified 'Vada'-resistance QTL was positioned to a 6.0 cM interval co-localizing with the *MILa*-locus on chromosome 2H.

A closer look to the size of the previously reported chromosomal regions carrying the powdery mildew resistance *MILa* locus revealed that accessibility of sufficiently dense markers has

historically been a limiting factor in precise localization of the QTL. The predicted size for detected QTL interval was rather large and not suitable for marker assisted selection (MAS) and / or map-based cloning (St.Clair, 2010). Once the closely linked markers are identified, they can be used for MAS. Prior to recent progresses in next-generation sequencing (NGS) technologies for rapid marker development, several approaches were used to increase the marker density of a genetic map by combining the previously generated mapping data to generate a consensus map. This method was applied by Wenzl et al. (2006) in barley and resulted into the construction of a consensus map containing 2,935 markers using the 7 DH and 3 RIL populations. They combined the generated DArT (Diversity arrays technology) markers data with previously mapped SSR (Simple sequence repeats), RFLP (Restriction Fragment Length Polymorphism), STS (sequence-tagged site) markers and loci influencing some agricultural traits. In another study, Stein et al. (2007) integrated the marker data (RFLP, SSR, SNP) from three DH mapping populations with prior data from 200 anchored markers to produce a 1,255 marker barley consensus map. Moreover, Varshney et al. (2007) generated a 775 SSR consensus map in barley by combining six independent genetic maps derived from different bi-parental populations. Although the integration of several genetic maps helped to generate a highly saturated genetic map, non-uniform data quality and high number of missing data made the consensus map construction a challenging and complicated approach.

NGS provides the possibility of cost-effective high-throughput *de novo* SNP discovery within the genome and parallel genotyping (Deschamps and Campbell, 2010). Multiple individuals can be rapidly sequenced with low cost and the detected SNPs can easily be converted into individual molecular markers for further application or directly used in high-density linkage map construction (Ruperao and Edwards, 2015). However, for crops with medium to large genomes, where much of the sequence is repetitive and the proportion of gene space is limited, a reduced-representation strategy is a practical alternative in sequencing which significantly improves cost effectiveness. In addition, sequencing the whole genome of every individual in a population is often unnecessary, when many biological questions can be answered using polymorphisms that are measured in a subset of genomic regions (Davey et al., 2011). Genotyping by sequencing (GBS) is based on the reduced-representation strategy using restriction digestion followed by direct sequencing the ends of a size-selected restriction fragment (Figure 4a). It is an efficient

method for discovering thousands of SNPs which can be directly used for high density linkage map construction (Elshire et al., 2011a; He et al., 2014a). Using GBS on bi-parental DH populations, Poland et al. (2012) genetically mapped 20,000 and 34,000 SNPs in wheat and barley, respectively. This strategy was shown to be efficient for genotyping a variety of species, including rice (Spindel et al., 2013), maize (Chen et al., 2014), oat (Huang et al., 2014) and other species. More recently, Chaffin et al. (2016) constructed a hexaploid oat high-density consensus linkage map consisting of 7,202 markers using GBS-derived SNPs on the progeny of 12 bi-parental RIL populations. The linkage groups from all mapping populations were individually constructed and compared to determine the conserved clusters. Later on, the linkage groups of each cluster combined into consensus chromosomes.

A second approach to reduce the complexity of the genome is the application of targeted enrichment strategies like an exome capture assay, which is a hybridization-based method designed to capture the exons of annotated genes (the ‘exome’) before sequencing (Bamshad et al., 2011) (Figure 4b). Since targeted sequencing is completely focused on specific regions, the overall costs per genome will be dramatically reduced, allowing high coverage depth of targets and as a consequence, the accurate variant and genotype calling (Mascher et al., 2014). It has been used in whole genome sequencing (WGS) of complex genomes like wheat and barley. Winfield et al. (2012) identified more than 350,000 putative SNP variants between the homoeologous genomes, A, B and D sub-genomes. However, in order to generate high-quality sequence data, the high sequence coverage (at least 30×) at the position of SNP variants was required since the wheat reference genome was not yet completed. Without such high rates of coverage, it was highly probable that many of the SNPs would be false and could lead to a considerable waste of effort in the failed validation experiments. Mascher et al. (2014) presented that exome capture on a subset of mutant and wild-type individuals in conjunction with bulked segregant analysis (BSA) was an appropriate approach to identify causative mutations in barley. However, this approach might suffer from the risk of missing causative gene in the design of capture probes whereas with WGS, all genome data will be obtained (Warr et al., 2015). Regardless of sequencing costs, the integrated approaches through combining the WGS and whole exome sequencing (WES) would be highly useful for variant discovery studies, as WES provides additional variants missed in low-coverage dataset (Belkadi et al., 2015; Warr et al.,

2015). An additional efficient method to rapidly and efficiently map genes under QTLs is BSA and RNA-sequencing, providing the capability to identify differentially expressed genes as well as SNPs different between the pools (Liu et al., 2012).

Although, construction of a genetic linkage map is a foundation for identification of genomic loci linked to phenotypic variants, the resolution of a genetic map depends on the number of recombination events occurring in meiosis (Liu, 1998). Hence, the high resolution mapping of the locus of interest is the key step in the process of isolating a gene of interest. In principal, the more individuals used for mapping, the more precise will be the resulting map. Map-based cloning relies on meiotic recombination events that are not uniformly distributed throughout the genome, Instead, the frequency of crossovers varies from centromeric to telomeric region (Mascher et al., 2017). Accordingly, for the required genetic resolution, a large number of meiotic events might be necessary to identify recombination events in close proximity to the gene. Thus, high resolution mapping starts with increasing the size of population and screenings of entire population with initially identified closely linked DNA markers to identify recombinants at the corresponding locus interval. This may require the development of further markers in the target interval (Lahaye et al., 1998; Ling et al., 2003; Pelliio et al., 2005). Prior to the release of barley reference genome, the mapping procedure was typically being continued until two markers flanking the gene of interest hit a single bacterial artificial chromosome (BAC) clone, so-called “chromosome landing” (Tanksley et al., 1995) and if it had not occurred, chromosome walking was principally required to identify the overlapping BAC clones and construct the physical contig spanning the target interval. Using sequence information of the BAC ends, the BAC library was being screened to identify the next adjacent overlapping BAC clone (Stein and Graner, 2004). Depending on the size of the gap required to being covered, this procedure was a laborious and time consuming task. However, by the construction of the barley reference genome and accessibility to the sequence data, there is no need for to invest further efforts into chromosome landing and chromosome walking. It is only required to find recombination events at the target interval until reach to a single candidate gene which is directly flanked by the closest markers (Gupta and Varshney, 2013). A part of barley genomic resources will be explained in following section.

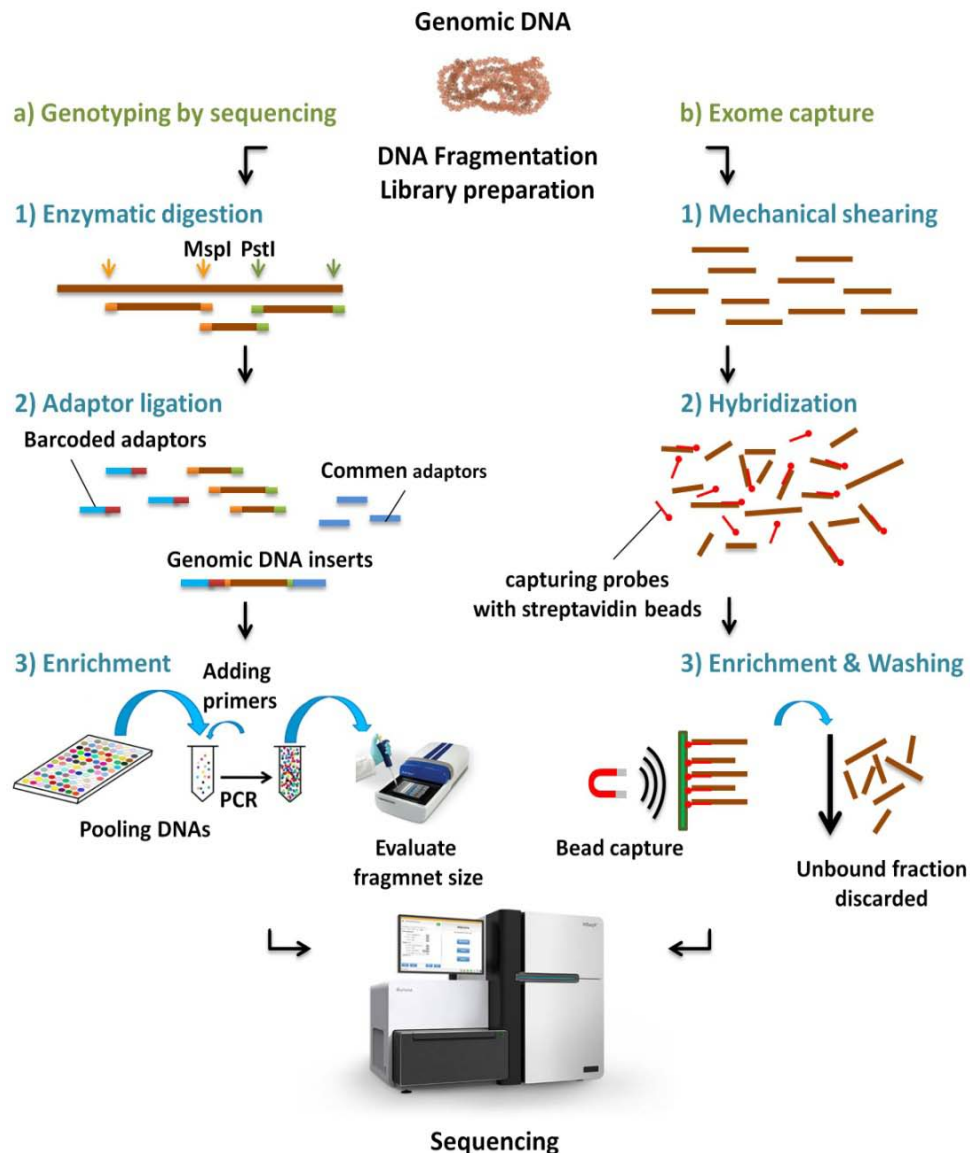


Figure 4: Schematic representation of the basic process of genotyping by sequencing and exome capture enrichment assays.

The gDNA extracted fragmented either by restriction enzymes or by mechanical shearing into small fragments to construct the genomic library. a) GBS libraries were prepared by ligating the digested DNA to unique nucleotide barcoded and common adaptors in 96-plex, followed by PCR amplification. A size selection is conducted prior to sequencing. b) exome capture: biotinylated oligonucleotide probes (baits) are used to selectively hybridize to target regions in the genome. Magnetic streptavidin beads are used to bind to the biotinylated probes, the non-targeted portion of the genome is washed away and PCR is used to enrich the sample for DNA from the target region, followed by sequencing (modified from Bamshad et al., 2011 and Elshire et al., 2011a).

1.8 Barley genomic infrastructure

The diploid nature of barley ($2n=14$) with high degree of inbreeding along with the ease of making genetic crosses, make this crop a favorable biological model for genetic and genomic studies (Saisho and Takeda, 2011). During the last two decades, comprehensive barley genomic resources have been developed that facilitate the analysis of the barley genome. A number of high density genetic maps including consensus maps from different mapping populations were developed (Wenzl et al., 2006; Varshney et al., 2007; Stein et al., 2007; Muñoz-Amatriaín et al., 2011) which are being utilized for various QTL discovery in barley (Szűcs et al., 2009; Sharma et al., 2011). Recent innovations in DNA sequencing technology facilitated the dissection of many genetically and biologically important complex traits in barley. In addition, the newly developed genome complexity reduction approaches like GBS and exome capture re-sequencing increased the efficiency of SNP discovery (Bamshad et al., 2011; Winfield et al., 2012; Poland et al., 2012; Mascher et al., 2013b) and marker development for gene identification in high resolution mapping and map-based cloning in barley (Silvar et al., 2012, 2013). In 2004, the first comprehensive oligonucleotide array, 22 K Barley 1 GeneChip, was designed for barley as a model for plants (Close et al., 2004). The array content was derived from 350,000 high-quality barley expressed sequence tags (ESTs) derived from 84 cDNA libraries representing various developmental stages. This has been widely used for barley genome analyses such as the construction of microarrays and DNA marker generation. Furthermore, a handful of BAC libraries from different barley cultivars have been generated which have been widely used for map-based cloning and barley physical map construction (Yu et al., 2000; Isidore et al., 2005; Saisho et al., 2007; Shi et al., 2010; Schulte et al., 2011; Yeo et al., 2016). The first BAC library was generated from a North American six-rowed malting cultivar 'Morex' with 313,344 gridded clones (6.3-fold haploid genome coverage (Yu et al., 2000). The cultivar 'Morex' was chosen because of its importance as a malting cultivar, but more importantly because of its resistance to several barley pathogens (spot blotch and certain races of stem rust). The construction of the BAC library was primarily intended for supporting gene isolation in barley. Likewise, two other libraries have been created, one from 'Cebada Capa', which is a leaf rust-resistant barley cultivar (Isidore et al., 2005) and one from the Japanese malting barley cultivar 'Haruna Nijo' (Saisho et al., 2007). This cultivar has been extensively used as a foundation genotype of current Japanese

breeding. A fourth library was constructed from a DH barley line ‘CS134’ which has boron tolerance, sodium exclusion, high grain zinc content and derived from the cross between the Australian malting variety ‘Clipper’ and the Algerian landrace ‘Sahara 3771’ (Shi et al., 2010). More recently another two non-gridded BAC libraries from cultivar ‘Vada’ and line ‘SusPtrit’ were constructed, which will allow the isolation of genes for partial and non-host resistances to rust and powdery mildew (Yeo et al., 2016). However, before the barley draft genome sequence became available, the efficiency of map-based gene isolation was rather limited by the lack of a complete physical map or a reference genome sequence. In 2012, the initial physical map-based barley draft genome sequence was completed through high information content fingerprinting and contig assembly of 571,000 BAC clones originating from six independent BAC libraries of cultivar ‘Morex’ (IBSC, 2012). In order to improve the genetic anchoring of the released barley sequence assembly, POPSEQ data (sequencing data derived for a segregating mapping population) was generated for genetically anchoring and ordering of *de novo* NGS assemblies (Mascher et al., 2013a). To come closer to barley sequencing consortium aim, barley physical genome maps was constructed by single-molecule optical mapping and chromosome conformation capture sequencing (Hi-C); aiming to assemble a contiguous sequence scaffolds representing the seven barley chromosomes (Mascher et al., 2017; Beier et al., 2017). These genomic resources facilitated gene isolation in map-based cloning of different barley genes e.g. genes controlling spike morphology (Poursarebani et al., 2015; Jost et al., 2016; Koppolu et al., 2013; Youssef et al., 2016) and continues to support the contextualization of sequence and comparative analysis of genome composition in barley with other *Triticeae* species, especially in non-recombining regions (Mascher et al., 2013b; Pfeifer et al., 2013; Zeng et al., 2015). A variety of recently developed web-based systems hosting barley genome and genomic data are freely accessible: IPK Blast Server (IBSC, 2012), MIPS PlantsDB (Nussbaumer et al., 2013), Ensembl Plants (Kersey et al., 2010, 2016) and Barlex (Colmsee et al., 2015). The latter is an integrated web-based database that accelerates the access to all developed genomic infrastructure in barley. It is a comprehensive database centered on the genome-wide physical map of barley (Colmsee et al., 2015).

1.9 The aims of this study

This study built on previous unpublished work of the Pathogen Stress Genomics research group of IPK Gatersleben towards mapping of putative powdery mildew resistance loci in barley. An initial collection of ~200 *Bgh* resistant barley accessions (available at the IPK Gatersleben genebank, (Meyer and Lehmann, 1979) were previously phenotyped *via* detached leaf assay (DLA) at the seedling stage during the years 2010-2011. The phenotyping was based on screening with seven modern, highly virulent isolates, three European [78P, D12-12 and CH 4.8] and four Israeli isolates [35, 69, 148 and 289] and revealed 35 resistant accessions, at least, to one of the tested isolates (Appendix 1). ‘HOR2573’, an Ethiopian landrace, was among the resistant accessions and was used to cross to ‘Morex’ which was susceptible to the tested *Bgh* isolates. An F₂ population was developed and served as starting material for genetic mapping. Among all seven modern *Bgh* isolates tested on parents, the isolate CH4.8 was selected for resistant scoring of F₂ segregating population. The phenotyping of F₂ generation was performed at the seedling stage *via* DLA in year 2012-2013. The population was genotyped by using a panel of 384 highly polymorphic SNP markers and an initial QTL analysis revealed two QTL for resistance to powdery mildew; a small QTL on 1HS and a strong one on 2HL. The position of the major QTL on 2HL coincided with the interval of previously reported barley powdery mildew resistance QTL at chromosome 2HL (Schweizer and Stein, 2011). Thus, the main objective of my thesis work was to perform high resolution genetic mapping of the identified QTL conferring resistances to powdery mildew in the barley RIL population ‘HOR2573 x Morex’ followed by physical delimitation of the target interval for the identification of potential candidate genes for powdery mildew resistance. To reach the study’s milestones, the following goals were pursued:

1. Comparison of the detected QTL conferring resistance to powdery mildew in different generations (F₂ and F₂S₅) of the barley mapping population;
2. High resolution QTL mapping;
3. Physical mapping of the interval of interest, by taking advantage of barley physical map resources;
4. Identification of potential candidate genes in the target interval;
5. Physical delimitation of the locus in a *Bgh* resistant genomic background by taking the advantage of availability of cultivar ‘Vada’ BAC library.

2 Materials and methods

2.1 Plant material

The F₁ plants derived from the cross between ‘HOR2573’ and ‘Morex’ were self-pollinated to produce an F₂ population, from which single seed descent was conducted and 95 F_{2:7}-derived lines were established as the RIL population of ‘HOR2573 × Morex’. The seed material of the RIL population was provided by the group of Pathogen Stress Genomics, IPK Gatersleben, Germany.

2.2 Phenotyping and experimental design

In order to assess reproducibility of powdery mildew disease scoring of the F₂S5 RIL mapping population, the phenotyping of the entire population was performed in three independent experiments. Within each experiment, eight seeds per RIL line were sown as eight biological replicates. Phenotyping was done 14 days after sowing using the second seedling leaf in a detached leaf assay. For this purpose, the plants were grown in trays at 17-20°C under long day conditions (16 h) in the greenhouse. The middle part of the second leaf was cut into two pieces (each 3 cm in length). These two leaf segments were considered as technical replicates for all lines in all three independent experiments. Detached leaves were placed surfaces upward in four-column plates on water agar (1%) containing benzimidazole (40 mg/l) as senescence inhibitor. In each column of one plate, five RILs were allocated randomly in combination with both positive (susceptible parent) and negative (resistant parent) controls. The prepared plates were inoculated with isolate CH4.8 at a spore density of 20–30 conidia mm⁻² under the inoculation tower. The inoculated detached leaves were kept in the incubator growth chamber under standard condition (with 20°C, 60% humidity, 16:8 photoperiod) and scored macroscopically at 7 days post inoculation (dpi). The disease intensity was rated based on infection area (%) according to Kølster et al. (1986) and Mains and Diktz (1930). Based on the infection area, the rating scores were finally grouped into two groups of resistant and susceptible. Plants included in the first two classes (class 1 and 2) with less than 25% leaf infection area were considered as resistant, while those included in classes 3 and 4 with leaf infection area $\geq 25\%$ were considered as susceptible.

2.3 Preparation of genomic DNA

Plant material for DNA extraction was grown under standard greenhouse conditions (16h day / 8h night, 20°C). Young leaves at 2-leaf stage were sampled and immediately transferred into liquid nitrogen. Different DNA isolation methods were used as described below.

2.3.1 Cetyltrimethyl Ammonium Bromide (CTAB)-based DNA isolation

For obtaining DNA yields higher than 20 µg, DNA was extracted using the modified cetyltrimethylammonium bromide-based (CTAB) method as described by Stein et al. (2001). In brief, the fresh leaves from 14 days old barley seedling were collected in 2 ml tubes (Sarstedt AG and Co. Nümbrecht, Germany) with a stainless steel ball (3.175 mm diameter) and immediately transfer to liquid nitrogen. The frozen leaves were ground using a mixer mill (Retsch, MM400, Germany) at 30 Hz frequency for 1 min to fine powder. Pre-warmed (65°C) CTAB extraction buffer was added to each tube and mixed properly. Once the samples were incubated for 30 min at 65°C, 800 µl of ice-cold (-20°C) Chloroform:Isoamylalcohol (24:1) was added to each sample and again incubated for 20 min at room temperature (RT, 20-25°C) in a REAX 2 overhead shaker (Heidolph, Schwabach, Germany). The tubes were centrifuged at 13,000 rpm (4°C) for 20 min. After centrifugation, the supernatant was transferred to a new 1.5 ml tube and treated with 5 µl RNase A [1,000 U/ml] (Carl Roth GmbH + Co. KG, Karlsruhe, Germany) for 15 min at 37°C. The DNA was precipitated by adding 570 µl isopropanol (-20°C) through inverting the tube until it well mixed. To pellet the DNA, centrifugation was done for 15 min (13,000 rpm, 4°C). A white pellet was clearly visible at this stage. The liquid phase was carefully removed as the pellet is loosely attached to the wall of the tube. For washing step, 1 ml of wash solution I (76% Ethanol, 200 mM Sodium acetate) was added to the samples and then samples were incubated on ice for 10 min. Following inoculation, the supernatant was carefully removed. The washing step continued by adding the wash solution II (76% Ethanol, 10 mM Ammonium acetate) and incubation time of 5 min on ice. It is necessary that all wash solution is completely removed. The pellet dried under a fume hood at RT. At the end, the DNA pellet was dissolved in 80 µl TE buffer (10 mM Tris / HCl pH 8.0, 1 mM EDTA).

2.3.2 Guanidine thiocyanate-based DNA isolation

For each sample, 6 cm fresh leaf material was placed in 1.1 ml 8-strip mini tubes in racks (96-well racked collection microtubes, Qiagen, Hilden, Germany) containing two 4 mm glass beads (Carl Roth GmbH + Co. KG, Karlsruhe, Germany) and frozen immediately with liquid nitrogen. The frozen leaf material was ground with a mixer mill (Retsch MM400, Germany) for a minimum of 1 minute at 30 Hz frequency. To remove the powder from the lids, a short spin with maximum speed was done. 600 µl of 65°C of preheated-extraction buffer (1M Guanidine thiocyanate, 2M NaCl, 30 mM Sodium acetate pH 6.0, 0.2 % Tween20) was added to each tube. The rack was shaken vigorously with a mixer mill (Retsch MM400, Germany) for a minimum of 1 minute at 30 Hz frequency until the solution homogenized completely. The rack was then incubated for at least 30 minutes at 65°C followed by centrifugation at 4,000 rpm at 10°C for 30 min. 480 µl of the supernatant was transferred to a 96-well acroprep advance filter plates (Thermo Fisher Scientific, Germany) followed by vacuum step with a vacuum manifold for 96-well plates. Once the well was empty, the pump was stopped and 900 µl of wash buffer (50 mM NaCl, 10 mM Tris / HCl pH 8.0, 1 mM EDTA, 70% ethanol) was added. Vacuum was re-applied and the washing step was repeated for a second time. The vacuum was maintained for 30 seconds after all wells were completely emptied. The 96-well acroprep advance filter plates were placed onto a Greiner 96-well standard microtiter plate (Thermo Fisher Scientific, Germany) and spun at 3,500 rpm for 3 min in order to remove the excess wash solution. The AcroPrep Advance plate was then placed onto a new NUNC 96-well plate (Thermo Fisher Scientific, Germany) and 100 µl of 65°C preheated TE light elution buffer (0.1 mM EDTA, 10 mM Tris / HCl pH 8.0) were added to each well. After 5 minutes, the plates were spun for 10 min at 3,500 rpm to elute the DNA.

2.4 Assessment of genomic DNA quality and quantity

2.4.1 Genomic DNA Quality through gel electrophoresis

To check the quality and concentration of extracted DNA samples through gel electrophoresis, 1% agarose (Invitrogen, Carlsbad, California, United States) in 1×TBE buffer (89 mM Tris, 89 mM Boric acid, 2 mM EDTA pH 8.0) was prepared. The concentration of DNA samples was

compared to a dilution series (50-250 ng) of standard λ -DNAs (Fermentas GmbH, St. Leon-Rot, Germany).

2.4.2 Genomic DNA Quantity through Qubit Fluorometer

The Qubit[®] Fluorometer enables a greater sensitivity and accuracy compared to UV absorbance measurements. The fluorescent dyes emit signals only if bound to specific target molecules, DNA, RNA and proteins. It is generally considered useful for checking genomic DNA quantitation before e.g. sequencing for small number (≤ 20) of samples. The DNA concentrations were measured using Qubit[®] 2.0 Fluorometer (Invitrogen, Carlsbad, California, United States) according to the manufacturer's protocol. The broad range (BR) Assay Kit (2-1000 ng) was used to quantify concentrations. In brief, a Qubit[™] working solution was prepared by diluting the Qubit[™] dsDNA BR reagent in Qubit[™] dsDNA BR buffer according to ratio 1:200 and kept in dark condition. To prepare both standard and isolated DNA samples for DNA quantification, 10 μ l of each standard DNA (standard 1: 0 ng/ μ l, standard 2: 100 ng/ μ l) and 1 μ l of each extracted DNA were mixed with 190 and 199 μ l of Qubit[™] working solution, respectively. All samples including the DNA standards were mixed thoroughly and centrifuged briefly to remove any bubbles. The DNA concentration of the samples was then measured using the Qubit[®] 2.0 Fluorometer.

2.4.3 Genomic DNA Quantity through Picogreen

For accurate DNA quantification for high number of samples (e.g. 20-20,000 samples) Quant-iT[™] PicoGreen[®] dsDNA assay kit (Invitrogen, Carlsbad, California, United States) and a Synergy HT microplate reader (BioTek, Bad Friedrichshall, Germany) were used. The assay is an ultra-sensitive fluorescent nucleic acid stain and well-adapted to high-throughput use, normally in a 96-well or 384-well plate. Before starting the experiment, an aqueous working solution of the Quant-iT[™] PicoGreen[®] reagent (component A) and λ DNA standard (component C) were kept in dark condition at room temperature for 10 minutes. Then a serial dilution of λ DNA standard ranging from 0.0 to 2000 ng/mL was made using TE (10 mM Tris, 1 mM EDTA, pH 7.5) and 50 μ l of aliquots was pipetted into the first two columns of a 384-well microplate (From A1 to P2). One column was kept empty (column 3) and then 50 μ l of diluted experimental DNA solution (1:500) in TE was loaded to each remaining wells (from column four onward). Meanwhile,

PicoGreen reagent was prepared by diluting the concentrated dimethyl sulfoxide (DMSO)-PicoGreen stock solution, provided in the PicoGreen kit, 1:200 with TE according to the kit instructions. 50 µl of PicoGreen reagent was added and mixed to all wells containing λDNA standards and experimental DNAs. Following incubation, the plate was briefly centrifuged to collect samples. The fluorescence was determined using a Synergy HT microplate reader. With filter-based measurements, the reader used a 485 nm, 20-nm bandwidth, excitation filter and a 528 nm, 20-nm bandwidth emission filter along with a 510 nm cutoff dichroic mirror. The auto-scale function optimizes the scale of the spectrum automatically during measurement.

2.5 Marker development and primer design

The cleaved amplified polymorphic sequence (CAPS) assay is a molecular DNA marker technology. In this method, the DNA fragments containing SNP(s) will be amplified through Polymerase chain reaction (PCR) and will be digested by a proper restriction endonuclease (RE), whose recognition sequence has been introduced by the SNP. Once the single nucleotide polymorphisms (SNPs) between resistant and susceptible genotypes were identified through GBS or exome capture assay, the corresponding sequences were utilized by SNP2CAPS software (Thiel et al., 2004). This software facilitates the computational conversion of SNPs into CAPS markers and assists to differentiate resistant and susceptible alleles based on fragment size polymorphism.

Primers used for marker development were designed using the online software Primer3 v. 0.4.0 (<http://bioinfo.ut.ee/primer3-0.4.0/>) (Koressaar and Remm, 2007; O'Halloran, 2015). Default parameters were used with minor modifications. Guanine-cytosine content (GC-content) was set within the range of 50-55% and the product size was adjusted according to the experimental requirement between 300-1000bp. The primer length was set between 19-21 bp and primer melting temperature (T_m) was adjusted around 60°C. In brief, the digestion reaction was performed in a 10 µl volume containing 5 µl of PCR product, 1 µl of appropriate 10× buffer (New England Biolabs, Hitchin, UK), 1 unit of enzyme (New England Biolabs, Hitchin, UK) and adjusted to final volume by adding ddH₂O. The reaction mix was incubated for one hour at recommended incubation temperature.

2.6 Polymerase chain reaction (PCR)

The DNA amplification was performed on GeneAmp PCR Systems 9700 (Applied Biosystems, Darmstadt, Germany). The reaction master mix was prepared in a total volume of 20 μ l containing of 2 μ l 10 \times PCR buffer [Tris-CL, KCL, (NH₄)₂SO₄, 15 mM MgCl₂] (Qiagen, Hilden, Germany), 2 μ l dNTP Mix [2 mM of each dNTP] (Fermentas, Fermentas, St. Leon-Rot, Germany), 1 μ l of each Primer [10 mM], 0.1 μ l Hot star *Taq* polymerase [5 units/ μ l] (Qiagen, Hilden, Germany) and 1 μ l DNA template [20 ng/ μ l] and filled up with double-distilled water to reach to the total volume. All DNA amplification reactions were done through a standard touchdown PCR profile consisting of two steps: initial denaturation for 15 min at 95°C, followed by four cycles of denaturation at 95°C / 30 s; annealing at 62°C / 30 s (decreasing by 1°C per cycle) followed by extension at 72°C / 60 s); then 35 cycles denaturation at 95°C / 30 s, annealing at 58°C / 30 s, and extension at 72°C / 60 s followed by a final extension step at 72°C / 7 min. Based on amplicon's length, the extension time was modified (1 min / 1 kb). The PCR-amplified products were resolved by 1.5-2.5% gel-electrophoresis based on the expected amplicon size. In General, 1.5% (w/v) agarose gel was prepared by melting 1.5 g of UltraPure™ Agarose (Invitrogen, Carlsbad, California, United States) in 100 ml of 1 \times TBE buffer (89 mM Tris-borate, pH 8.3; 2 mM Na₂EDTA) (Sambrook et al., 1989). The gel was run in an electrophoresis chamber (Bio-Rad Laboratories GmbH, Munich, Germany), the running buffer (1 \times TBE buffer) was added to chamber with a depth of 3 mm over the surface of the gel. The voltage gradients were adjusted based on the distance between the electrodes. For visualization of DNA molecules, the gel was stained by adding ethidium bromide (EtBr) to 0.5 μ g/ml final concentration.

2.7 Purification of PCR products for cycle-sequencing

PCR products were purified using the NucleoFast 96 PCR Kit (Macherey-Nagel, Germany) according to the manufacturer's instructions. In brief, the total volume for each PCR tube was adjusted to 100 μ l with nuclease-free water and loaded directly onto the NucleoFast® 96 PCR filter membrane. Then a vacuum was applied to collect the PCR product on the surface of the ultrafiltration membrane while contaminants were filtered to waste. Additional 100 μ l of nuclease-free water was added to the samples and repeated the vacuum step. The purified PCR product was recovered directly from the membrane using Recovery Buffer by using 10 min shaking on Titramax 100 (Heidolph Instruments GmbH, Schwabach, Germany) and transferred

into new 96-well plate (Fisher Scientific GmbH, Schwerte, Germany). The concentration of purified PCR products was determined visually by agarose gel electrophoresis by comparison with defined dilution series (1 µg-100 ng) of λDNA (Fermentas GmbH, St. Leon-Rot, Germany).

2.8 Sequencing and data analysis

2.8.1 Sanger sequencing of PCR amplicon

Sanger sequencing was performed in-house at the Genome Center, IPK Gatersleben, Germany. Data were generated through cycle sequencing with BigDye Terminator (BigDye[®] Terminator v3.1, Applied Biosystems, Darmstadt, Germany) chemistry using purified PCR products as template according to the manufacturer's instructions. Samples for sequencing were prepared in a total volume of 10 µl including 5 µl of purified PCR product with normalized concentration (ca. 10 ng/100 bp) as well as 1 µl of forward/reverse primer (5 µM each) and 4 µl BigDye Premix.

2.8.2 Genotyping by Sequencing (GBS)

Prior to library preparation, the genomic DNA was quantified using PicoGreen (Invitrogen, Carlsbad, California, United States) and normalized to 20 µl of 10 ng/µl (200 ng total) in 96-well plates. Genomic DNA (200 ng) was digested with a combination of two restriction enzymes, *Pst*I-HF (CTGCAG, NEB Inc., Ipswich, UK) and *Msp*I (CCGG, NEB Inc.) The digestion reaction was prepared in a total volume of 20 µl, consisting of 10 µl genomic DNA (200 ng), 10× NEB buffer 4 and 10× BSA (NEB Inc.). For direct downstream adapter ligation (without additional purification steps), the samples were incubated at 65°C for 20 min to inactivate any restriction enzymes. Adapter ligation and following adapter fill-in were done according to Meyer and Kircher (2010). Eight microliters of eluted DNA solution was used for the indexing PCR, which was done in 50 µl volume with a final concentration of 1× Phusion HF buffer, 2 mM each dNTP, 200 µM primer IS4_indPCR.P5 (Meyer and Kirchner, 2010), 200 µM indexing primer and 0.02 U/µl Phusion Hot Start Flex (NEB Inc., Ipswich, UK). The amplification was done with initial incubation at 98°C for 30 s followed by 16 cycles amplification (98°C for 10 s, 60°C for 30 s, 72°C for 5 s) and a final extension step (72°C, 10 min). The PCR products were purified by using Carboxyl-coated magnetic beads (SPRI beads) and then eluted in 25 µl elution buffer. The DNA concentration was measured using the Quant-iT PicoGreen dsDNA assay kit (Life Technologies GmbH) and a Synergy HT microplate reader (BioTek, Bad Friedrichshall,

Germany). Afterwards, the indexed samples were pooled together in equimolar ratios. For size selection, 500 ng pooled DNA was size fractionated electrophoretically using a 2% agarose gel (Invitrogen, Carlsbad, California, United States) and SYBR Gold (Invitrogen, Carlsbad, California, United States) staining. The DNA fragments with a size of 150-600 bp were recovered from the gel using a MinElute Spin column according to the manufacturer's instructions (Qiagen, Hilden, Germany). For quality control of DNA, the GBS library was analyzed with an Agilent 2100 Bioanalyzer (Agilent Technology, Santa Clara) using the Agilent High Sensitivity DNA kit. Finally, the quantification control of the library was performed using qPCR according to Mascher et al. (2013b). The concentration was determined based on the standard curve and the average size of the GBS library.

2.8.3 Exome capture sequencing

Exome capture re-sequencing was done on homozygous RILs comprising a recombination within the 2HL powdery mildew resistance QTL interval. The construction of exome capture libraries and sequencing were done based on previously established procedures (Mascher et al., 2013b). In brief, the genomic DNA (1 µg) was mechanically sheared to 200-300 bp fragments by using ultra sonication with the CovarisTM S220 Sonicator (Covaris Inc., Woburn, MA, USA), with following settings: 175W Peak Incident Power, Duty Factor 10%, 100 seconds treatment time and 200 cycles per burst. Size selection was controlled with Agilent High Sensitivity DNA Assay on Agilent 2100 Bioanalyzer (Agilent Technologies, Santa Clara, CA, USA). Sequencing library preparation was performed with Illumina TruSeq DNA Sample Preparation Kit (Illumina, San Diego, CA, USA) according to the manufacturer's instructions. Adapter ligated DNA products were selected according to their size (320-420 bp) by excision from a SYBR-Gold stained agarose gel. Correctly ligated DNA fragments were enriched using a pre-capture LM-PCR reaction (ligation-mediated PCR) and purified as described by Mascher et al. (2013b). The concentration of the adapter ligated DNA was determined with Qubit[®] dsDNA HS (High Sensitivity) Assay (Invitrogen, Carlsbad, CA, USA) according to the manufacturer's protocol (described in 2.4) and analyzed using an Agilent 2100 Bioanalyzer (Agilent Technology, Santa Clara) on a DNA 7500 chip (between 250 and 500 bp). The hybridization of the amplified sample library was only continued if the amount of the library was higher than 1 µg and the obtained fragment size in a range between 250 and 500 bp. 10 µl of Sequence Capture Developer Reagent

(Roche, Indianapolis, IN, USA) were added to 1 μg of the amplified library just before hybridization. Adding 1 μl of the TruSeq HE Universal Oligo 1 (1 mM) to 1 μl of the appropriate TS-INV-HE Index Oligo (1 mM) blocks the universal segment of TruSeq DNA library adapters during the sequence captures hybridization. The TS-INV-HE Index Oligos were blocked the corresponding indexed segment of the TruSeq DNA library adapters. After drying the mixture in a SpeedVac at 60°C, 7.5 μl 2 \times Sequence Capture (SC) Hybridization Buffer and 3 μl Hybridization Component A were added to each dried sample. The hybridization cocktail was mixed for 10 s, collected by short spin centrifugation and denatured in a heating block (95°C, 10 min). Samples were transferred to 0.2 ml PCR tubes and mixed gently with 4.5 μl exome Library. The incubation of hybridization mixture (15 μl) was done in a thermocycler for 64-72 h at 47°C.

Before use, the provided NimbleGen SC Wash Buffers, the Bead Wash Buffer and Stringent Wash Buffer were diluted to 1 \times working solutions (Roche, Indianapolis, IN, USA). Streptavidin Dynabeads (M-270, Invitrogen) were fully mixed, added (50 μl per hybridization) into 1.5 ml tubes. For purification step, tubes were placed in DynaMag-2 magnet (Invitrogen) until liquid became clear. Following, the supernatant was discarded and 100 μl of Bead Wash Buffer were added. Tubes were vortexed again, placed back in the DynaMag-2 magnet, the buffer was removed, and the washing was repeated. Afterwards, Dynabeads were re-suspended in Bead Wash Buffer (50 μl), transferred into PCR plates. After removing buffer, the hybridization sample was added to the Dynabeads and mixed gently. The captured sample was bound to the Dynabeads by inoculation in a thermocycler (lid heated to 57°C) at 47°C for 45 min. The sample was vortexed for 3 s in every 15 min to make sure that the Dynabeads remained in suspension. Following hybridization of the DNA to the Dynabeads, 100 μl preheated SC Wash Buffer I (47°C for 2 h) was added and vortexed for 10 s. The suspension was transferred to a 1.5-ml tube and placed in the DynaMag-2 magnet. The supernatant was discarded once it became clear. Washing was continued by adding 200 μl pre-heated Stringent Wash Buffer (47°C for 2 h). During the incubation, the samples were mixed by pipetting. After bead purification using the DynaMag-2 magnet, the supernatant was discarded and the washing step with Stringent Wash Buffer was repeated. Purification of dynabeads plus bound DNA was re-performed using DynaMag-2 device. Again 200 μl Wash Buffer I was added and the samples were mixed thoroughly for 2 min. After magnetic separation, the buffer was removed and washing step with 200 μl Wash Buffer II and 200 μl Wash Buffer III were done as mentioned before. The bead-bound captured library was

eluted in 50 µl double-distilled water. Following affinity purification, post-capture library amplification was performed. The LM-PCR master mix was prepared in total volume of 200 µl containing 100 µl Phusion High-Fidelity PCR Master Mix (2×, New England BioLabs GmbH), 50 µl of bead-bound captured library, Illumina sequencing adapters (2 IM TS-PCR Oligo 1 and 2 IM TS-PCR Oligo 2). The master mix was divided into two 0.2-ml PCR tubes. For LM-PCR amplification cycling conditions were adjusted on: initial incubation at 98°C for 30 s, followed by 16 cycles of 98°C for 10 s, 60°C for 30 s and 72°C for 30 s. The final extension time was set for 5 min at 72°C. The combined LM-PCR products were purified using Qiaquick PCR purification kit (Qiagen, Hilden) based on the manufacturer's protocol. One ml of Qiagen PBI buffer was added to the sample and the total amount was transferred to a Qiaquick column placed in a collection tube. Centrifugation was performed at 13,000 rpm for 1 min. For washing, 750 µl Qiagen PE buffer was added to the column which was centrifuged at 13,000 rpm (1 min). The flow-through was discarded and the column re-centrifuged with the same power for 1 min. DNA was eluted by adding 50 µl preheated elution buffer (50°C), incubated for 5 min and centrifuged (13,000 rpm, 1 min). The size of captured libraries was checked electrophoretically using the Agilent 2100 Bioanalyzer (Agilent Technologies, Santa Clara, CA, USA) and a DNA 7500 chip. The size of the post capture enriched sequencing libraries was between 250-500 bp. The quantification of library was performed by qPCR according to Mascher et al. (2013b).

2.9 Genetic linkage analysis

Genetic linkage analysis was done using JoinMap[®] 4.0 software (Van Ooijen, 2006) as described by the manual's instructions. Homozygous susceptible, heterozygous and homozygous resistant allele calls were defined as a, h and b, respectively; missing data were indicated by a dash. A regression mapping algorithm and Kosambi's mapping function were selected to construct the linkage map. Markers were grouped into seven groups based on Logarithm of Odds (LOD: >5) groupings. In order to have better visualization of maps from each linkage group, MapChart software was used (Voorrips, 2002). Since the GBS reads mapped against the barley reference genome, the physical position of each SNP was defined. Therefore, all obtained SNP marker from GBS data are entitled with their corresponding physical position on the barley reference genome sequence.

2.10 Physical mapping and BAC library screening

A non-gridded BAC library of cultivar ‘Vada’ (Yeo et al., 2016) was used to identify BAC clones representing the orthologous interval corresponding to the 2HL powdery mildew resistance characterized on the basis of the ‘Morex’ reference sequence. This approach allows rapid screening of the genomic library for target clones by using a PCR-based approach. The ‘Vada’ BAC library contains 116 BAC pools, named V1 to V116; consisting of 1,435 BAC clones with estimated insert sizes between 67-98 kb.

2.10.1 Identification of positive BAC pools

The first step was to identify BAC pools containing target clones for the QTL region. This was performed through PCR with primers corresponding to flanking and co-segregating markers in the region of interest and using the plasmid DNA isolated from each pool (20-fold diluted) as template. PCR reactions were carried out in a final volume of 20 μ l. The genomic DNA of cv. ‘Morex’ and ‘HOR2573’ were used as positive controls. Amplification was checked on 1.5% agarose gel stained with EtBr. The presence of a bright band with the expected amplicon size was used as an indication that the corresponding pool was positive for the presence of the target sequence.

2.10.2 BAC monoclonal isolation

For each positive BAC pool, a sample from the stock was diluted 10,000-fold in d_0 H₂O. A 50 μ l aliquot of the dilution was added to 20 ml of lysogeny broth (LB) medium containing the selective antibiotic Chloramphenicol and was plated into a 384-well plate. The 384-well plates were incubated for 16 h at 37°C and then replicated onto square Petri dishes (144 cm²) containing solid LB medium (LBA) supplemented with 34 μ g/ml of chloramphenicol (CAM). The colonies that grew from the 384-wells (each well still containing multiple BAC clones) were column-pooled by scraping the solid media using a pipette tip and transferred to a tube containing 150 μ l of distilled water. A total of 24 column pools per plate were sampled this way, diluted 10-fold and used as template in a PCR reaction with final volume 20 μ l and cycling conditions (94°C for 5 min, followed by 35 cycles at 98°C for 10 s, 60°C for 30 s and 72°C for 30 s, and a final extension step at 72°C for 1 min). After the identification of a positive column pool, the 16 wells in that column were tested to identify the well(s) containing the target BAC clone; in this step a

10-fold dilution of the culture media was used as template in a PCR reaction of final volume of 20 μ l and by applying the same cycling conditions (94°C for 5 min, followed by 35 cycles at 98°C for 10 s, 60°C for 30 s and 72°C for 30 s, and a final extension step at 72°C for 1 min). The content of the positive well was diluted 100,000-fold and a second 384-well plate was prepared, replicated and PCR-screened as described above, except for the addition of 34 μ g/ml of CAM to the liquid LB medium. Once a positive well was identified for this second 384-well plate, its content was diluted either 10,000 or 100,000-fold, plated onto selective LBA and incubated for 16 h at 37°C. Single colonies were picked and individually transferred to tubes containing 100 μ l of selective LB medium. After a period of 16 h growing at 37°C, the culture media was used as template in a PCR reaction in final volume 20 μ l and previously mentioned cycling conditions to detect positive BAC monoclonal.

2.10.3 BAC clone sequencing

BAC clone sequencing was performed in-house at the Genome Center, IPK Gatersleben. Briefly, pooled BACs were fragmented in a microfuge by passing the DNA through the small orifice of a g-Tube (Covaris, MA, USA) twice at 5,600 rpm for 10 min and size selected using two rounds of 0.45 \times AMPure beads (Beckman Coulter, CA, USA). SMRTbell libraries were created using the 'Procedure and Checklist-20 kb template preparation using BluePippin™ Size Selection' protocol. The obtained fragments were end-repaired and then ligated to SMRT hairpin adapters using SMRT template kit. Briefly, the library was loaded on a BluePippin system (Sage Science, Inc., Beverly, MA, USA) to select the SMRTbell templates. The resulting average insert size was ~8 kb based on 2100 Bioanalyzer instrument (Agilent Technologies, Santa Clara, CA, USA). Sequencing primers were annealed to the hairpins of the SMRTbell templates followed by binding with the P5 sequencing polymerase and MagBeads (Pacific Biosciences, Menlo Park, CA, USA) and sequenced on a Pacific Biosciences (PacBio) Sequel.

2.11 Statistics of the phenotypic analysis

The three independent phenotyping experiments were treated as three environments. The phenotypic data analysis was performed using the software ASReml-R 3.0 (Butler et al., 2009). The mean infection area in each experiment (considered as environment) was used to calculate the best linear unbiased estimates (BLUEs) with the following model:

$$y_{ijmno} = \mu + g_i + l_o + (gl)_{io} + s_{jo} + p_{jmo} + c_{jmn} + e_{ijmno},$$

Where y_{ijmno} is the phenotypic performance of i^{th} genotype in n^{th} column of m^{th} plate in j^{th} inoculation tower of o^{th} environment, μ is the intercept, g_i is the effect of i^{th} genotype, l_o is the effect of o^{th} environment, $(gl)_{io}$ is the interaction between i^{th} genotype and o^{th} environment, s_{jo} is the effect of j^{th} inoculation tower in o^{th} environment, p_{jmo} is the effect of m^{th} plate in j^{th} inoculation tower of o^{th} environment, c_{jmn} is the effect of n^{th} column in m^{th} plate of j^{th} inoculation tower in o^{th} environment, and e_{ijmno} is the error of y_{ijmno} . For BLUEs estimation, only μ and g_i were treated as fixed effects and for heritability estimation, all the effects were treated as random except μ . The heritability can be calculated with the following equation:

$$h^2 = \frac{\sigma_g^2}{\sigma_g^2 + \frac{\sigma_{gl}^2}{Nr.env} + \frac{\sigma_e^2}{Nr.env * Nr.rep}}$$

The Significance test of variance components was performed. For repeatability estimation, all the effects were treated as random except μ . The repeatability can be calculated with the following equation:

$$r = \frac{\sigma_g^2}{\sigma_g^2 + \frac{\sigma_e^2}{Nr.rep}}$$

2.12 QTL analysis

The QTL analysis was performed using GenStat v16 software (VSN International, Hemel Hempstead, Hertfordshire, UK). An initial genome-wide scan was carried out by simple interval mapping (SIM) to obtain candidate QTL positions. These can be used as cofactors in subsequent scans (composite interval mapping). One or more rounds of composite interval mapping (CIM) was done, implying a genome-wide scan for QTL effects in the presence of cofactors, which were usually potential QTL positions detected at previous steps. Following back-selection from a set of candidate QTL, a final set of estimated QTL effects was obtained. The LOD significance threshold ($\alpha=0.05$) was estimated by 1000 permutation tests.

3 Results

3.1 Low resolution mapping identified a major locus for seedling stage resistance to barley powdery mildew on chromosome 2H

3.1.1 Phenotypic data analysis

Based on an unpublished study conducted by the group of Pathogen Stress Genomics, IPK Gatersleben, resistance to powdery mildew was mapped in an F₂ population derived from a cross between barley landrace accession ‘HOR2573’ and cultivar ‘Morex’. Two QTL conferring resistance to the *Bgh* isolate CH4.8 were identified; a minor QTL on chromosome 1HS and a major QTL on chromosome 2HL explaining ~27% of the phenotypic variation (Appendix 2). To verify the identified QTL and also to determine the gene underlying these QTL, an F₂S5 RIL population was developed through single seed descent and provided at start of the project. The phenotyping of the F₂S5 RIL mapping population was conducted through three independent experiments with the same *Bgh* isolate, CH4.8. Based on the previous results in the F₂ generation, the disease severity in RIL population was scored based on the estimated area covered by pathogen infection (%) according to Kølster et al. (1986) and Mains and Diktz (1930) (Figure 5). The distribution of powdery mildew disease severity for each phenotyping experiment and across all three experiments is shown in Figure 6. The infected leaf area scores ranged between 0% and 100% with an interval of 10%. Parental lines displayed the following phenotyping scores; ‘HOR2573’ with ≤2.5% and ‘Morex’ with ≥ 80% leaf infection area. The phenotyping scores on the parental lines were consistent among all the experiments.

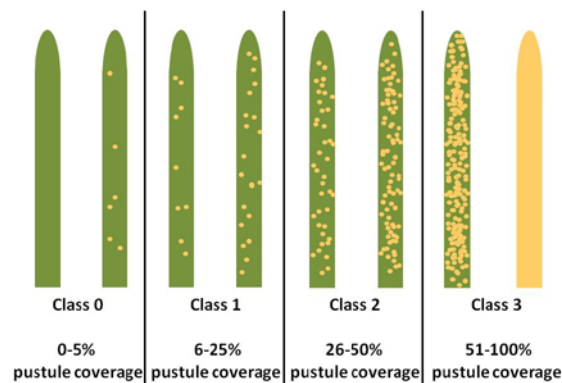


Figure 5: Schematic illustration for the quantitative classification of barley susceptibility against powdery mildew according to symptom severity.

Heritability for powdery mildew resistance was $h^2 = 0.98$ in all three independent phenotyping experiments, indicating that the most of phenotypic variation was genetically determined (Table 1). The calculated repeatability for all experiments was ≥ 0.99 , meaning that the data was highly reproducible.

Table 1: Variance component and significance across experiments.

Item	Variance component	P values	Significance
Genotype	421.3	8.42E-83	***
Exp	9.5	5.12E-02	
Geno:Exp	20.8	5.44E-02	
Plate	2.2	5.40E-02	
Column	6.4	7.51E-02	
error	125.3		
Heritability	0.98		

*, **, and *** indicate $P < 0.05$, $P < 0.01$ and $P < 0.001$ levels of probability, respectively.

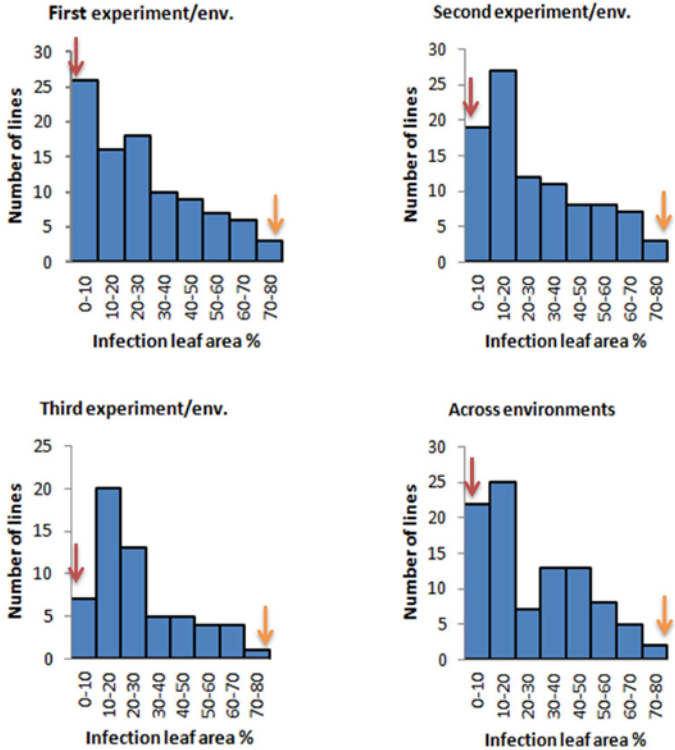


Figure 6: Distribution of powdery mildew disease severity of ‘HOR2573 × Morex’ population through three independent phenotyping experiments.

Arrows display the performance of resistant (red) and susceptible (orange) parents, respectively.

To evaluate the correlation of phenotypic measurement between each two independent experiments, the *linear correlation coefficient*, called r was calculated (Figure 7). Significant correlations were observed among all three phenotyping experiments. The values of r were 0.93, 0.91 and 0.94 between the first and second, second and third, and first and third experiments, respectively. Together with the distribution of phenotypic scores in the F2S5 population, the analysis of phenotypic data indicated very good inoculation / infection efficiency in all the three experiments. For all experiments, the resistant and susceptible parents of the population were included as negative and positive controls, respectively.

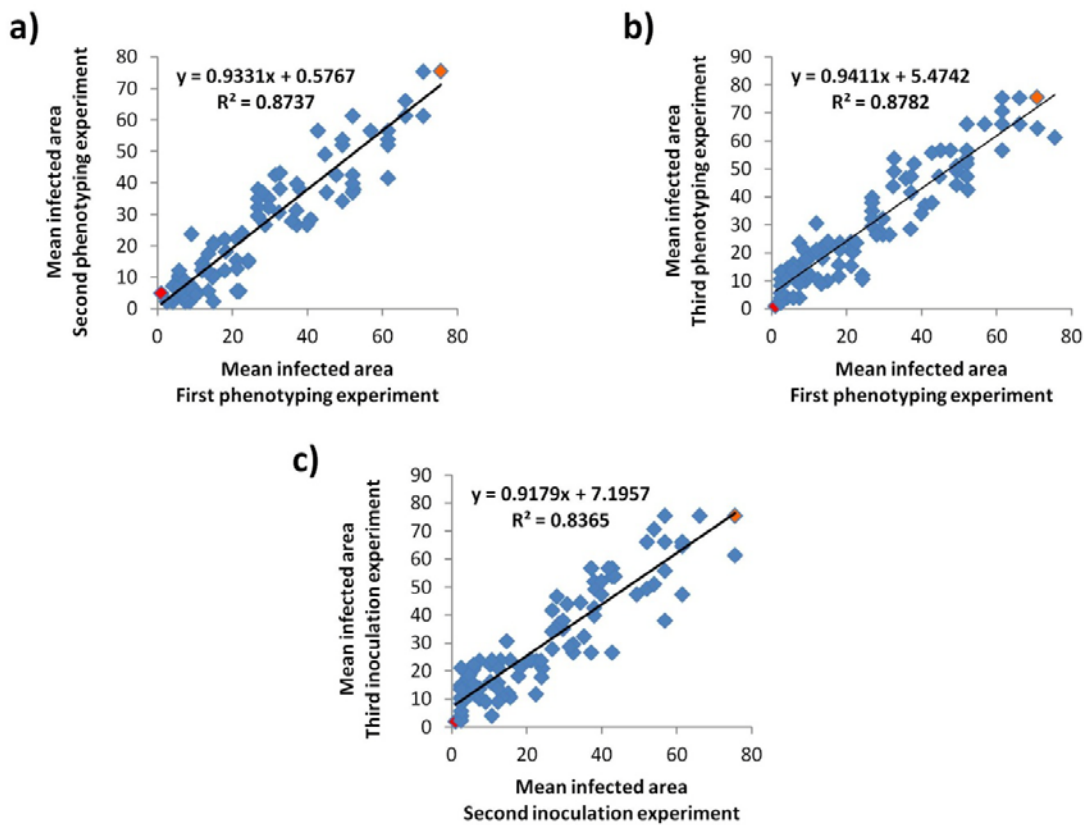


Figure 7: Performance evaluation of phenotyping scoring.

a) Scatterplot of disease scoring for experiment one versus experiment two. b) Scatterplot of disease scoring for experiment one versus experiment three. c) Scatterplot of disease scoring for experiment two versus experiment three. Red and orange dots represent the performance of resistant and susceptible parents, respectively.

3.1.2 Genotyping of the RIL population

In order to create a high density genetic map and to allocate precisely any resistance QTL segregating in the RIL population, all 95 RILs (F2S4) including parents were genotyped using the GBS approach. Genotype calls were filtered in order to select only SNPs matching the default criteria. The default parameters were defined for a RIL population by Mascher et al. (2013b), considering the expected residual heterozygosity of 1-2% in the population presented in this study. In total, 46,689 and 15,798 SNPs were obtained genome-wide at minimum sequence read coverage of two- or six-fold, respectively. Furthermore, to reduce the computational errors in JoinMap[®] 4.0, SNPs with more than 10% missing data were excluded from further analysis. This approach delivered 10,644 genome-wide SNPs at minimum two-fold read coverage with 1,843 SNPs being located on chromosome 2H (Table 2). In principle, the more sequencing coverage, the higher accuracy of variant calls will be; meaning that with higher levels of sequencing coverage, each base is covered by a greater number of aligned sequence reads. Hence, variant calls can be made with a higher degree of confidence. Therefore, a set of 1,394 genome-wide SNPs with robust variant calls (six-fold read coverage) were utilized to construct a genetic linkage map (Figure 8).

Table 2: Number of detected SNPs derived from GBS before and after filtration in two levels of read coverage.

Chromosome	SNP before filtration (Including missing data)		SNP after filtration (Missing data ≤ 10%)	
	2×	6×	2×	6×
1H	6,328	1,894	1,274	154
2H	7,196	2,771	1,843	252
3H	7,151	2,420	1,658	191
4H	5,046	1,554	1,056	137
5H	6,619	2,497	1,669	269
6H	7,153	2,030	1,341	171
7H	7,196	2,632	1,803	220
Total	46,689	15,798	10,644	1,394

The relatively high proportion of missing data in the GBS run was typical and related to the number of samples per sequencing lane.

The high-density genetic linkage map of the RIL population consisted of seven linkage groups (LOD = 5.0). Chromosome assignment of the linkage groups was accomplished on the basis of the locus coordinates determined during read mapping against the barley reference genome assembly (IBSC, 2012). The number of markers on different chromosomes ranged from 154 (1H) to 269 (5H), which were distributed evenly on each chromosome. The marker density varied from 1.1 for chromosome 4H (137 SNPs /119.7 cM) to 1.9 for chromosome 2H (252 SNPs /134.4 cM) (Table 3).

Table 3: Summary of the genetic linkage map constructed based on 1,394 SNP markers derived from GBS in the barley RIL population.

Chromosome	Markers	Ave. Marker density (N/cM)	Genetic Length (cM)	Physical Length (bp)
1H	154	1.2	130.5	555,702,863
2H	252	1.9	134.4	763,520,364
3H	191	1.3	152.0	680,094,686
4H	137	1.1	119.7	645,472,783
5H	269	1.7	161.1	663,621,891
6H	171	1.3	130.5	582,493,418
7H	220	1.3	171.8	656,152,933
Total	1,394	1.4	1000.0	4,547,058,938

The accuracy of the genetic linkage map was checked through the observed consistency between the physical order of markers and their genetic positions (IBSC, 2012). The framework linkage map's size per chromosome was in the range of 119.7 cM (4H) -171.8 cM (7H), with a total map length of 1000 cM, in the similar range as reported for other genetic maps of barley (Stein et al., 2007; Close et al., 2009; Mascher et al., 2013c).

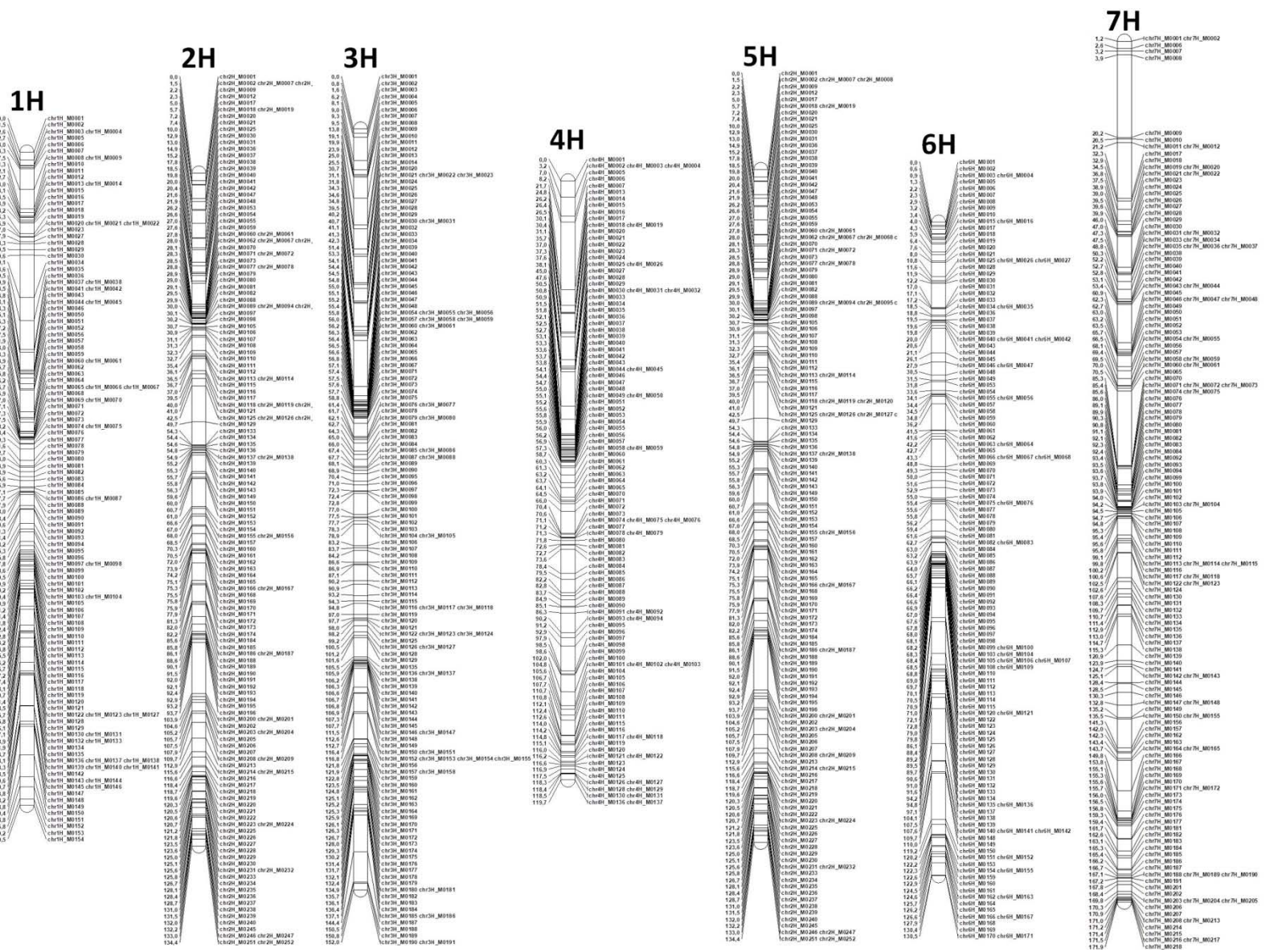


Figure 8: Genetic linkage map of F2S5 'HOR2573 x Morex' composed of 1,394 GBS-derived SNPs markers on seven barley linkage groups.

3.1.3 QTL mapping for powdery mildew resistance

A QTL analysis was performed using genotypic and phenotypic data of the RIL population. The three independent phenotyping experiments were treated as three environments. Linkage analysis for single trait in single / multiple environment(s) for both Interval Mapping and Composite Interval Mapping (CIM) methods yielded the same major QTL with LOD peaks of 48, 53 and 46 on the long arm of chromosome 2H for all three environments, respectively (Figure 9). The QTL interval was stable across all environments explaining an average of 73.3% of the phenotypic variance in the first, 74.7 % of the phenotypic variance in the second and 71.4 % of the phenotypic variance in the third environment (Table 4).

Table 4: Summary of QTL found for *Bgh* resistance in F2S5 generation of ‘HOR2573 x Morex’ population.

Exp./Env.	Chromosome	Markers_interval ¹	Interval size(bp) ²	LOD score	R ²	Additive effect
1	2H	M238_M252	3,482,164	48.55	0.73	-17.36
2	2H	M238_M252	3,482,164	53.16	0.75	-17.62
3	2H	M238_M252	3,482,164	45.97	0.71	-17.23

¹ 95% confidence interval ²The physical coordinates of the 95% confidence interval flanked by markers M238 and M252 on barley reference genome: 762,829,007 and 766,311,171 bp, respectively.

QTL mapping identified a single major QTL assigned to a 95% confidence interval of 3.0 cM flanked by markers M238 and M252. The physical position of this QTL overlapped with the physical position of the major QTL positioned on 2H in F2 generation. This QTL was flanked by marker, ge00372s01 and ge00260s01, corresponding to bp-positions 750,535,187 and 758,850,944 Mbp (Appendix 2). The detected QTL in all three independent phenotyping experiments were supported by statistically significance LOD scores ranging between 46 and 53, and strong R²-values classifying it is as a major QTL (Romero et al., 2014; Kumar et al., 2018; Wang et al., 2018). In addition, this QTL was the only one that contributed significantly to the trait of interest explaining on average 73.3% of phenotypic variation. This indicates that this resistance QTL is a single locus, controlling the trait of interest. The physical distances estimated between markers M238 and M252 corresponded to a ~3.5 Mbp physical distance based on

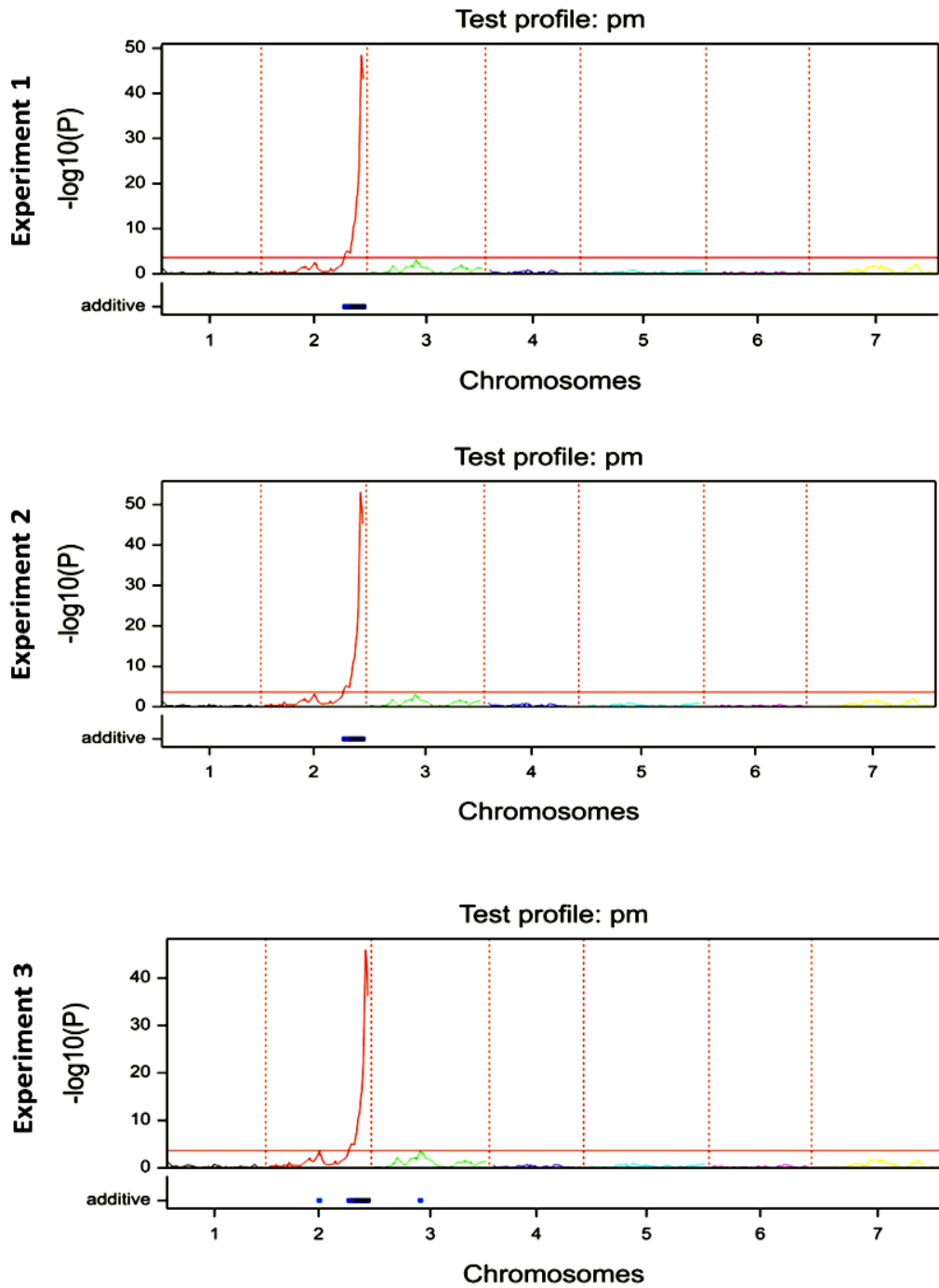


Figure 9: Results of the QTL mapping analysis of F2S5 population ‘HOR2573 × Morex’ in each phenotyping experiment (environment).

Three independent QTL mapping experiments were performed. In each experiment, the Logarithm (base 10) of odds (LOD) score revealed a single significant peak LOD value on chromosome 2HL.

the barley reference genome assembly, comprising at least 108 putative genes within this interval (Appendix 3).

The strength and the effect of the identified QTL on phenotypic variation suggested that the powdery mildew resistance from ‘HOR2573’ was most likely controlled by a single major gene. To validate this possibility, disease scoring was re-performed with two qualitative classes (resistant vs. susceptible class) independently from the previous phenotyping scores in order to obtain unbiased results. The qualitative scoring was subsequently assessed according to predefined criteria (resistant: $\leq 25\%$ infected area, susceptible: $>25\%$) in plant disease qualitative scoring (Figure 10).

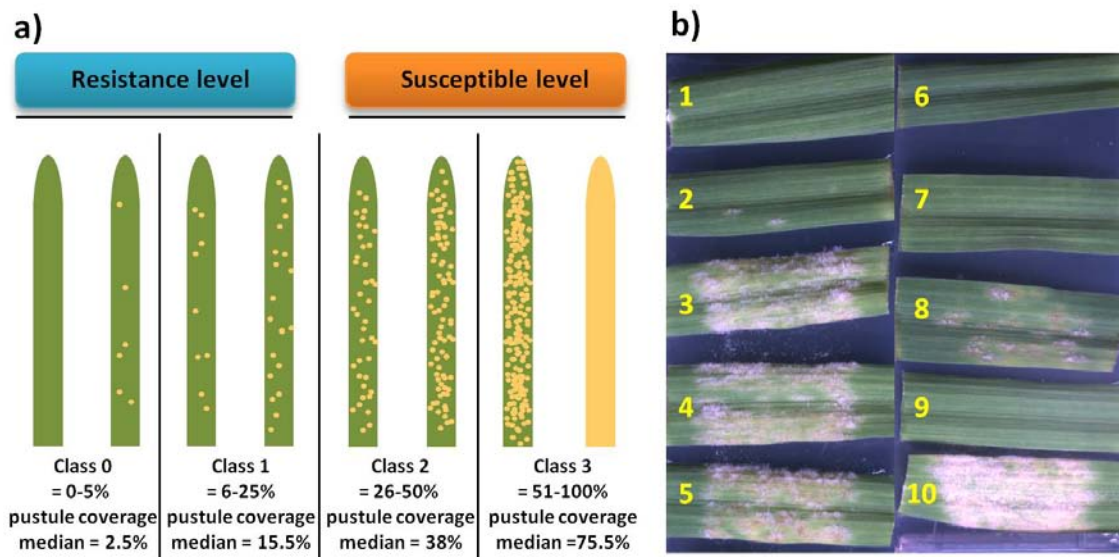


Figure 10: Schematic illustration for qualitative scoring of susceptibility to powdery mildew in barley based on DLA.

a) Quantitative and qualitative phenotyping scoring scale used to evaluate the powdery mildew infection severity b) Disease symptom on inoculated leaf segments 7 days post inoculation using the *Bgh* isolate CH4.8. Leaf number 1 and 6: resistant parent (negative control, class 0), leaf number 3 and 10: susceptible parent (positive control, class 3), other leaves are progeny; leaf number 4, 5 and 8 (examples of class 2).

Based on the qualitative evaluation, 51 out of 95 RILs were consistently scored as resistant whereas 44 RILs were scored as susceptible plants. This is consistent with the expected inheritance pattern of a monogenic Mendelian factor [$1:1$, $X^2 = 0.5156 < 3.841$ at the certainty

level of ($1 - P$ value = 0.95) with the degrees of freedom (d.f. = 1)]. In all three phenotyping experiments, the parental controls were included and phenotyped and the resistant parent ‘HOR2573’ always represented the highest resistance score (class 0) whereas maximum susceptibility was always recorded for ‘Morex’, the susceptible parent (class 3) documenting high inoculation/infection efficiency. The obtained results strongly confirmed the presence of a single major dominant locus / gene controlling powdery mildew resistance in the population ‘Hor2573 x Morex’.

3.2 Overlap of the mildew resistance locus with previously identified mildew resistance QTL

Several significant QTL near the distal end of this chromosomal region have repeatedly been reported to be associated with powdery mildew resistance (von Korff et al., 2005; Marcel et al., 2007; Schweizer and Stein, 2011). The ‘*Laevigatum*’ quantitative resistance gene (known as *MILa*) conferring resistance to barley powdery mildew was also mapped to this region (Giese et al., 1993; Backes et al., 2003). This region was further investigated by Marcel et al. (2007) for resistance against the leaf rust and powdery mildew using near-isogenic lines (NIL) which resulted to identification of smaller interval for ‘*Laevigatum*’ powdery mildew resistance QTL on barley chromosome 2HL (personal communication with Dr. Rients Niks, Wageningen University, the Netherlands). In order to assess the overlap between the location of the resistance locus in ‘HOR2573 × Morex’ population with the identified *MILa*-QTL, the sequence information of corresponding flanking and co-segregation genetic markers of the *MILa*-QTL was kindly provided by Dr. Niks for the current study. The genetic marker sequences were blasted against the barley reference genome. The result showed that all *MILa*-QTL related markers (WBE142, WBE138, MWG2200, WBE141, and WBE145) were anchored within M238-M252 interval (Figure 11), potentially suggesting that the same locus might explain powdery mildew resistance in ‘Vada’ (derived from ‘*Laevigatum*’) and ‘HOR2573’ which can harbor different alleles or different genes. Therefore, it was proposed to name the resistance locus from ‘HOR2573’ “*MILa-H*”, indicating that the resistance-conferring allele in this locus was derived from the Ethiopian landrace ‘HOR2573’. The acronym ‘HOR’ stands for ‘*Hordeum*’. The information of flanking and co-segregating markers with *MILa*- locus is provided in Table 5.

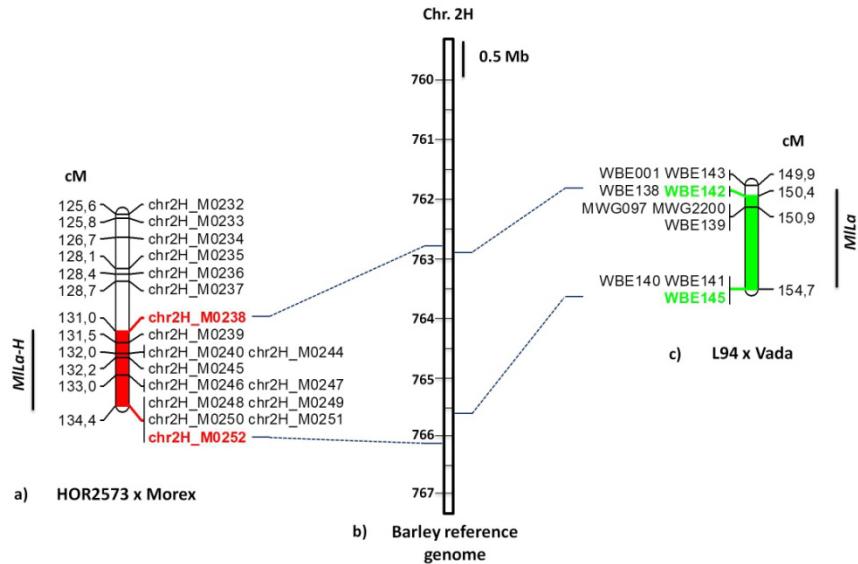


Figure 11: Physical position of the powdery mildew resistance *MILa-H* locus originated from ‘HOR2573’ and quantitative resistance locus *MILa* derived from ‘Vada’ on the barley reference genome.

a) Genetic mapping of *MILa-H* locus on chromosome 2H in F2S5 ‘HOR2573 × Morex’ population. The flanking markers and the genetic interval are highlighted in red. b) A part of barley reference genome (distal end of barley chromosome 2HL). Numbers on the left side indicate the position, in cM. c) The Interval of identified *MILa* locus in NIL population ‘L94 × Vada’ (personal communication with Dr. Niks). The genetic interval and closest flanking markers are highlighted in green.

Table 5: List of flanking and co-segregating DNA markers with the *MILa* locus in ‘L94 × Vada’ population.

Marker ID	Chromosome	Physical coordinates	Status to <i>MILa</i> locus
WBE142	2HL	762,952,935	closest marker proximally
WBE138	2HL	763,962,153	closest marker proximally
MWG2200	2HL	764,068,119	co-segregating with <i>MILa</i>
WBE141	2HL	764,432,251	co-segregating with <i>MILa</i>
WBE145	2HL	765,633,903	closest marker distally

¹Physical coordinates based on the barley reference genome (Mascher et al., 2017)

3.3 High resolution genetic mapping of the 2HL resistance locus

The analysis of variation observed within a bi-parental population for a trait of interest usually starts with a primary QTL mapping step which localizes all major loci responsible for the trait variation. The interval of the identified QTL within a chromosome might represent a genetic distance of 5-30 cM and might contain up to several hundreds of genes, depending on the region of the chromosome. The challenge is then to increase the genetic resolution with the intention that the QTL interval becomes delimited to a small chromosome region, preferably including only one gene. In this regard, positional cloning is a fundamental approach that can be set up to clone the QTL of interest. This approach is based on linkage disequilibrium (non-random assortment of alleles at different loci) that proves the correlation between the trait value and the smallest chromosome segment flanked by molecular markers (Varshney and Tuberosa, 2007). In the current study, the identified interval carrying the resistance locus *MILa-H* is rather big, approximately 3 cM containing 108 predicted genes according to the barley reference genome. In order to delimit this large interval, an increase in the mapping resolution was required which could be obtained by producing a new, large mapping population; however, this was undeniably a time-consuming task (at least 6 months for spring barley). In order to save time, the development of mapping population from the residual heterozygous lines (RHL) was considered as a rapid, efficient and promising alternative approach for high resolution mapping of the locus. In fact, the RHL is a recombinant inbred line that harbors a heterozygous region in the target interval which can be used as F₂-like population for high resolution mapping. This approach had been successfully implemented for fine mapping and map-based cloning of numerous genes in soybean (Yamanaka et al., 2005), rice (Yu et al., 2008) and maize (Pan et al., 2017).

In the current study, three RHLs were identified from GBS data on the F2S4 RIL population harboring a heterozygous region where the resistance locus was located. In addition, a survey of the initial phenotyping results for these three lines (RHL145, RHL567 and RHL836) exhibited a phenotypic segregation for powdery mildew resistance in all three phenotyping experiments (Table 6), verifying the heterozygous status of these lines. However, in order to have rigorous proof concerning the heterozygous status of these three selected RHLs for the respective region, the total read coverage plus the number of alternative allele coverage at target interval were re-evaluated; confirming that selected lines were heterozygous for the target interval (Table 7). The

table is an expanded view of the whole GBS data points for the three selected RHLs in the respective region of the genome.

Table 6: Observed phenotypic variation among eight biological replicates for RHLs 145, 567, 836 in response to powdery mildew (infected leaf area %) through three independent phenotyping experiments.

Infected leaf area % (Experiment one¹)								
	Plant 1	Plant 2	Plant 3	Plant 4	Plant 5	Plant 6	Plant 7	Plant 8
RHL 145	80	5	10	10	50	25	5	10
RHL 567	80	25	60	10	25	1	5	5
RHL 836	1	5	25	15	25	50	20	60
Infected leaf area % (Experiment two¹)								
RHL 145	80	50	10	10	10	5	25	10
RHL 567	5	20	5	10	25	85	50	10
RHL 836	5	1	1	20	25	50	40	60
Infected leaf area % (Experiment three¹)								
RHL 145	70	5	50	25	20	5	20	5
RHL 567	10	1	20	25	5	50	1	90
RHL 836	50	30	5	90	5	25	5	10

¹The parental lines were included in all three phenotyping experiments as positive and negative controls. The percentage of leaf area affected by powdery mildew among eight biological replicates for RHLs 145, 567 and 836 (three independent phenotyping experiments) exhibit variation for disease response, suggesting heterozygosity for the putative disease resistance locus.

Table 7: Allele coverage of heterozygous variants at the QTL interval for three RHLs 145, 567 and 836.

Position (bp)	Genotype	Ref./Alt. allele ¹	Quality of reads ²	Total coverage ³	Alt_ coverage ⁴
CH2_758926583	145	C/T	93	10	5
CH2_759410274	145	C/T	99	10	6
CH2_760762352	145	G/A	99	13	7
CH2_763972104	145	G/A	99	11	5
CH2_765158649	145	C/G	99	13	6
CH2_765158681	145	A/C	99	14	6
CH2_766311166	145	G/A	99	18	10
CH2_766311169	145	A/G	99	18	10
CH2_766311171	145	T/C	99	18	10
CH2_766311199	145	G/A	99	19	10
CH2_766311206	145	T/G	99	19	10
CH2_759291307	567	C/G	96	12	7
CH2_759291308	567	G/A	99	12	7
CH2_759410274	567	C/T	99	12	7
CH2_760762352	567	G/A	99	14	7
CH2_763044999	567	G/A	90	17	9
CH2_763045023	567	G/C	99	17	9
CH2_763045048	567	C/A	99	17	9
CH2_763045073	567	A/C	97	17	9
CH2_764288462	567	T/C	90	9	5
CH2_758760671	836	C/T	99	24	12
CH2_758926583	836	C/T	99	24	12
CH2_759291307	836	C/G	99	25	13
CH2_759291308	836	G/A	99	25	13
CH2_759410274	836	C/T	99	22	13
CH2_760113401	836	A/G	99	48	22
CH2_760762352	836	G/A	99	29	14
CH2_763044999	836	G/A	99	19	11
CH2_763045023	836	G/C	99	19	11
CH2_763045048	836	C/A	99	19	11
CH2_763045073	836	A/C	99	19	11
CH2_763972104	836	G/A	99	28	13
CH2_764288462	836	T/C	99	18	8
CH2_765158649	836	C/G	99	24	12
CH2_765158681	836	A/C	99	22	10

¹ Ref. stands for the allele at barley reference sequence cv. 'Morex'/ Alt. for allele at resistant parent (HOR2573). ² Qualifies allele call is 99% accurate, with a 1% chance of error. ³ Total number of reads covering the respective SNP. ⁴ The number of reads supporting the alternative allele.

Another critical step for positional cloning is to estimate the size of the mapping population required for high resolution mapping, which is a rather difficult task because the meiotic recombination frequency varies along chromosomes (Muñoz-Amatriaín et al., 2015). The genetic distance between the target locus and a molecular marker (a known physical location on a chromosome) is indirectly concluded by number of meiotic recombination events that can break the co-segregation of the phenotype (the target locus) with respective molecular marker. In fine mapping, the optimal resolution is to reach to a physical interval containing only one single gene delimited by recombination(s) to be flanked by marker(s) on either side. As a result, the frequency of recombination event (R, kb / cM) in the respective genome region is a critical parameter to determine the size of the mapping population. In order to predict the size of mapping population required to be genotyped for delimiting the interval of *MILa-H* locus into a single gene, the recombination frequency was calculated by dividing the length of a physical sub-region (M238-M252) in kilobase pair by the length of the corresponding genetic sub-region in centimorgans. The initial low-resolution mapping revealed that the resistance locus mapped in an interval flanked by M238 and M252, with recombination frequency of ~ 1160.6 kb / cM around the locus. This value is on average 2000 kb / cM in distal regions of the barley chromosomes (Muñoz-Amatriaín et al., 2015). According to the equation,

$$N = \text{Log} (1 - P) / \text{Log} (1 - D/100R)$$

Where, *P* is threshold probability of success (e.g., 0.95), *N* is the number of meiotic gametes (chromosomes) that must be genotyped, *D* is expected distance between flanking molecular markers (kb), and *R* is recombination frequency (kb / cM) (Dinka et al., 2007). Based on this formula, 9,984 gametes or 4,992 lines are needed to be genotyped to detect a minimum of one recombination per defined physical interval. However, due to the limitation in initial seed stock, the high resolution mapping and marker saturation was initiated by screening phenotypically and genotypically of 1001 lines from the three selected RHLs. This allowed me to save time considering the fact that once the target interval was reduced, an additional population derived from progeny would be screened to increase the resolution. The resistance evaluation of RHL-population was done with the same *Bgh* isolate, CH4.8, used in the previous phenotyping experiments. The phenotyping analysis of the RHL-population resulted in the identification of 742 resistant and 259 susceptible lines. The observed segregation pattern reconfirmed that

powdery mildew resistance in the developed F₂-like mapping population was controlled by a single dominant gene ($\chi^2 = 0.407 < 2.706$ and P value = 0.1) with the degrees of freedom (d.f. = 1). The segregation pattern was also evaluated individually in each RHL subfamily (RHL145, RHL567, RHL836), verifying the monogenic dominant inheritance of the *MILa-H* locus (Table 8).

Table 8: Phenotypic segregation pattern of each residual heterozygous sub family for resistance to the powdery mildew isolate.

Sub-family	Number of resistant lines	Number of susceptible lines	χ^2
RHL145	369	117	0,22
RHL567	205	74	0,34
RHL836	168	68	1,83

For genotyping of RHL-population, three CAPS markers (M3, M7 and M8) were developed by taking the advantage of GBS-derived SNPs within the locus interval according to their physical position on the barley reference genome (Table 9) and were used for screening the 1,001 individuals. To reduce the risk of the target locus being lost, markers were selected with sufficient physical distance to contain the entire locus interval; meaning that although M3 and M8 were outside of the 95% confidence interval, they were still located in the locus interval.

Table 9: List of CAPS markers used for initial high resolution mapping.

Marker ID	Physical position	Enzyme	HOR2573 Fragment size (bp)	Morex Fragment size (bp)
M3	758,760,670	<i>AvaII</i>	<u>645</u> ¹ /165/89/12	<u>498</u> ¹ /165/ <u>147</u> ¹ /89/12
M7	764,288,462	<i>BauI</i>	<u>390</u> ¹ /127	<u>517</u> ¹
M8	760,762,352	<i>SapI</i>	<u>807</u> ¹	<u>507</u> ¹ ,300

¹The diagnostic fragments are underlined.

From the genotyping of all 1,001 individuals, a total of 141 recombinants were identified between the three selected markers (Figure 12b), of which 47 and 94 recombination events occurred between M3 and M8 and between M8 and M7, respectively. The resistance locus mapped into a 3.5 Mbp interval flanked by M8 and M7. From 94 recombination events between M8 and M7, 69 proximal cross-over occurred between M8 and the resistance locus whereas for M7, only 5 distal cross-over with the resistant locus were observed. The remaining 20 recombination events within the M8-M7 interval occurred between a heterozygous and homozygous resistance allele. The number of observed recombination events between flanking markers and the resistant locus indicated that the resistance locus was located close to marker M7.

Looking for further polymorphic SNPs in the six-fold read coverage GBS dataset revealed seven putative SNPs for further marker development between M8 and M7 interval. Some of them were very closely located to each other (<50 bp) which resulted in only three putative informative markers to narrow down the interval. In order to get the robust SNP calls within the target interval required for the marker saturation with high degree of confidence, the exome capture assay was employed on a number of selected recombinants with extreme phenotypes to the *Bgh* isolate (either highly susceptible or highly resistance). Based on exome capture data analysis, 295 SNPs (with six-fold read coverage) were identified between the flanking marker M8 and M7. Of which eight polymorphic SNPs were selected according to their physical position on the barley reference genome and converted to CAPS markers. A subsequent CAPS-based screening of the current informative recombinants (69+5+20) resulted in saturation of the interval with 11 additional markers (Table 10). The analysis of the observed recombinants positioned the resistance locus between marker M27 and M31, delimiting the interval from 3.5 Mbp to 1.1 Mbp. In this interval, five markers M21, M23, M25, M20 and M30 were co-segregating with the resistance locus. Both flanking markers M27 and M31 displayed 5 recombination events at either side of the locus, meaning that 10 recombinants in total were identified within this target interval (Figure 12c).

Table 10: List of CAPS markers derived from GBS and exome capture data used to narrow down the target interval.

Marker ID	Source	Physical position ¹	Enzyme	HOR fragment size (bp)	Morex fragment size (bp)
M15	Exome cap.	760,881,528	<i>TaqI</i>	<u>256</u> ² ,228,205	<u>689</u> ²
M17	Exome cap.	761,623,897	<i>TaqI</i>	<u>424</u> ² ,171,165,141	<u>595</u> ² ,166,141
M19	Exome cap.	762,152,404	<i>AccI</i>	<u>840</u> ² ,149	<u>758</u> ² ,149,71
M26	Exome cap.	762,463,641	<i>MspII</i>	<u>615</u> ² ,237	<u>454</u> ² ,237,161
M27	GBS	762,827,447	<i>XmnI</i>	<u>702</u> ²	<u>448</u> ² ,254
M21	Exome cap.	762,994,364	<i>SspI</i>	<u>445</u> ² ,163	<u>608</u> ²
M29	GBS	763,121,737	<i>EspI</i>	<u>690</u> ² ,177,5	<u>484</u> ² ,201,177,5,5
M30	Exome cap.	763,201,116	<i>FauI</i>	<u>863</u> ²	<u>483</u> ² ,38
M23	Exome cap.	763,346,522	<i>AccI</i>	<u>828</u> ²	<u>639</u> ² ,104,76
M25	Exome cap.	763,552,756	<i>MmeI</i>	<u>980</u> ²	<u>680</u> ² ,273
M31	GBS	763,961,402	<i>AccI</i>	<u>646</u> ² ,233	<u>512</u> ² ,233,134

¹Markers are listed in physical order based on the barley reference genome (Mascher et al., 2017).

²The diagnostic fragments are underlined.

To increase the genetic resolution in the vicinity of the target locus and identify additional recombinants, an additional 940 F₂-like lines (the subsequent progeny) were sown and screened for the recombination events by utilizing the flanking marker M27 and M31 plus the first and the last co-segregating markers (M21 and M25). The screening results confirmed the complete linkage between co-segregating markers and the resistance locus, along with identification of an additional 11 recombinants for the interval of interest.

All identified recombinants within the target interval (10+11) were subsequently screened by the newly designed markers; being developed based on either reliable detected SNPs at lower coverage from GBS or exome capture data. For instance, there were 18 GBS derived SNPs at six-fold read coverage between M27 and M21 (proximal side of the resistance locus), however, only one of these SNPs could potentially be used for narrowing down the interval as the other SNPs were located very close to each other (with a physical distance ranging from 10 to 2,500 bp), therefore, being not informative for further marker saturation. Since no recombination event could be expected in such tight distances, the SNP calls with lower coverage were utilized for

marker development. These selected SNPs were common between GBS and exome capture data. This situation was rather different on the distal side of the resistance locus where only one GBS derived SNP calls at lower coverage could potentially be used for the screening. Hence, two additional markers (M14_22 and 28N14_4) were developed based on non-redundant sequence information of ‘Morex’ BAC contigs (IBSC, 2012). For this, the PCR amplicon from each designed primer pair was sequenced by Sanger sequencing and the potential polymorphisms between the parents were identified. In case of the presence of polymorphism between two parents, the primer pairs were employed as a marker to check the polymorphism status in the progeny. The analysis of the identified 21 recombinants (10+11) within M27-M31 using all above-mentioned markers (Table 11) led to further narrowing down of the target interval to 850 kb, flanked by marker G2x_4 and M14_22, containing only two recombinants at either side of the resistance locus (Figure 12d). Considering the average gene density in the distal regions of barley chromosomes (13 genes per Mb), it was predicted that this interval might carry genes according to the size of interval (~850 kb). In addition, by considering the fact that at least 3000 more F₂-like lines (as already calculated by the formula) had to be screened to find one recombination between these markers, an alternative approach was used which will be explained in the following section.

Table 11: List of markers derived from GBS and exome capture data used in Sanger sequencing to narrow down the target interval.

Marker ID	Resource	Physical position ¹	Morex allele/HOR2573 allele
G2x_1	GBS	762,828,965	A/G
G2x_2	GBS	762,834,763	G/A
G2x_3	GBS	762,862,503	G/C
G2x_4	GBS	762,893,276	A/G
G2x_6	GBS	762,951,125	G/A
ExC_1	Exome cap.	763,695,010	C/G
M14_22	Kmasker	763,746,838	G/C
28N14_4	Kmasker	763,881,395	T/C
G2x_10	GBS	763,901,902	A/C

¹Physical coordinates based on the barley reference genome (Mascher et al., 2017).

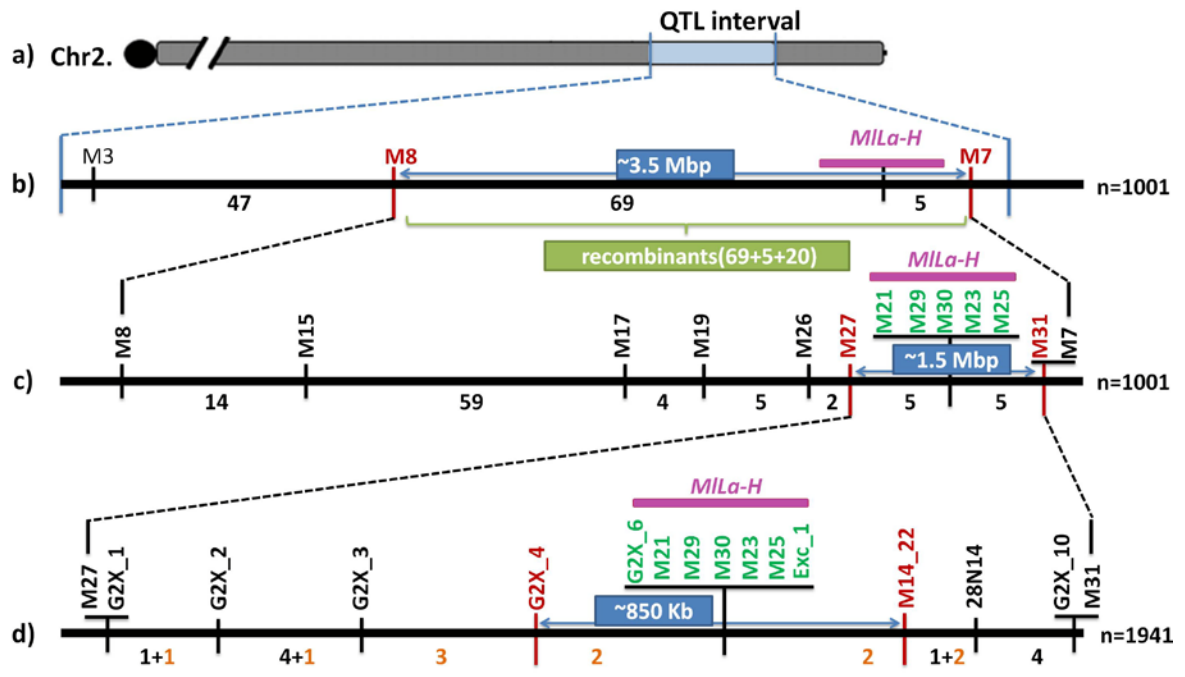


Figure 12: High resolution mapping of the powdery mildew resistance locus *MILa-H*.

a) The genomic region containing the *MILa-H* locus on the long arm of barley chromosome 2H is shown in blue, which was identified through QTL analysis. b) The screening of initial 1,001 F₂-like lines by the three CAPS markers (M3, M8 and M7) led to identification of 141 recombinants at this interval. In addition, the *MILa-H* was mapped between M8 and M7. c) The chromosomal region between M8 and M7 was saturated with additional markers developed by taking advantage of SNP resources from GBS and exome capture re-sequencing of resistant versus susceptible genotypes, resulting in the reducing of target interval to 1.1 Mbp with remaining 10 recombinants at this interval. d) Additional 940 F₂-like lines (the subsequent progeny) were screened by the flanking marker M27 and M31 plus the first and the last co-segregating markers (M21 and M25) in the co-segregating marker cluster. This led to identification of additional 11 recombinants. d) All the identified recombinants (10+11) from the initial and subsequent generations at the target interval flanked by M27 and M31 were screened with additional developed markers. This resulted in narrowing down of the target interval to 850 kb. In each step the flanking markers are highlighted in red. The physical distance between two flanking markers is written in dark blue box. The co-segregating markers with the phenotype (the target locus is shown in pink) are highlighted in green. The number of recombination events between markers is shown below the black line which presents the barley reference genome. The identified additional 11 recombinant lines are highlighted in orange.

3.4 *In silico* based candidate gene identification at the *MILa-H* locus

The map-based reference sequence of barley was constructed through whole-genome shotgun / mate-pair sequencing and assembly of individual BAC clones. The BAC sequences were organized into so-called sequence clusters (groups of overlapping BAC sequences). These BACs have been ordered by Hi-C data (3D chromosome conformation capture sequencing). This Hi-C map assigned each BAC cluster to a consecutive position along the chromosome, from the short arm telomere to the long arm telomere producing barley chromosome pseudomolecule sequences (Beier et al., 2017); a contiguous sequence file representing individual chromosomes but still containing assembly gaps.

The *MILa-H* interval, defined by the flanking markers G2x_4 and M14_22, is represented in the chromosome 2H pseudomolecule sequence by ten individually sequenced BAC clones forming a single sequence cluster (cluster_241) constituted of 143 partial sequences from the individual BAC assemblies (Appendix 4). These ten BAC clones are located on the minimum tiling path (MTP), indicating the minimal set of overlapping clones needed to provide complete coverage of this chromosomal region. In fact, any candidate gene of the *MILa-H* locus, if present in cv. 'Morex', must be contained in this piece of barley genome sequence.

In order to understand the distribution of the closest flanking markers (G2x_4 and M14_22) and co-segregating markers on the overlapping BAC clones, the markers were anchored using nucleotide BLAST search against the barley BAC assembly (http://webblast.ipk-gatersleben.de/barley_ibsc/viroblast.php). The proximal flanking marker (G2x_4) and the first co-segregating marker (G2x_6) were assigned to two adjacent BAC clones HVVMRXALLMA0276H13 and HVVMRXALLMA0301J16, respectively with 57.8 kb distance from each other. The distal flanking marker (M14_22) and last co-segregating marker (ExC_1) were located on two non-adjacent BAC clones, HVVMRX83KHA0013M14 and HVVMRXALLMA0013I07, respectively with a physical distance of ~52 kb (Figure 13b, c). According to the distribution pattern of co-segregating markers on BACs, the smallest physical interval that must harbor the resistance gene was predicted to be in a physical distance of approximately 702 kb between BAC clone HVVMRXALLMA0301J16 and HVVMRXALLMA0013I07. Using the barley genome explorer, Barlex (<https://apex.ipk-gatersleben.de/apex/f?p=284:10>), the predicted gene models on the respective BAC clone were

retrieved and summarized (Table 12). For most genes a putative functional annotation was available (Mascher et al. 2017).

Powdery mildew resistance conferred by the *MILa-H* locus, derived from ‘HOR2573’, is dominantly inherited, race-specific and involves a hypersensitive response-like programmed cell death at a microscopic level. This pattern of resistance indicates the involvement of NLRs or RLKs, thus it was anticipated that the delimited target interval (~850 kb) of the *MILa-H* locus would contain candidate genes belonging to the expected classes of resistance gene analogs (R genes). According to predicted biological function, four genes of this interval belonged to disease resistance gene families that could be considered as potential candidate genes for the *MILa-H* locus. The position of each R gene on the overlapping BAC clones is shown in Figure 13c. In addition, the structure of each R gene is depicted in Figure 13d.

Table 12: Summary of the overlapping BAC clones with flanking and co segregating markers information in the *MILa-H* interval.

BAC ID ¹	Gene ID ²	Functional annotation ³	DNA marker ID ⁴
HVVMRXALLMA0276H13			proximal flanking marker
HVVMRXALLMA0301J16	<i>HORVU2Hr1G126250</i>	R gene (LRR-RLK)	M21
	<i>HORVU2Hr1G126290</i>	unknown function	
	<i>HORVU2Hr1G126350</i>	homolog to SCAR protein	
HVVMRX83KHA0131O13	LC gene ⁵		M29
HVVMRXALLHC0076A01	<i>HORVU2Hr1G126380</i>	R gene (NBS-LRR)	M30
HVVMRXALLMA0320H13	No gene		
HVVMRXALLEA0216D09	<i>HORVU2Hr1G126440</i>	R gene (NBS-LRR)	M23
HVVMRXALLMA0013I07	<i>HORVU2Hr1G126510</i>	R gene (NBS-LRR)	M25
HVVMRXALLEA0301J21	No gene		
HVVMRXALLMA0105H07	<i>HORVU2Hr1G126540</i>	homology with Amidase superfamily	ExC_1
HVVMRX83KHA0013M14			distal flanking marker

¹The overlapping BAC clones cv. ‘Morex’ spanning the delimited *MILa-H* interval based on minimum tilling path (MTP). ²All gene models with full gene ID are high confidence (HC) genes. The genes located on each BAC clone is written in front of each BAC ID. ³The function of the genes were predicted using automated gene annotation of the barley reference based on four independent datasets for gene evidence information including 1) RNA sequencing (RNA-seq) data 2) reference protein predictions from barley, rice, *Brachypodium* and sorghum 3) published barley full-length complementary DNA (fl-cDNA) sequences; and 4) newly generated barley PacBio Iso-Seq data (Mascher et al., 2017). ⁴ The column represents the corresponding BAC clone for each flanking and co-segregating marker in the *MILa-H* interval. ⁵Low confidence gene; barley contains about 41,000 gene-like sequences including potential *pseudogenes* that they did not agree with at least one of the four reference genomes; rice, sorghum, *Brachypodium* and *Arabidopsis*.

The annotation of the barley reference sequence (Mascher et al. 2017) comprises high-confidence (HC) and low-confidence (LC) gene models. Low-confidence genes are sequences of transcripts that lack homology to other genomes and are missing support from a gene family, whereas HC genes have homology to at least one reference genome like sorghum, rice, *Brachypodium* or *Arabidopsis*. For the *MILa-H* target interval seven HC genes and 17 LC genes were predicted. However, since the annotation of 'Morex' BAC clones was conducted automatically, it is possible that some genes located on the BAC clones might have been unnoticed (Mascher et al., 2017). Therefore, it was necessary to perform the re-annotation of the non-redundant sequence of the BAC clones spanning the *MILa-H* interval independent from the gene models. Due to the fact that the barley genome has a high content (>80%) of repetitive sequences, the unique sequences of the target region were extracted using the Kmasker-web tool (<http://webblast.ipk-gatersleben.de/kmasker/>). The obtained unique sequences were used for a Nucleotide Similarity Search using BLASTN against non-redundant DNA/protein database to identify the best hits. The result of annotation was then compared to the predicted genes to confirm that this region was not previously annotated during automated annotation by IBSC. This *de novo* annotation of genes for the sequence of the *MILa-H* interval allowed to reject the possibility of any overlooked gene/ORF during automated annotation. In addition, it was critical to confirm the structural annotation of gene models in the *MILa-H* interval through sequence comparison with the closest orthologs since the automated annotation of the barley reference sequence (Mascher et al., 2017) might contain small fraction of inaccuracies. For this purpose, the protein sequence of each gene model was used to perform protein similarity search using BLASTP against non-redundant protein sequence (nr) database. The protein sequence of the best hit from one of the closet species (rice, bread wheat, and Tausch's goat grass; *Aegilops tauschii*) was selected for alignment using TBLASTN against the barley reference genome to get the corresponding physical coordinates. Based on physical coordinates, the corresponding genomic sequence was extracted in barley and subsequently exons and introns were determined. The obtained result was then compared to the result of the automated barley gene annotation, indicating that the two disease resistance gene models in this interval, *HORVU2Hr1G126380* and *HORVU2Hr1G126510*, had an incomplete open reading frame (ORF) in the automated annotation (Table 13). Detailed information of the comparative analysis results for these four resistance genes in other species are provided in Table 14.

Table 13: Manual annotation of four resistance gene models within the *MILa-H* interval compared to the barley automated gene annotation.

	<i>HORVU2Hr1G126250</i>				<i>HORVU2Hr1G126380</i>				<i>HORVU2Hr1G126440</i>				<i>HORVU2Hr1G126510</i>			
	LRR-RLK protein family				NBS-LRR protein family				NBS-LRR protein family				NBS-LRR protein family			
	Exon	Gene size (kb)	CDS (bp)	Protein (aa)	Exon	Gene size (kb)	CDS (bp)	Protein (aa)	Exon	Gene size (kb)	CDS (bp)	Protein (aa)	Exon	Gene size (kb)	CDS (bp)	Protein (aa)
Automated¹	2	3.85	3,507	1,168	1	2.20	2,208	735	4	15.84	3,247	1,081	3	7.01	3,729	1,242
Manual	2	3.85	3,507	1,168	4	17.96	3,504	1,167	4	15.84	3,247	1,081	4	7.68	3,729	1,242

¹(IBSC, 2012)

Table 14: List of orthologous loci in rice, bread wheat and tausch's goatgrass for the four resistance gene models in the *MILa-H* interval

Species	<i>HORVU2Hr1G126250</i>				<i>HORVU2Hr1G126380</i>				<i>HORVU2Hr1G126440</i>				<i>HORVU2Hr1G126510</i>			
	LRR-RLK protein family ¹				NBS-LRR protein family ¹				NBS-LRR protein family ¹				NBS-LRR protein family ¹			
	Exon	Gene size (kb)	CDS (bp)	Protein (aa)	Exon	Gene size (kb)	CDS (bp)	Protein (aa)	Exon	Gene size (kb)	CDS (bp)	Protein (aa)	Exon	Gene size (kb)	CDS (bp)	Protein (aa)
<i>O. sativa</i> <i>ssp. japonica</i>	<i>Os11t0628000</i>				<i>Os11g0213700</i>				<i>Os11t0212000</i>				<i>Os11g0213800</i>			
	2	3.50	3318	1105	4	3.65	2748	915	4	5.84	3264	1087	3	2.05	1224	407
<i>T. aestivum</i>	<i>2BL_TGACv1_129540_AA0387780</i>				<i>2BL_TGACv1_130529_AA0412970</i>				<i>2AL_TGACv1_092893_AA0266350</i>				<i>2BL_TGACv1_130529_AA0412970</i>			
	2	4.22	3486	1161	4	4.2	2514	837	4	8.26	3378	1125	4	4.2	2514	837
<i>A. tauschii</i>	<i>F775_13446</i>				<i>F775_16265</i>				<i>F775_16266</i>				<i>F775_16265</i>			
	2	3.58	3450	1149	2	3.88	2106	701	1	1.14	1137	378	2	3.88	2106	701

¹The biological function of each gene has been checked in orthologous genes. They all confirm the predicted the annotated biological function for four gene models.

In addition, for the other three gene models (*HORVU2Hr1G126290*, *HORVU2Hr1G126350* and *HORVU2Hr1G126540*) in the *MILa-H* interval, the structural re-annotation was performed using the same approach. To support the confidence of the analysis, orthology prediction was performed in several species (Table 16). The comparison analysis showed that the automated gene annotation for the two gene models *HORVU2Hr1G126290* and *HORVU2Hr1G126540* were incomplete. The summary of manual annotation for these three gene models is presented in Table 15. The result showed that the *HORVU2Hr1G126290* gene model was not characterized in any crop species. The comparison of protein sequence between this gene and its orthologs revealed that it gained a premature stop codon in the coding sequence leading to a shorter protein sequence. A survey on public available gene expression data of this gene model from different plant tissues (IBSC, 2012) showed that this gene only expressed in tissues taken from developing grains, palea and rachis, meaning that the truncated protein product may still be functional. The manual annotation of the *HORVU2Hr1G126540* gene model showed that 592 bp of the 5' coding region was not present in the automated annotation. The gene expression dataset presented that this gene was highly expressed in developing grains. In contrast, the *HORVU2Hr1G126350* gene model had an early premature stop codon in the ORF, made it truncated and nonfunctional, that was also verified by checking the gene expression dataset, meaning that it was not expressed in any tissue. From this result, none of these gene models had a role in resistance to plant pathogens or plant / pathogen interaction; therefore they were excluded for any further analysis.

Furthermore, regarding the R genes in this interval, the comparison of CDS sequence of *HORVU2Hr1G126380* (as query) and *HORVU2Hr1G126510* (as query) through pairwise sequence alignment indicated 90% identity in 95% of the query coverage. It was a clear clue why these two gene models hit a same gene model in wheat and *Aegilops*. In fact, the high homology between the genes of the same family is highly expected due to the presence of highly conserved domains. The degree of homology was also checked for *HORVU2Hr1G126440* (with the same query), showing 81% identity in 79% of query coverage which implied on their high homology. To get a clear view, the CDS sequence homology between two gene models *2AL_TGACv1_092893_AA0266350* and *2BL_TGACv1_130529_AA0412970* in wheat was also checked, indicating that they were homoeologues with 70% identity in 84% coverage. This degree of homology coupled with high density of R gene from NBS-LRR family could be probably the result of genome evolution, the presumed duplication and diversification which generate an alternative recognition capability for the pathogen attack. Beyond this, according to

the result of manual re-annotation for these three genes (*HORVU2Hr1G126380*, *HORVU2Hr1G126440* and *HORVU2Hr1G126510*), they contained the same number of exons but they vary greatly in size (Table 12). A further analysis at the gene structure of *HORVU2Hr1G126380* in the barley reference genome revealed the presence of an intron with size of ~ 12.8 kb between exon 2 and 3 resulted from a retrotransposons LTR insertion which was also observed for gene model *HORVU2Hr1G126440* with a shorter (~5kb) insertion. This insertion of a big transposable element between exons in *HORVU2Hr1G126380* gene model might have disturbed the function as this R gene in 'Morex'.

Table 15: Manual annotation of the three other HC genes models within the *MILa-H* interval compared to the barley automated gene annotation.

	<i>HORVU2Hr1G126290</i>				<i>HORVU2Hr1G126350</i>				<i>HORVU2Hr1G12540</i>			
	uncharacterized protein				homology with SCAR family				homology with Amidase superfamily			
	Exon	Gene size (kb)	CDS (bp)	Protein (aa)	Exon	Gene size (kb)	CDS (bp)	Protein (aa)	Exon	Gene size (kb)	CDS (bp)	Protein (aa)
Automated¹	3	2.53	791	258	4	854	569	67	4	1.66	1024	340
Manual	5	4.56	791	258	4	854	569	67	6	5.67	1616	397

¹(IBSC, 2012)

Table 16: List of orthologous loci in closest crop model species to the three predicted gene models in the *MILa-H* interval

	<i>HORVU2Hr1G126290</i>				<i>HORVU2Hr1G126350</i>				<i>HORVU2Hr1G126540</i>			
Species ¹	uncharacterized protein				homology with SCAR family				homology with Amidase superfamily			
	Exon	Gene size (kb)	CDS (bp)	Protein (aa)	Exon	Gene size (kb)	CDS (bp)	Protein (aa)	Exon	Gene size (kb)	CDS (bp)	Protein (aa)
<i>O. sativa</i> ssp. <i>japonica</i>	<i>Os06t0325500</i>				<i>Os03g0816900</i>				<i>Os04g0118100</i>			
	12	4.99	1713	570	8	5.71	3466	1155	8	3.02	1515	435
<i>T. aestivum</i>	<i>7AS_TGACv1_571224_AA1846080</i>				<i>5BL_TGACv1_404151_AA1286960</i>				<i>2BL_TGACv1_129339_AA0379320</i>			
	13	6.05	1134	377	10	9.87	7382	2344	7	5.67	1751	442
<i>S. bicolor</i>	<i>SORBI_3010G133400</i>				<i>SORBI_3001G038800</i>				<i>SORBI_3002G378000</i>			
	12	6.44	1536	511	11	9.9	6841	2108	9	6.99	5818	437
<i>B. distachyon</i>	<i>BRADI1G42620</i>				<i>BRADI1G04000</i>				<i>BRADI5G27490</i>			
	12	6.33	1643	547	11	9.8	7243	2303	7	2.35	1688	440

¹ The full name of the crop species used in analysis: rice (*Oryza sativa*), bread wheat (*Triticum aestivum*), sorghum (*Sorghum bicolor*) and stiff brome (*Brachypodium distachyon*)

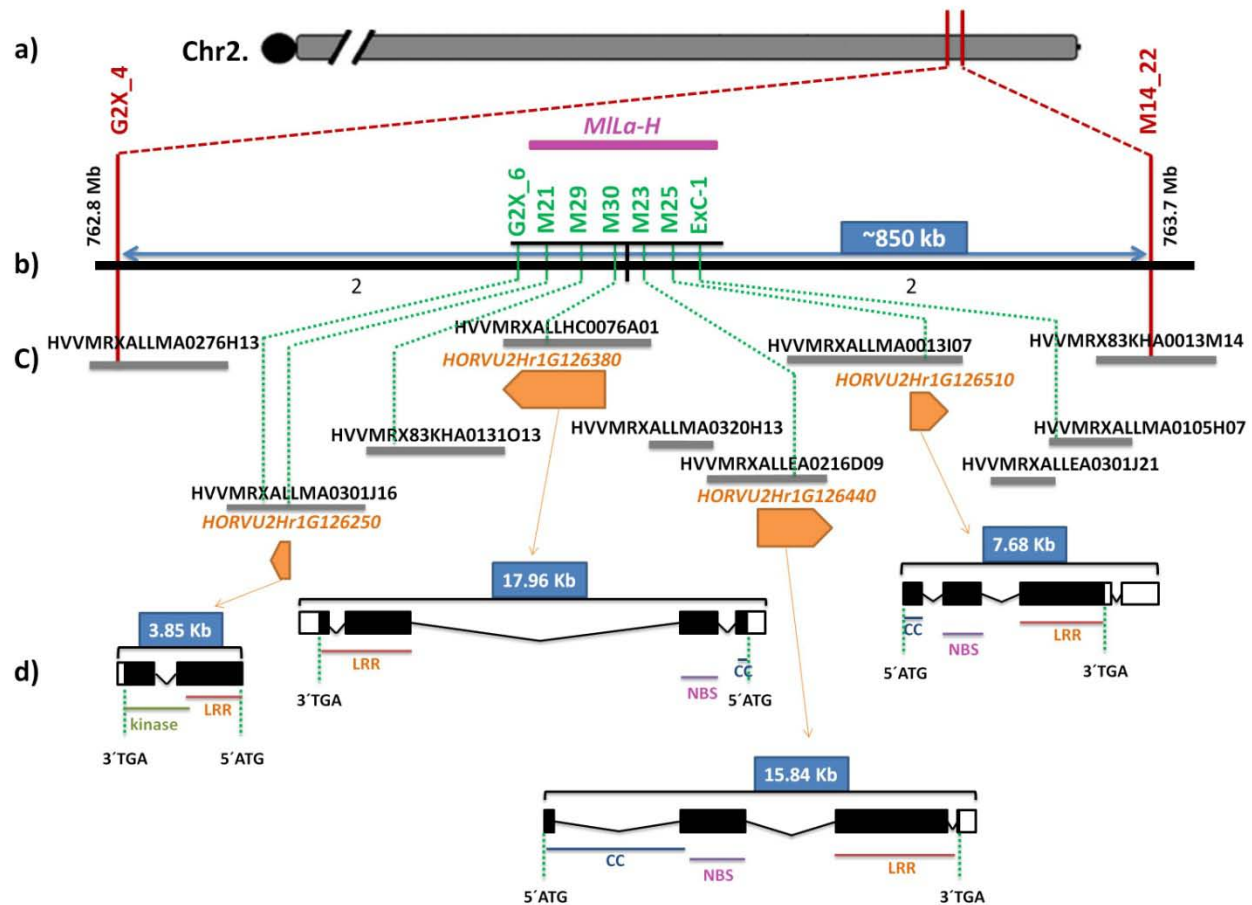


Figure 13: *In silico* characterization of the *MILa-H* locus interval

a) The target interval containing the *MILa-H* locus as delimited by high resolution mapping is indicated by two red vertical lines (position of the closest flanking markers). b) Expanded view of the delimited target interval on physical scale according to the barley reference genome. The red vertical lines stand for flanking markers and the physical position of flanking markers is written beside the DNA marker ID. Markers co-segregating with the resistance locus (*MILa-H*) are highlighted in green and they are physically ordered according to the barley reference sequence. The black solid line represents the chromosome 2H pseudomolecule. The number of recombination events between flanking marker at either side of co-segregating markers is written below the black line. c) The overlapped BAC clones spanning the *MILa-H* interval based on minimum tiling path are shown as gray bars. The position of each DNA marker is shown on BAC clones by dashed green lines. The name of BAC clones is written above the gray line. The four resistance genes are shown in orange pentagons with the corresponding ID above them. The direction of pentagons shows which strand of DNA was sequenced and represents the direction of genes on the reference genome d) The structure of each R gene model in cv. 'Morex' (used for the barley genome reference and as the susceptible parent in this study) is represented in black (exon) and white (untranslated regions) boxes. The distance between boxes represents the introns. The size of each gene is written in blue boxes above of each gene model. The corresponding protein domains are written below exons. The start and stop codons are written according to the direction of genes.

3.5 Re-sequencing of potential candidate genes in ‘HOR2573’ identified potentially causative mutations

Four R genes were identified in the *MILa-H* interval providing intuitive candidate resistance genes. In absence of higher genetic resolution, which could help to rule out some of the candidates by recombination, it is crucial to generate any other evidence, which would allow for identifying the final *MILa-H* candidate gene. The first strategy was to survey sequence differences in the four candidate genes between resistant and susceptible genotypes. All four candidate genes were re-sequenced from the resistant parent ‘HOR2573’ and compared to the ‘Morex’ sequences which is representative for the susceptible parent. For this purpose, several PCR primer pairs were designed based on the barley reference sequence information in order to amplify the entire coding sequence of each gene. The re-sequencing results are summarized in Table 17. All four candidate genes showed the presence of different types of polymorphisms from single nucleotide changes to medium and / or large scale insertions and deletions leading either to amino acid changes and / or premature stop codons compared to susceptible parent cv. ‘Morex’ (Figure 14). The sequence comparison of the first disease resistance gene model (*HORVU2Hr1G126250*) between parental lines revealed 20 SNPs, including 4 synonymous and 16 nonsynonymous SNPs, leading to amino acid changes in both LRR and kinase domains (Figure 14a). The re-sequencing result of the second disease resistance gene model (*HORVU2Hr1G126380*) from resistant parent’s genome ‘HOR2573’ showed that a 42 bp deletion plus a 53 bp insertion occurred in different parts of the second exon, corresponding to the LRR domain (Figure 14b).

The re-sequencing of the third disease resistance gene model, *HORVU2Hr1G126440*, revealed the presence of two paralogs of this gene in ‘HOR2573’, the resistant genotype. One copy is 100% identical to the ‘Morex’ allele (not shown in the Figure 14) and likely represents the orthologous gene. The other copy (putative paralog) showed several SNPs in the exons plus a single bp insertion in the first exon and two consecutive nucleotide changes in the second exon predicted to induce a frame-shift, thus, the *HORVU2Hr1G126440* paralog of ‘HOR2573’ likely represented a pseudogene. Furthermore, the comparison of the predicted protein sequences from resistant and susceptible parents suggested that due to the frame shift, the LRR domain was absent, leading to loss of function status of this gene model in ‘HOR2573’ (Figure 14c). Two

paralogs were also observed in 'HOR2573' for the gene model *HORVU2Hr1G126510*. One copy was 100% identical to the 'Morex' allele (not shown in the Figure 14) and likely represented the orthologous gene whereas the putative 'HOR2573' paralog carried a 4 bp deletion in the first exon, leading to a frame shift and pre-mature stop codon, thus, the *HORVU2Hr1G126510* paralog also likely represented a pseudogene (Figure 14d).

From these results HORVU2Hr1G126250 was favored as the primary candidate gene for *MILa-H* based resistance since it exhibited 4 synonymous and 16 nonsynonymous SNPs, leading to amino acid changes in both the LRR and kinase domains. It can be speculated that these polymorphisms have introduced novel properties to the LRR domain in regard to race-specificity in 'HOR2573', however, this needs to be subject of further functional testing.

Table 17: Summary of sequence analysis of four disease resistance homologs within target interval from 'HOR2573' (resistance parent).

Gene ID	SNP position	SNP Morex/HOR2573	aa change/frame shift	Note
<i>HORVU2Hr1G126250</i>	71	C/T	Pro/Ser	EXON 1
	163	A/C	Arg/Ser	EXON 1
	254	C/G	Arg/Gly	EXON 1
	517	T/C	-	EXON 1
	705	G/A	Ser/Asn	EXON 1
	877	G/A	-	EXON 1
	1399	T/C	-	EXON 1
	1667	A/G	Lys/Glu	EXON 1
	2343	C/T	Thr/Ile	EXON 1
	2519	G/T	Val/Leu	EXON 1
	2819	C/T	His/Tyr	EXON 1
	2840	T/C	Tyr/His	EXON 1
	2904	G/C	Gly/Ala	EXON 1
	2978	A/G	Asn/Asp	EXON 1
	3188	A/G	Arg/Gly	EXON 2
	3220	A/T	Glu/Asp	EXON 2
	3344	T/G	Leu/Glu	EXON 2
3345	T/A	-	EXON 2	
3372	T/C	Met/Thr	EXON 2	
3384	G/A	Arg/His	EXON 2	
<i>HORVU2Hr1G126380</i>	364-406	42 bp deletion	frame shift and premature stop codon	EXON 2
	511-564	53 bp insertion		EXON 2
<i>HORVU2Hr1G126440</i>	29	1 bp insertion	frame shift and premature stop codon	EXON 1
	30	C/G		EXON 2
	31	G/C		EXON 2
<i>HORVU2Hr1G126510</i>	45-49	4 bp deletion	frame shift and premature stop codon	EXON 1

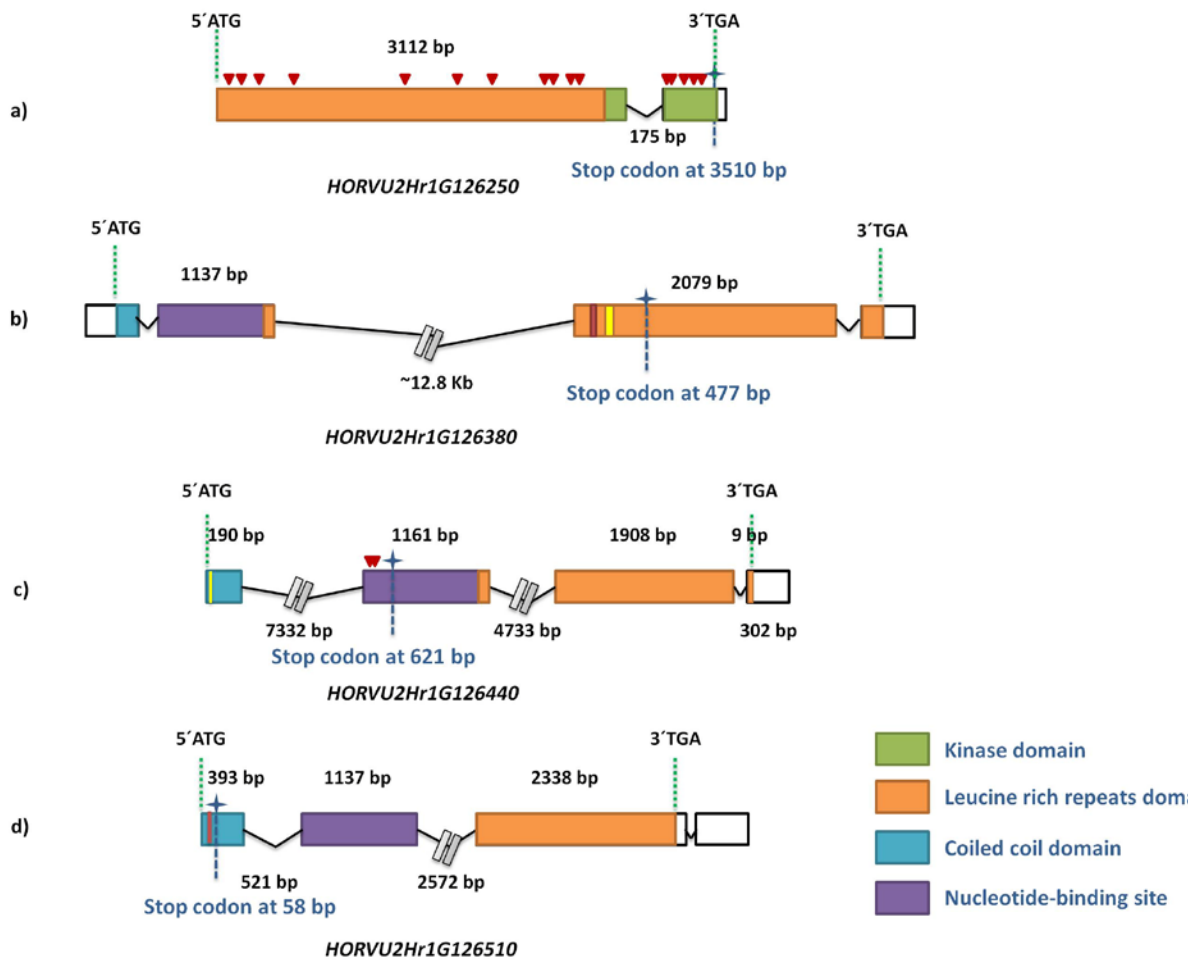


Figure 14: Characterization of the four potential candidate genes in the *MILa-H* interval through re-sequencing in the resistant parent 'HOR2573'.

The structure of each gene model in 'HOR2573' is shown (a-d). All four resistance genes were sequenced from the resistant parent genome. The PCR primers were designed from the corresponding gene in cv. 'Morex'. The ID of each gene model is written under gene structure. The colored and white boxes represent exons and UTRs, respectively. The color code green, orange, violet and blue display the protein domains standing for kinase, leucine rich repeats, nucleotide-binding site and coiled coil domains, respectively. The size of each exon is written above the boxes. The distance between boxes shows the intron size. For the large intron sizes, the distance has been truncated. Premature stop codons are indicated by asterisks with identified position at the bottom of vertical dashed line. The non-synonymous SNPs are indicated by red triangles. Insertions and deletions are depicted with vertical red and yellow lines.

3.6 Physical map construction for the *MILa-H* locus in a powdery mildew resistant haplotype

Analysis and annotation of the *MILa-H* locus was based on a reference sequence derived from a genotype (Morex), which does not carry a functional powdery mildew resistance gene against the tested *Bgh* isolate (CH4.8). In fact, without knowing the exact sequence of the *MILa-H* region of a resistant haplotype, any conclusion regarding the identification of candidate genes is premature. The commonly observed presence/absence variation (PAV) in R genes in *Arabidopsis* (Grant et al., 1998; Henk et al., 1999; Stahl et al., 1999; Tian et al., 2002) could raise doubts of the final list of potential candidate genes within the current target interval characterized on the basis of the 'Morex' sequence. The actual resistance gene might be under PAV, meaning that it can be present in 'HOR2573' but absent in the susceptible parent (Morex). For instance, the analysis of *Rpm1* in *Arabidopsis*, a gene conferring resistance to *Pseudomonas syringae*, suggested that P/A polymorphism of the *Rpm1* directly corresponded to the resistance phenotypes of individual lines (Stahl et al., 1999). There are several strategies that could be taken into consideration to determine the PAV in two genotypes. The most straightforward method is to construct the physical map of the region of interest by screening a BAC library of the resistant genotype by the *MILa-H* flanking and co-segregating markers. A BAC library for the resistant parent, 'HOR2573' was not available in frame of this thesis, however, as an alternative strategy, a BAC library of the genotype 'Vada', carrying the *Laevigatum* type powdery mildew resistance was available for this strategy (Yeo et al., 2016). As explained previously (Figure 11), the physical interval of the resistance locus *MILa-H* overlapped with the *Laevigatum* resistance locus characterized in the 'L94 × Vada' population. Based on the hypothesis that 'HOR2573' and 'Vada' might carry different or the same resistance conferring alleles at the *MILa/MILa-H* loci, a physical map of the resistance locus derived from the genotype 'Vada' might reveal additional R-gene candidates that are absent in the 'Morex' haplotype and the reference sequence. The screening of the 'Vada' BAC library with flanking markers (G2x_4 and M14_22), the co-segregating markers (G2x_6, M21, M29, M30, M23, M25 and M14_31) and two additional markers (G2x_6 and M14_31) resulted in the identification of six positive BAC pools (V10, V34, V51, V54, V55 and V88). From each positive BAC pool, a single monoclonal was isolated (see section 2.10) and confirmed by the marker used for screening the library. The confirmed isolated monoclonals were draft sequenced and assembled, resulting in four contigs (V_C1 to V_C4). The

distribution of ‘Vada’ first draft assembly along the *MILa-H* interval based on the barley genome reference is depicted in Figure 15. Since the DNA sample of each ‘Vada’ BAC was not barcoded separately before the sequencing, the construction of a continuous contig covering the entire interval was hampered by the presence of repetitive sequences within the target region. The summary of sequence comparison of the ‘Vada’ draft BAC assemblies and the markers PCR amplicon is presented in Table 18. The result showed that all the markers at the *MILa-H* interval were present on the draft ‘Vada’ BAC assembly. In addition, a structural variation (large inversion) was identified between the ‘Vada’ and ‘Morex’ haplotypes as both BAC V34 and BAC V69 (hit by M21) were also hit by M23 and M25 at the *MILa-H* interval (Figure 15) indicating that the *HORVU2Hr1G126440* and *HORVU2Hr1G126510* gene models have most likely two paralogs in the ‘Vada’ haplotype, similar as what was observed in the their re-sequencing results in ‘HOR2573’ genome. Furthermore, the CDS sequence of the *HORVU2Hr1G126250* gene model, as the best potential candidate gene was selected from the barley reference genome and blasted against all ‘Vada’ BAC contigs. The result showed that this gene model was present in V_C1 contig, showing 85% identity (SNPs polymorphisms) with the corresponding gene in ‘Morex’. In addition, the ORF of this gene model obtained from re-sequencing result of ‘HOR2573’ was compared to the corresponding gene model in ‘Vada’; indicating that they had 88% identity to each other, with eight common SNPs.

Table 18: Summary of sequence comparison result between draft ‘Vada’ assemblies and the markers PCR amplicon.

Query	Vada	Identity (%)	q_len (bp)	Mismatch (#)	Gap (#)	ref_start match	ref_end match	E_val.	bitscore
V10_M25	V_C4	100	689	0	0	47,851	48,539	0.0	1,273
V34_M21	V_C1	100	714	0	0	101,978	102,691	0.0	1,319
V34_M23	V_C2	89.7	713	73	0	41,390	42,102	0.0	913
V51_M25	V_C4	100	689	0	0	47,851	48,539	0.0	1,273
V51_M23	V_C2	100	714	0	0	101,978	102,691	0.0	1,319
V55_M14_31	V_C3	99	555	1	0	19,148	19,702	0.0	1,020
V55_M14_22	V_C3	100	459	0	0	10,855	10,397	0.0	848
V88_M29	V_C1	100	796	0	0	21,172	21,967	0.0	1,471
V88_M30	V_C1	100	776	0	0	25,656	26,431	0.0	1,434
V88_G2x_6	V_C1	100	1,001	0	0	121,615	122,615	0.0	1,849
V54_G2x_4	V_C1	100	736	0	0	24,174	23,439	0.0	1,360

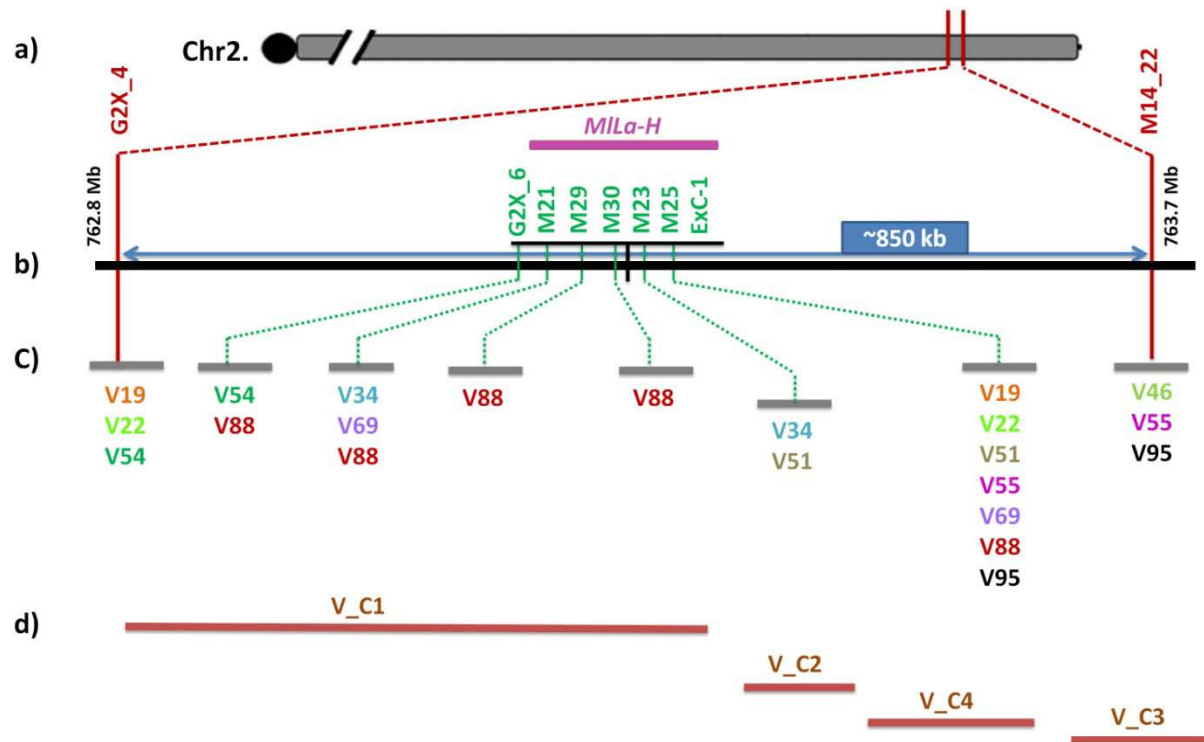


Figure 15: Schematic illustration of the physical map construction for the *MILa-H* interval in ‘Vada’ draft assembly.

a) The target interval containing the *MILa-H* locus as delimited by high resolution mapping on barley chromosome is indicated by two red vertical lines (position of the closest flanking markers). b) Expanded view of the delimited target interval on physical scale according to the barley reference genome. The red vertical lines stand for flanking markers and the physical position of flanking markers is written beside the DNA marker ID. Markers co-segregating with the resistance locus (*MILa-H*) are highlighted in green and they are physically ordered according to the barley reference genome sequence. The black solid line represents the chromosome 2HL pseudomolecule c) The positive ‘Vada’ BAC pools. The DNA markers in the *MILa-H* interval were used to screen the ‘Vada’ BAC library. For each marker the corresponding positive ‘Vada’ BAC clones spanning the *MILa-H* interval are written below a gray line. The common BAC clones between markers are highlighted with the same colors. d) The sequence comparison of the PCR amplicon from each ‘Vada’ BACs was aligned to ‘Vada’ draft BAC assembly. The name of each assembled contig is written above the dark orange line.

4 Discussion

This study reports the result of using barley genomic resources and state-of-the-art technologies to gain insights into a resistance locus called *MILa-H*, located on the telomeric region of the barley chromosome 2H. The locus interval corresponds to the interval of *MILa*, derived from *H. laevigatum*, a well-documented powdery mildew resistance locus. Due to its durability – a result of its intermediate reaction type – the *MILa* locus has garnered much attention from barley breeders and was immediately introduced into the modern barley varieties ‘Minerva’ and ‘Vada’ (Dros, 1957). The critical nature of *MILa* has long attracted considerable interest in localizing the gene on barley chromosomes through continuous advances in molecular markers. However, in all previous studies, the target region carrying the *MILa* locus was mapped within a large interval and the flanking markers were not precise enough for either MAS or map-based cloning of the candidate gene. The initial genetically assignment of the *MILa* locus at the distal end of barley chromosome 2H was reported by Hilbers et al. (1992) in ‘1B-87 × Vada’ population using the first barley linkage maps constructed by Graner et al. (1991). Hilbers and his colleagues positioned the *MILa* locus within an interval with the size of 13 cM, flanked by MWG66 (proximal to *MILa*) and MWG97. Giese et al. (1993) confirmed the reported interval and reduced it to 10 cM by adding extra RLFP markers provided by Shin et al. (1990). Furthermore, Backes et al. (2003) conducted a QTL analysis again on ‘1B-87 × Vada’ population in order to find novel chromosomal regions carrying resistance genes against powdery mildew and leaf rust. This led to the assignment of the *MILa*-locus distally to the last marker (MWG539) on chromosome 2H. In ‘L94 × Vada’ population, saturation of the genetic region carrying the *MILa* gene with the previously reported molecular markers as well as additional molecular markers led to assignment of the *MILa* interval to an interval with the size of 4.3 cM, flanked by marker WBE138 and WBE145 with two co-segregating markers MWG2200 and WBE141 (Marcel et al., 2007). By anchoring of the both flanking and co-segregating genetic markers of *MILa*-QTL from NIL population to the physical interval of *MILa-H* in the current study (Figure 11), it can be postulated that the same resistance locus contributes to the resistance in ‘Vada’ (derived from ‘*Laevigatum*’) and ‘HOR2573’, maybe with different alleles.

4.1 Fine mapping allowed to map the *MILa-H* locus in a 850 kb interval

The current study presents the first high resolution genetic map of a dominant powdery mildew resistance locus corresponding to the *MILa* locus interval. This effort positioned the *MILa-H* locus within an 850-kb region carrying four disease resistance gene homologs. The resolution achieved in this experiment is considerable, although the initial mapping of the *MILa-H* locus shows a slight deviation of the observed recombination frequency from the average predicted value for the telomeric region of the barley chromosomes: the observed physical to genetic distance ratio at the *MILa-H* locus was ~ 1.16 Mb/cM, whereas an average predicted recombination frequency of 2 Mb/cM was determined for distal regions of the barley chromosomes (Ariyadasa et al., 2014). This discrepancy as well as the observed cluster of several co-segregating markers with the resistance locus may indicate that the recombination frequency was suppressed by chromosomal rearrangements. Therefore, further increase of the genetic resolution through recombination to disclose some of the candidates might be impossible. The presence of structural variation (large inversion) identified between the resistant (Vada) and susceptible (Morex) haplotypes (discussed in 4.3) offers further support for this finding (Figure 15). A genome reference survey from various species, including rice, *Arabidopsis*, and barley, provides general agreement on the widespread occurrence of local rearrangement among R genes triggered by the evolutionary event between plants and their pathogens (Meyers et al., 2003; Monosi et al., 2004; IBSC, 2012). This is clearly demonstrated in Hanemann et al.'s (2009) study on fine mapping of the *Rrs2* gene conferring resistance to barley leaf scald. At the genetic resolution provided by 4,721 F2 plants, the *Rrs2* gene was fine mapped to an interval of 0.08 cM containing several co-segregating markers with the locus. Although this size of the population was already predicted based on the recombination rate in the interval, to break the co-segregation of markers, the size of the mapping population was doubled. However, the population re-enlargement did not result in a higher genetic resolution of the *Rrs2* locus. The haplotype analysis showed a large linkage block extending over several hundred kb derived from a local chromosomal rearrangement in all cultivars carrying the *Rrs2* gene, which was not found in non-*Rrs2* cultivars. Similarly, Wei et al. (1999) identified a strongly suppressed recombination within a delimited 240-kb interval carrying the barley *Mla* powdery mildew resistance cluster on the barley chromosome 1H, caused by a lack of proper pairing and subsequent strand exchange between homologous regions in the parents. Analogous results were found for *Ty-2* resistance to

Tomato yellow leaf curl virus (Wolters et al., 2015) and for *Mi-1* resistance of tomato to root-knot nematode (Seah et al., 2004), both introgressed from wild relatives.

4.2 A gene encoding LRR-RLK protein is the best candidate gene in the *MiLa-H* interval

It has been already noted that ‘HOR2573’ responds to the several tested *Bgh* isolates including CH4.8 by triggering hypersensitive cell death at early stages during the interaction with pathogen (unpublished data, personal communication with Dr. Patrick Schweizer). This study highlights the presence of four disease resistance gene analogs in the delimited *MiLa-H* interval, one gene belongs to RLK and the rest to the NBS-LLR gene family, the two most represented groups of R genes, in context of dominant race-specific resistance which make each of them potentially a candidate gene for the *MiLa-H* locus.

The re-sequencing analysis of three out of four R genes within the *MiLa-H* interval from ‘HOR2573’ displays functional polymorphisms from SNPs to medium and / or large-scale insertions and deletions leading to premature stop codons compared to susceptible parent cv. ‘Morex’. These findings exclude those three genes as candidate genes for the *MiLa-H* locus, as all the structural variations are likely to lead to loss of function in the resistant genotype. In the gene model *HORVU2Hr1G126380*, predicted to encode a NBS-LRR gene, the frame-shifting deletion and insertion were observed in LRR domain leading to the premature stop codon and a probable loss of function of the domain. The LRR domain in R genes have a specific function as site of protein-protein interaction for the recognition of pathogen effectors (Dangl and McDowell, 2006; Ye et al., 2017). Previous studies showed that the LRR domain and its sequence are essential for the recognition of the pathogen, and a mutation in different motifs of LRR domain in R genes could change the gene function either to the partial or complete loss of function of NB-LRR genes (Warren et al., 1998). Gassmann et al. (1999) showed that the transformation of the genomic sequence of *Arabidopsis RPS4*, a member of NBS-LRR family conferring resistance to *Pseudomonas syringae* pv Tomato strain, causing premature stop codons in LRR domain impeded the function of *RPS4*. It is then unlikely that a NBS-LRR gene with a severely truncated LRR domain would be a resistance gene. A similar situation has been also observed in *HORVU2Hr1G126510* gene model, in which the presence of early premature stop codon occurred in CC domain, first functional domain of the protein, making it a pseudogene. In the

HORVU2Hr1G126440 gene model, a premature stop codon occurs in the NB domain predicted to cause loss of function too.

Interestingly, the sequencing results of these four R genes from the resistant parent point toward the gene model *HORVU2Hr1G126250* to be the best candidate for the *MILa-H* locus among the list of potential candidate genes. From the structural annotation, this gene model belongs to the Receptor-Like Serine / Threonine Kinase (RSTK) gene family; meaning that it contains an extracellular region, a single membrane spanning domain and an intracellular kinase domain (Becraft, 2002). The kinase domain independent from other domains can be involved in both elicitor/effector recognition and also serine / threonine phosphorylation (Bogdanove and Martin, 2000). It phosphorylates the OH group on the side chain of serine or threonine residues, resulting in a functional change of the target protein by modifying enzyme activity, changing its and probably other proteins' cellular locations in order to finally trigger the resistance (Dhanasekaran and Reddy, 1998). This gene family is highly diverse in the number of domains, for instance, the tomato *Pto* is a well known cytoplasmic serine / threonine kinase which does not have a ligand binding motif, yet, directly binds to *AvrPto*, the pathogen effector and involves in basal signaling pathway (Bogdanove and Martin, 2000). In barley, *Rpg1*, another race-specific stem rust-resistant gene that encodes a serine / threonine kinase protein was identified to have the similar mechanism like the tomato *Pto*. It has two tandem kinase domains which is a novel structure for proteins contributing in disease resistance in plants (Brueggeman et al., 2002). However, the major group of RSTK contain LRR domain, the extracellular region that is recognized by the repeated sequence LxxLxLxxNxLxx. A typical LRR belongs to the 3, 6, 12, or 24 repeat subfamily of LRR (Kajava, 1998). The structural annotation of the gene model *HORVU2Hr1G126250* implies that this gene contains an extracellular LRR domain with 6 repeats. The resistant parent's genome contains 4 synonymous and 16 nonsynonymous SNPs for this gene compared to 'Morex', leading to amino acid changes in both LRR and kinase domains. Among the four R genes in this cluster, this gene is the only one with meaningful non-synonymous polymorphisms. The study of divergence between ancestral copies of LRR-RLK represented that some LRR-RLK characterized by fixation of a higher number of non-synonymous than synonymous mutations at some amino acid sites, highlighting the emergence of probably new advantageous functions for these R genes (Dufayard et al., 2017). It has been reported that both LRR and kinase domains are under different selective pressures according to their roles in resistance response. The LRR

domain has often the experience of a diversifying selection phase, obtaining new advantageous genetic variants, most likely in order to recognize the new virulent pathogen effectors, while the kinase domain is typically under purifying / negative selection leading to the removal of alleles that are deleterious such as functional and structural restrictions involved in signal transduction (Zhang et al., 2006).

Although the comparative sequencing analysis of the putative candidate genes in this target interval would provide the clear evidence on potential candidate gene, further investigations are still required to determine the function of the potential candidate gene, *HORVU2Hr1G126250*, as well as the other three NBS-LRR genes in the *MILa-H* locus. The gene functional analysis can be performed either through the over-expression of the gene of interest and silencing using RNA interference (RNAi)-based silencing or so-called Transient induced gene silencing assay (TIGS). Both approaches have been developed over the years and proven to be valuable tools for identification the gene function (Ihlow et al., 2008; Douchkov et al., 2014). The TIGS and overexpression constructs can be generated in plasmid vectors pIPKTA9 and pIPKTA30 as defined by previous studies (Schweizer et al., 1999; Douchkov et al., 2005). The approach for both techniques is rather the same; meaning that full length of cDNA of the genes (from 'HOR2573') are cloned into the hairpin vector pIPKTA9 (overexpression construct) and pIPKTA30 (RNAi constructs) for TIGS assay as described previously by Douchkov et al. (2005) and are bombarded into leaf segments, followed by inoculation by the isolate CH4.8. It is expected that overexpression of the genes that doesn't provide resistance on susceptible plants should result in super-susceptibility whereas the overexpression of the responsible gene for the trait on susceptible parent / genotypes leads to resistance. In transient gene silencing, the constructs will be checked in both susceptible and resistant parents to assess their phenotypes (Schweizer et al., 1999). In comparison with the stable transformation, both assays can be performed in 10 days and the function of genes can be assessed without the generation of transgenic plants. The only negative point is rather the typical variation in results using biolistic particle delivery system; however, it can easily be solved by higher technical replicates.

If *HORVU2Hr1G126250* is validated, the question of the causal SNPs will still be relevant. To rule out whether the polymorphisms in LRR domain or kinase region alter the resistance to powdery mildew, the chimeric gene constructs (different combinations of these two domains of

the *HORVU2Hr1G126250* gene from both ‘HOR2573’ and ‘Morex’) can be produced and introduced into the susceptible parent, ‘Morex’. The transformed plants can then be inoculated with the *Bgh* isolate CH4.8. Depending on the results, it can be concluded which domain is responsible for the trait of interest.

4.3 Is another gene present in the *MILa-H* interval?

Even if *HORVU2Hr1G126250* is a good candidate, it cannot be ruled out that the resistance is provided by presence / absence variation (PAV) of a resistance gene between resistant and susceptible genotypes, meaning that the candidate gene might be missing from the genome of a susceptible genotype. As a well-known event, the plant genomes evolution has occurred through whole genome duplication and insertion / deletion (Indels) leading to some gene losses. Such broad rearrangement events can lead to PAV and structural variations (SVs) in plant genomes between and within species (Griffiths et al., 1999). Indeed, these segmental duplications as well as transposons, increase the genome redundancy (reviewed by Flagel and Wendel, 2009) providing situations for the unequal crossing-over between misaligned sequences. Several studies have underlined the high possibility of identification of PAV between genotypes with contrasting phenotypes. Grant et al. (1998) studied the structure of *Rpm1* conferring resistance to *Pseudomonas syringae*, pv *maculicola* in nine *Arabidopsis* accessions and they found that all four disease-resistant accessions have a nearly identical haplotype (with few SNPs difference) to the reference allele (resistant genotype) while the five susceptible accessions contain a null haplotype implying that the entire *Rpm1* gene (3.7 kb of nucleotide sequence) was absent. This finding suggests the functional polymorphism in an R gene locus can occur from PAV of genes. The structural variation might also be observed by variable number of homologs in each haplotype which is the most prevalent PAV in multigene loci (Bergelson et al., 1998). For instance, the structural comparison of *Rpp5*, a multigene locus in a downy mildew resistant *Arabidopsis* ecotype, Landsberg erecta (Ler) with a susceptible ecotype, Columbia (Col-0) revealed the presence of ten *Rpp5* homologs in the entire Ler haplotype whereas *Rpp5* haplotype in *Col-0* consisted of eight homologs. They proposed the *Rpp5* locus contained dynamic gene clusters with capability to adapt fast to a new pathogen variant through modification of recognition regions, implying that these regions have been most likely experienced a diversifying and purifying selection (Noël et al., 1999). The structural analysis in both *Rpm1* and *Rpp5* clearly showed this

variation was directly associated with the phenotype. Thus, the availability of the complete DNA sequence of the *MILa-H* interval from both susceptible and resistant genotypes would allow for analyzing and comparing the intraspecific variations including PAV, copy number variation (CNV) and SV at this locus.

To obtain evidence of the presence of a similar inversion or PAV in the *MILa-H* locus in 'HOR2573', two state of the art approaches are proposed to further investigate the target region. The first approach is targeted chromosome-based cloning (TACCA) through long-range assembly (Thind et al., 2017). It combines short-read Illumina sequences of a single chromosome sorted by flow cytometry with proximity ligation of *in vitro*-reconstituted chromatin, also known as Chicago (Putnam et al., 2016). Developing high-quality *de novo* assemblies from the flow-sorted barley chromosome 2H can be a way to study the *MILa-H* locus in 'HOR2573'. Such libraries are easier to handle, allowing to *de novo* assemble a complete chromosome with a limited cost to detect structural variation and simplify contig assembly compared to the whole-genome BAC libraries where the sequences are mapped on a reference genome (Doležel et al., 2007). This approach was applied in hexaploid wheat with the complex genome for rapid cloning of agriculturally important genes (Thind et al., 2017). In this approach, the mitotic chromosomes are classified through flow cytometry according to light scatter and fluorescence parameters. The chromosome of interest is then purified by flow sorting (Vrána et al., 2000) and will be sequenced.

The large size of the barley genome (~5.1 Gb) and the highly repetitive nature of its genome make the barley whole genome sequencing with sufficient read coverage costly. In the present study, despite the high-density linkage map construction and further marker development, the detection of small chromosomal inversion in the identified locus interval is impossible. In addition, mapping the chromosome breakpoints using traditional methods like *in situ* hybridization through fluorescent dye-labeled BAC clones (BAC-FISH) is rather laborious and the obtained resolution is often insufficient to clearly identify the disrupted gene in particular for the inverted segment with the size of ≤ 500 kb. Therefore, the sequencing of a single chromosome is an invaluable tool to decipher small structural variations. Moreover, the telomeric region of barley chromosomes are known to be rich in genes, and particularly in disease resistance genes (Dilbirligi et al., 2005; Schweizer and Stein, 2011; Surana et al., 2017). Several significant QTL

near the distal end of this chromosomal region have repeatedly been reported to be associated with disease resistance (von Korff et al., 2005b; Marcel et al., 2007; Schweizer and Stein, 2011). Therefore, the sequencing of flow-sorted chromosome 2H from 'HOR2573', as a barley resistance genotype will add valuable genomics data in this region that may significantly benefit to other disease resistance researches. Chen et al. (2008) showed that the sequencing of flow-sorted derivative chromosomes is a well-designed approach to resolve the chromosome composition and map-based breakpoints on the chromosome with an error margin of less than 1,000 bp. Mayer et al. (2009) showed that by combining NGS and chromosome sorting, they could gain insight into the gene content of an entire Triticeae chromosome. In this approach, ~40% of sequence-tagged genes were anchored to barley chromosome 1H through the conjunction with high-resolution synteny data from rice and sorghum. Using NGS of the mitotic flow-sorted chromosome along with synteny-based comparisons with other grass genomes, the challenge of sequence assembly by excluding a large proportion of repetitive sequences in the barley genome was significantly reduced (IBSC, 2012). Hernandez et al. (2012) reported that this technique has facilitated the construction of an ordered gene map of the wheat chromosome 4A and the precise localization of the various translocation and inversion breakpoints on this chromosome.

Targeted Locus Amplification (TLA) is another interesting approach that recently being introduced by Cergentis, in a close collaboration with several Medical Center universities in the Netherland (de Vree et al., 2014). This technique can be used to target the region of interest (e.g. the *MILa-H* locus interval), and to sequence a highly interval-enriched library and assemble this interval with a cost even lower than the sequencing of the flow cytometry sorted chromosome. This approach can uncover all the possible genetic variation including structural variants in the targeted region. It relies on a method similar to Circularized Chromosome Conformation Capture (4C) technique, with a slight modification. Likewise 4C, the TLA is based on the basis of the crosslinking of physically proximal sequences, but in the TLA, the selected region is completely amplified; meaning that the entire genes in this interval are sequenced (De Vree et al. , 2014) whereas in 4C approach only the end of each ligated DNA fragments are sequenced (Zhao et al., 2006). Using this technique a wide range of chromosomal rearrangements including breakpoint as well as SNVs and Indels can be detected which allow extensive characterization of targeted regions and haplotyping across large genomic intervals. De Vree et al. (2014) identified the

chromosomal rearrangements across 81 kb and mapped the breakpoints at base-pair resolution of the mutated *BRCA1* gene, a well-known tumor suppressor gene in human. They showed that by using TLA approach, a single anchor primer pair inside the gene can amplify sequences across the 81-kb *BRCA1* gene whereas in the PCR-based exon sequencing methods previously used in clinics, ≥ 30 amplicons spanning the region had to be analyzed to identify the harmful mutations in this region. Since the 4C technique is already established and routinely being used in the Genomics of Genetic Resources group, in IPK Gatersleben, a slight modification of the protocol (using extra digestion enzyme and one single specific primer pair for each gene in the *MILa-H* interval) may be sufficient to investigate easily the structural variation within this region.

As time and budget constraints did not allow to perform this experiment, the construction of the *MILa-H* physical map using available ‘Vada’ BAC library was taken as an alternative approach. Considering the fact that the *Mla* locus interval (derived from resistance cultivar ‘Vada’) overlaps with the physical position of the *MILa-H* locus (Figure 11), the use of ‘Vada’ BAC library for physical map construction of this interval would provide important clues on the structure of the *MILa-H* locus in a resistant haplotype. However, it is important to note that in case of detection of PAV of an R gene between ‘Vada’ and ‘Morex’, this has to be verified in ‘HOR2573’. The complementary approaches such as gene expression analysis and / or TIGS for the respective gene can validate whether the identified R gene in ‘Vada’ is responsible for resistance in ‘HOR2573’ as well. The draft of ‘Vada’ BAC contig assembly for the *MILa-H* locus showed a considerable SV (large inversion) within the interval between resistant (Vada) and susceptible (Morex) haplotypes. The result suggests a model in which a chromosomal segment carrying the two *HORVU2Hr1G126440* and *HORVU2Hr1G126510* models was experienced a duplication caused by misalignment of regions that shared high sequence homology. This is then followed by the inversion of a segment in this region (Figure 16). This proposed model also fits well with the finding of paralogs in ‘HOR2573’ re-sequencing results for these two gene models and suggests that these R genes have most likely experienced local rearrangement during the evolutionary history in this interval.

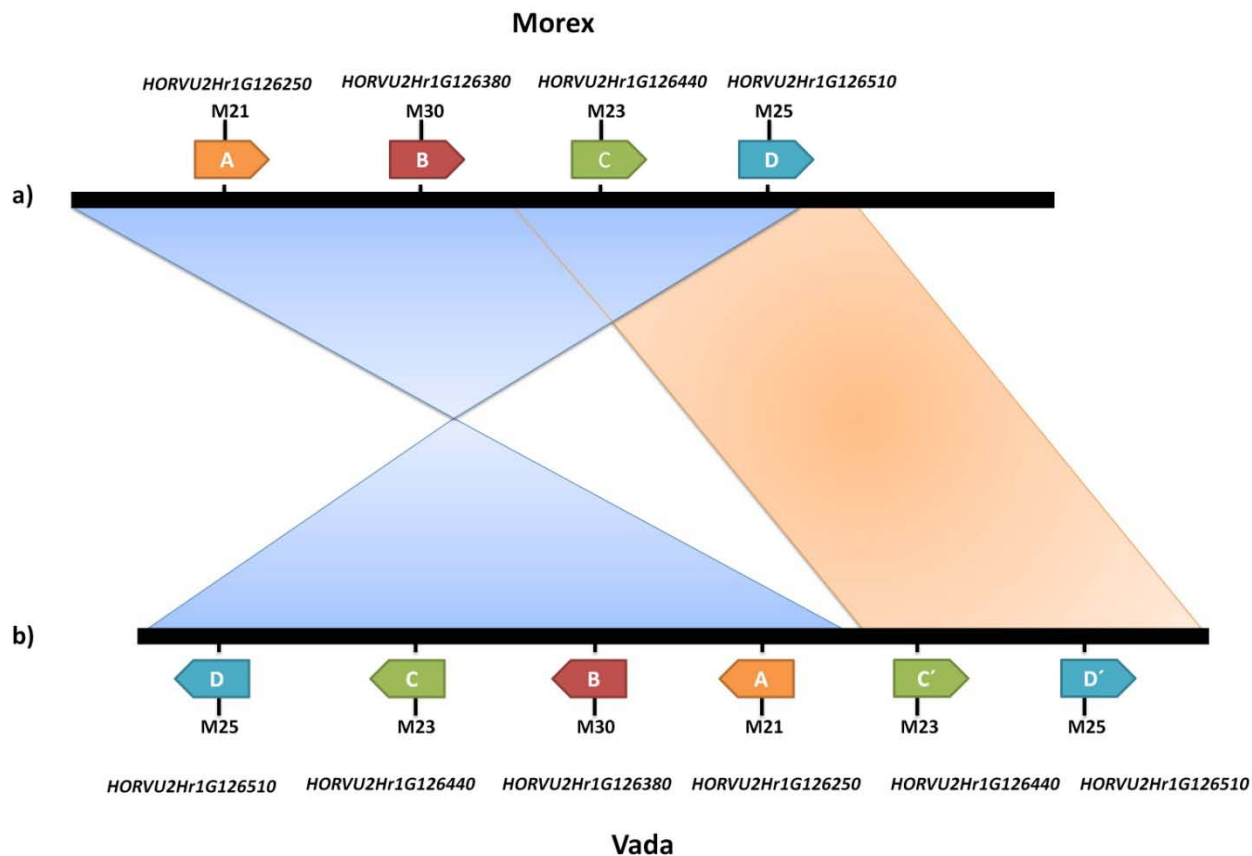


Figure 16: Schematic illustration of the structural variation within the *MILa-H* locus interval between resistant (Vada) and susceptible (Morex) haplotype

a) The Structure *MILa-H* locus interval in the barley reference genome (cv. Morex) b) The proposed model for the structure *MILa-H* locus interval in ‘Vada’ based on draft ‘Vada’ BAC assembly. The model suggests the presence of SV (large inversion) between ‘Vada’ and ‘Morex’ haplotypes. The chromosomal region carrying gene C and D has experienced a duplication (highlighted in light orange) followed by the inversion of the segmental region containing gene A, B, C and D (highlighted in light blue). The Black solid line stands for the *MILa-H* locus interval. The colorful pentagons present the R genes in the *MILa-H* interval. The name of each gene is written below each pentagon.

In addition, although the published barley pseudomolecule is a highly contiguous reference genome sequence, the comparative approaches to the diverse barley individuals’ assembly are highly recommended while the different individuals may have different translocations and inversions. In this regards, IPK groups recently produced the genome assembly of three barley genotypes, Barke (a two-row spring barley cultivar), FT11 (*H. spontaneum*) and HOR10350 (an

Ethiopian barley landrace) based on Illumina sequencing data assembled with NRGene's DeNovoMAGIC™ software (Prof. Dr. Nils Stein and Dr. Martin Mascher, personal communication). The assembly of these three genotypes, in particular 'HOR10350' which is close to 'HOR2573' in barley diversity can permit to further investigate the *MILa-H* interval by unraveling a part of the structural variations that exist in barley.

4.4 Genetic mapping and its successors: advanced tools for defining the gene location

The current study highlights the use of GBS technology for the construction of a high-density linkage map of a barley RIL population. In the low resolution mapping step, by taking the advantages of GBS along with the accurate phenotyping assessment, the *MILa-H* locus was initially assigned within an interval of 3 cM, corresponding to 3.5 Mbp at the physical scale. For the high resolution mapping step, the SNPs derived by GBS were being easily converted to individuals CAPS markers to saturate the target region, screen the recombinants and reduce the target interval. The low cost of GBS, makes it an attractive approach to create a dense genetic map and to allocate precisely any resistance QTL interval in mapping and breeding populations. As the amount and quality of generated sequence data per run keep increasing, GBS has become a cost-competitive alternative to other whole-genome genotyping platforms (Elshire et al., 2011b). In addition, for crops with big genomes like barley, this technique is technically less challenging compared to exome sequencing owing to reduced sample handling and few PCR and purification steps, making it a highly rapid approach (He et al., 2014b). In fact, following the DNA extraction, the library preparation for 200 lines takes only less than one week. Although creating a dense genetic map is an important step in the genetic mapping of a locus, increasing the size of mapping population and marker saturation within the target interval are essential steps to obtain a higher resolution at the chromosomal region containing the target gene. In the current study, a cluster of related disease resistance genes, RLK and NBS-LRR genes, were located in close physical proximity at the targeted interval. The deviation of the observed recombination frequency from the average predicted value for the telomeric region of the barley chromosomes offers clear clues for suppressed recombination at this interval which was also detected in 'Vada' haplotype. In this situation, the population size enlargement cannot help to obtain a higher resolution. Resistance gene enrichment sequencing (RenSeq) approach is an innovative approach that could have been used instead of classical gene mapping to further facilitate the candidate

gene identification process (Jupe et al., 2013). It can be used for mapping of resistance loci in segregating populations but also for rapid cloning of R genes *via* its combination with mutagenesis (Mutagenesis and Resistance gene enrichment sequencing: MutRenSeq). The latter approach is especially useful in the regions where dissection of the resistance locus through recombination is not realistic like the situation observed in current study (Steuernagel et al., 2016). Both RenSeq and MutRenSeq approaches are based on enrichment sequencing, eliminating the necessity to sequence the whole genome. In fact, all genomic regions complementary to the R-encoding genes of the reference genome are captured by baits of 120 nucleotides (Steuernagel et al., 2017). This provides an opportunity to explore the allelic diversity at R genes. Jupe et al. (2013) applied RenSeq to identify NBS-LRR alleles that co-segregate with the underlying resistance in a wild potato population that was segregating for late blight resistance. This approach highly facilitated the development of the closest markers for the *Rpi-rzc1* gene conferring broad-spectrum resistance to potato late blight within a cluster of candidate R genes (Śliwka et al., 2012). Both approaches can be applied to quickly map all functional R genes to control important crop diseases, and to identify previously uncharacterized R encoding sequences (Jupe et al., 2012, 2013; Steuernagel et al., 2016). Jupe et al. (2013) demonstrated that a large fraction of the identified R loci mapped on genomic regions for which no gene models were provided by the Potato Genome Sequencing Consortium (PGSC). Thus, it is highly proposed to consider RenSeq as a helpful technique to improve the current barley reference genome annotations for R genes. In the current study, it was shown that the automated annotation for two R genes located in the *MILa-H* interval, was incomplete and gene prediction software failed to annotate some parts/exons. This might also be true for the rest of the genome. Using RenSeq, it was realized that many R genes that were annotated by PGSC as partial, were in reality full length, with large gaps/missing some sequences (Jupe et al., 2012; Steuernagel et al., 2016). The main limitations in assemblies are direct consequences of extreme abundance of repetitive elements in the genome, and the severely reduced frequency of meiotic recombination in pericentromeric regions (Mascher et al., 2017). As in RenSeq, the complexity of the genome is significantly reduced in a non-random manner, this limitation might be overcome. Nevertheless, Steuernagel et al. (2016) reported that by using Illumina 250-bp paired-end sequencing reads in RenSeq and MutRenSeq, they also faced difficulties to bridge a gap by a 2,920-bp intron located between two exons of *Sr22* gene. This could be due to the short reads obtained from Illumina sequencing as well as high sequence similarity of large R gene sub-families which might cause

some misassemblies or some incompleteness of predicted annotations (Steuernagel et al., 2017). This limitation could be overcome if the DNA and even, RNA samples of respective individuals are being sequenced using a long-read sequencing technology such as PacBio (Steuernagel et al., 2016; Witek et al., 2016; Bevan et al., 2017). One drawback of RenSeq is that the broad sequence diversity among parental R gene families prohibited the identification of the individual R genes responsible for resistance which can be easily be solved by using MutRenSeq. Steuernagel et al. (2016) used RenSeq in combination with mutagenesis to identify R genes that mediate resistance. By using ethyl methanesulfonate (EMS)-derived loss of function mutants, and crossing with the wild-type resistant genotype, they created the independent M₂ families and did screening for susceptible mutants in each family. In conjunction with a *Triticeae* NBS-LRR-specific bait library and sequencing of the wild-type and susceptible mutants, they successfully cloned two major dominant wheat stem rust genes, *Sr22* and *Sr45*. This approach is a very novel and practical approach for the cloning of R genes regardless of where they reside within the genome (on telomeric or centromeric regions) and whether they have experienced suppression recombination due to SV or not (Jupe et al., 2012; Bevan et al., 2017). By EMS mutagenesis of the resistant plant (HOR2573) in the current study and creation of independent M₂ families and screening for susceptible mutants for various disease resistant traits like resistance to leaf rust, leaf blight, powdery mildew and etc., all the possible resistance genes present in this accession can be identified. For the target enrichment, it is proposed to add the annotated RLK family genes from *Triticeae* gene recourses to available *Triticeae* NBS-LRR-specific bait library and do sequencing of the wild-type and susceptible-mutants, data analysis and finally candidate calling. For mapping, *de novo* assembly of the enriched sequences of the resistant wild-type can be used as a reference. This approach provides important clues on SV and PAV within R genes on the genome-wide scale (Steuernagel et al., 2017). The key advantages of this approach are that it is highly rapid compared to classical map-based cloning approach (<24 months), without a need for fine mapping and the construction of physical contig spanning the target interval. Furthermore, this approach allows to rescue R genes from crop wild relatives-introgressions (from *H. bulbosum*) or barley accessions found in Genebanks which are not currently being used in breeding program owing to linkage drag, and provide an opportunity to clone rapidly R genes that could be used in multi-R gene pyramiding efforts, a strategy that promises more durable disease resistance in crops (Bevan et al., 2017; Steuernagel et al., 2017).

4.5 Can the durability of *MILa-H* be increased by allele or gene pyramiding?

The development of barley varieties with durable resistance to powdery mildew has been one of the objectives in disease resistance breeding programs. In barley, several types of race-specific mildew resistance genes have already been identified. Most of them have been mapped or tagged with DNA-markers. The resistance alleles derived from *Mla*, *MILa*, *Mlk*, *Mlg*, *Mlh*, and *aMlra* have been used in European barley cultivars (Jørgensen and Wolfe, 1994; Czembor J. H. and Czembor H. J., 2001). From those, the identified resistance alleles at *Mla* locus are highly popular among breeders, as they provide resistance against barley powdery mildew specific races (Boyd et al., 1995; Seeholzer et al., 2010). Another popular locus among breeders is *MILa* as it is characterized by intermediate reaction type or partial resistance. In this study, the identified locus called *MILa-H* confers major race-specific (qualitative) resistance against a powdery mildew pathogen. Compared to quantitative resistance (conferred by several genes with small effects), this type of resistance is easy to incorporate into breeding programs, however, it is often not durable because of rapid changes in the pathogen virulence (Parlevliet, 2002). Combining multiple highly effective R genes, each covering a broad race spectrum, with many known successes is a practical approach to prevent or delay the development of boom-and-bust cycles commonly observed in the deployment of single R genes. The best-documented gene pyramiding is the combination of wheat stem and leaf rust resistance genes that controlled the corresponding diseases in wheat since the mid-1950s (McIntosh and Brown, 1997). Although the emergence of new wheat stem rust race 'U99' in the late 1990s in Uganda overcame this pyramid (Singh et al., 2008), controlling a wheat major pathogen for 25 years is an incredible success.

The overlapping of the *MILa* locus interval with the *MILa-H* locus possibly means that these two loci are two different genes or different alleles of the same gene. Combination of the two R genes is expected to extend the durability of R-gene as the pathogen will have to evolve multiple Avr genes simultaneously to gain virulence on such pyramided lines which is very unlikely event (McDonald and Linde, 2002). Different allelic variants of the same R gene can also be combined as an alternative to the stacking of different R genes. By crossing transgenic lines having different alleles, a combination of various alleles can be achieved. There are several promising examples of how genetic diversity at a locus can also be exploited for improving resistance. Using this approach, Bieri et al. (2004) increased powdery mildew specificities by developing pyramided

lines containing both the *Mla1* and *Mla6*, alleles at the *Mla* locus in barley. Chen et al. (2008) improved flax rust resistance by combining *L6* with the *L2* or *L10* alleles in one line. To determine the relationship between two loci, the complementation test is a common approach that can be performed; e.g. in current study, the test can be carried out by crossing ‘HOR2573’ with ‘Vada’ as they have the powdery mildew resistance gene at the same chromosome region and, checking the segregation pattern in F₂ plants. But the conclusion can be difficult to make as, if there is two genes in high linkage disequilibrium, their segregation in the absence of recombination can be mistaken for the segregation of two alleles of a single gene. Thus, checking these two loci at the sequence level is only way to identify the causal polymorphisms and to determine whether they are two genes or different alleles of the same gene. Following the identification of the relationship between these two loci, the next step is to check whether they are compatible with each other as well as with the genetic background. Functional incompatibilities between resistance genes / alleles and also with the genetic background often cause limitation in combination of different R genes or alleles. In fact, some pairwise combinations of different alleles might result in suppression of resistance and can negatively interfere with the allele-pyramiding approach. Incompatibility between resistance genes / allele may lead to autoimmunity (Bombliès and Weigel, 2007) and with the genetic background may result in weakened or loss of resistance activity (Chen et al., 2013). Stirnweis et al. (2014) demonstrated that incompatibility among alleles of an NBS-LRR resistance gene can cause suppression of resistance. Their findings suggested that the expression of closely related NB-LRR resistance genes or alleles in the same genotype can lead to dominant-negative interactions. In contrast, Koller et al. (2018) showed that pyramiding of transgenic *Pm3* alleles in wheat enhanced powdery mildew field resistance. Plant development and yield resistant scores of the pyramided lines were highly similar to the average scores of the respective parental lines, and therefore, the allele pyramiding did not cause any negative effects on the resistance. A promising approach that can be utilized for compatibility check of different alleles / genes in pyramiding is targeted genome editing using clustered regularly interspaced short palindromic repeat (CRISPR-associated protein 9 (Cas9) system (Gilbert et al., 2013). This system can also offers valuable clues for other aspects of this locus like, the candidate gene confirmation and the identification of causal polymorphism. Compared to the classical cross-breeding, this approach is a fast and efficient way to introduce either multiple R genes into an existing cultivar or multiple alleles into one single gene. It provides an opportunity to develop simultaneously unlimited combinations of targeted gene / allele

pyramided lines (Ainley et al., 2013) and to assess their phenotypes (reviewed by Barakate and Stephens (2016)). By the development of CRISPR/Cas9, its application in disease resistance has been significantly increased in recent years. Macovei et al. (2018) developed new sources of resistance to *tungro spherical virus* (RTSV) in rice in a significantly shorter time compared to traditional breeding. Using three different gRNAs' regions surrounding encoding the YVV residues in *elf4G* was targeted leading to resistant phenotype to RTSV. The mutations were successfully transmitted to the next generation. Wang et al. (2014) targeted simultaneously editing of three *MLO* loci, which encode proteins that were shown to suppress defenses against powdery mildew diseases in other plants. Loss-of-function *mlo* alleles lead to broad-spectrum and durable resistance. The inoculation result of the leaves of the *tamlo-aabdd* plants showed resistant phenotype, though the leaves of wild-type plants were highly infected. The generated *tamlo-aabdd* alleles in the elite wheat cultivars can serve as prime starting materials for durable and broad-spectrum resistance in bread wheat breeding programs. It is proposed by using this approach, different targeted gene / allele pyramided lines containing *MILa-H* and *MILa* can be developed and then assess their compatibilities to each other. In addition, their combinations with other R genes can add valuable information to the current knowledge.

5 Outlook

The reported high resolution mapping and physical map construction of the resistance locus *MILa-H* display the fundamental steps for map-based cloning of the respective gene. The fine mapping of the target interval revealed the presence of four disease resistance gene homologs belonging to RLK and NBS-LRR gene families at this locus, which are the potential candidate genes for the race-specific resistance phenotype. Although the comparative sequencing analysis of these putative candidate genes between resistant and susceptible parents strongly suggests that *HORVU2Hr1G126250* is the best candidate gene, to validate it, further investigation of this locus are required. In the present work, various novel and practical approaches for additional analysis at this locus have already been discussed in comprehensive details. Those approaches will definitely add extra values to the current work. However, as an outlook, the two main approaches that were already planned will be shortly reminded. Even if *HORVU2Hr1G126250* is the best candidate gene, functional analysis is necessary to validate its function for the observed phenotype. High throughput RNA interference (RNAi) system for transient-induced gene silencing (TIGS) has been developed to categorize genes underlying the trait (Douchkov et al., 2005; McGinnis, 2010; Mohr et al., 2010). Using this system, the function of the candidate genes will be tested for their phenotype in both susceptible and resistant genotypes. In the present study, even if the entire procedure of gene functional analysis *via* TIGS method was not manageable within the agreed time framework of Ph.D. project, all the required initial tasks have already been performed and prepared. The infrastructure at IPK is fully equipped for such transient analysis and the work is now ongoing in collaboration with Pathogen Stress Genomics research group, IPK, Gatersleben in order to be included in a peer-reviewed publication which is in preparation.

Furthermore, it is indispensable to find out whether the resistance phenotype is conferred by the presence of an additional resistance gene which is absent from the barley reference genome (cv. 'Morex' - the susceptible parent of the current population). Given that the intervals of *MILa* and *MILa-H* are overlapping, the newly constructed non-gridded 'Vada' BAC library (Yeo et al., 2016) was screened with the *MILa-H* locus' flanking markers as well as the co-segregating markers to investigate PAV of a resistance gene between resistant and susceptible haplotypes. This allowed me to understand the structure of this locus by reconstruction of its physical map in a resistant haplotype. Since the group of Genomics of Genetic Resources in IPK, Gatersleben is

newly equipped with a PacBio sequencer, the sequencing of the positive single BAC clones has been already scheduled and currently is in progress. This approach will allow to perform *de novo* assembly of the target interval, and to detect SV, PAV, and CNV in a resistant haplotype. The obtained result has to be validated through one of the previously discussed approaches in 'HOR2573' as well.

6 Summary

This study successfully addressed the high resolution mapping of a resistance locus interval, *MILa-H* located on 2HL chromosomal region in barley. To reach the project milestones, the low resolution mapping was performed on an F2S5 population derived from a cross between susceptible cv. ‘Morex’ and resistant barley accession ‘HOR2573’, consisted of 95 RILs by taking the advantage of GBS genotyping as well as an accurate phenotyping assessment. A single major QTL was assigned to an interval of 3.5 Mbp with 95% confidence, co-localizing with the interval of earlier reported *Laevigatum* resistance gene, *MILa*. The identified QTL in the F2S5 confirmed the previously detected QTL in the F2 population. More importantly, this QTL was the only one that significantly contributed to the resistance, explaining on average 73.3% of phenotypic variation, indicating that the resistance in this cross is provided by a single locus. The qualitative re-evaluation of this mapping population revealed that the segregation ratio of resistant to susceptible lines was consistent with the expected inheritance pattern of a monogenic Mendelian factor, indicating that a single dominant gene was involved in the resistance to the tested *Bgh* isolate in this population. The constructed high-density genetic linkage map facilitated fine-scale mapping of the resistance interval. A total of 1,941 F₂-like plants were screened by developed CAPS markers based on GBS derived SNPs and 155 recombinant lines were detected, resulting in further narrowing down of the interval to 850 kb.

The delimited target interval contained seven annotated HC genes; of which four genes belong to two most represented groups of R genes, in context of dominant race-specific resistance, making them potential candidate genes for the *MILa-H* locus. Three out of four R genes within the *MILa-H* interval from ‘HOR2573’ showed the functional polymorphisms, from SNPs to medium and / or large-scale insertions and deletions, leading to premature stop codons in comparison with the susceptible parent cv. ‘Morex’. These findings exclude those three genes as candidate genes for the *MILa-H* locus, since all the structural variations were likely to lead to loss of function in the resistant genotype. The sequencing results of these four R genes from the resistant parent point toward the gene model *HORVU2Hr1G126250* to be the best candidate for the *MILa-H* locus among the list of potential candidate genes. This gene belongs to LRR-RLK family that includes a large number of resistance genes to bacteria and fungi and contained 4 synonymous and 16 nonsynonymous polymorphisms between ‘Morex’ and ‘HOR2573’. Nevertheless, there is also a

high chance that resistance is provided by presence / absence polymorphism of a resistance gene between resistant and susceptible genotypes. Therefore, to understand the structure of the *MILa-H* locus, a BAC library of the genotype 'Vada', carrying the *Laevigatum* resistance gene was screened with flanking and co-segregating markers of the *MILa-H* interval to identify the positive BAC pools. From each positive BAC pool, a single monoclonal was isolated and confirmed through Sanger sequencing of PCR amplicons. The initial sequencing analysis of the single monoclonals led to the identification of a large inversion in the resistant haplotype (Vada) compared to susceptible (Morex) haplotype; indicating that 'HOR2573' probably contains a similar structure variation and any further increase of the genetic resolution at the *MILa-H* locus through mapping population enlargement would not help to disclose some of the candidates through recombination. Based on the current draft assembly of 'Vada' single monoclonals, the identification of PAV of a resistance gene between resistant and susceptible haplotypes are not achievable. Nevertheless, all the isolated 'Vada' monoclonals will be re-sequenced by the use of long-read sequencing PacBio technology and that would allow to figure out the complete structure of this locus in a resistant haplotype. The functional analysis of the best candidate, *HORVU2Hr1G126250*, in this interval through TIGS or overexpression analysis would allow to confirm its implication in the resistant phenotype as well.

7 References

- Ainley, W.M., Sastry-Dent, L., Welter, M.E., Murray, M.G., Zeitler, B., Amora, R., Corbin, D.R., Miles, R.R., Arnold, N.L., Strange, T.L., Simpson, M.A., Cao, Z., Carroll, C., Pawelczak, K.S., Blue, R., West, K., Rowland, L.M., Perkins, D., Samuel, P., Dewes, C.M., Shen, L., Sriram, S., Evans, S.L., Rebar, E.J., Zhang, L., Gregory, P.D., Urnov, F.D., Webb, S.R., Petolino, J.F., 2013. Trait stacking via targeted genome editing. *Plant Biotechnol. J.* 11, 1126–1134. <https://doi.org/10.1111/pbi.12107>
- Alemayehu, F., 1995. Genetic variation between and within Ethiopian barley landraces with emphasis on durable disease resistance. [Agricultural University], Wageningen.
- Aljanabi, S.M., Parmessur, Y., Kross, H., Dhayan, S., Saumtally, S., Ramdoyal, K., Autrey, L.J.C., Dookun-Saumtally, A., 2007. Identification of a major quantitative trait locus (QTL) for yellow spot (*Mycovellosiella koepkei*) disease resistance in sugarcane. *Mol. Breed.* 19, 1–14. <https://doi.org/10.1007/s11032-006-9008-3>
- Allaby, R.G., 2015. Barley domestication: the end of a central dogma? *Genome Biol.* 16, 176. <https://doi.org/10.1186/s13059-015-0743-9>
- Ameline-Torregrosa, C., Wang, B.-B., O’Bleness, M.S., Deshpande, S., Zhu, H., Roe, B., Young, N.D., Cannon, S.B., 2008. Identification and Characterization of Nucleotide-Binding Site-Leucine-Rich Repeat Genes in the Model Plant *Medicago truncatula*. *Plant Physiol.* 146, 5–21. <https://doi.org/10.1104/pp.107.104588>
- Ariyadasa, R., Mascher, M., Nussbaumer, T., Schulte, D., Frenkel, Z., Poursarebani, N., Zhou, R., Steuernagel, B., Gundlach, H., Taudien, S., Felder, M., Platzer, M., Himmelbach, A., Schmutzer, T., Hedley, P.E., Muehlbauer, G.J., Scholz, U., Korol, A., Mayer, K.F.X., Waugh, R., Langridge, P., Graner, A., Stein, N., 2014. A Sequence-Ready Physical Map of Barley Anchored Genetically by Two Million Single-Nucleotide Polymorphisms. *Plant Physiol.* 164, 412–423. <https://doi.org/10.1104/pp.113.228213>
- Arya, P., Kumar, G., Acharya, V., Singh, A.K., 2014. Genome-Wide Identification and Expression Analysis of NBS-Encoding Genes in *Malus x domestica* and Expansion of NBS Genes Family in *Rosaceae*. *PLOS ONE* 9, e107987. <https://doi.org/10.1371/journal.pone.0107987>
- Asfaw, Z., 2000. Genes in the Field: On-farm Conservation of Crop Diversity. IDRC.
- Ayliffe, M., Periyannan, S.K., Feechan, A., Dry, I., Schumann, U., Wang, M.-B., Pryor, A., Lagudah, E., 2013. A Simple Method for Comparing Fungal Biomass in Infected Plant Tissues. *Mol. Plant. Microbe Interact.* 26, 658–667. <https://doi.org/10.1094/MPMI-12-12-0291-R>
- Backes, G., Madsen, L., Jaiser, H., Stougaard, J., Herz, M., Mohler, V., Jahoor, A., 2003. Localisation of genes for resistance against *Blumeria graminis* f.sp. *hordei* and *Puccinia graminis* in a cross between a barley cultivar and a wild barley (*Hordeum vulgare* ssp.

- spontaneum*) line. *Theor. Appl. Genet.* 106, 353–362. <https://doi.org/10.1007/s00122-002-1148-1>
- Backes, G., Schwarz, G., Wenzel, G., Jahoor, A., 1996. Short Communication Comparison between QTL analysis of powdery mildew resistance in barley based on detached primary leaves and on field data. *Plant Breed.* 115, 419–421. <https://doi.org/10.1111/j.1439-0523.1996.tb00946.x>
- Badr, A., M, K., Sch, R., Rabey, H.E., Effgen, S., Ibrahim, H.H., Pozzi, C., Rohde, W., Salamini, F., 2000. On the Origin and Domestication History of Barley (*Hordeum vulgare*). *Mol. Biol. Evol.* 17, 499–510. <https://doi.org/10.1093/oxfordjournals.molbev.a026330>
- Bamshad, M.J., Ng, S.B., Bigham, A.W., Tabor, H.K., Emond, M.J., Nickerson, D.A., Shendure, J., 2011. Exome sequencing as a tool for Mendelian disease gene discovery. *Nat. Rev. Genet.* 12, nrg3031. <https://doi.org/10.1038/nrg3031>
- Barakate, A., Stephens, J., 2016. An Overview of CRISPR-Based Tools and Their Improvements: New Opportunities in Understanding Plant–Pathogen Interactions for Better Crop Protection. *Front. Plant Sci.* 7. <https://doi.org/10.3389/fpls.2016.00765>
- Becraft, P.W., 2002. Receptor Kinase Signaling in Plant Development. *Annu. Rev. Cell Dev. Biol.* 18, 163–192. <https://doi.org/10.1146/annurev.cellbio.18.012502.083431>
- Beier, S., Himmelbach, A., Colmsee, C., Zhang, X.-Q., Barrero, R.A., Zhang, Q., Li, L., Bayer, M., Bolser, D., Taudien, S., 2017. Construction of a map-based reference genome sequence for barley, *Hordeum vulgare* L. *Sci. Data* 4.
- Belkadi, A., Bolze, A., Itan, Y., Cobat, A., Vincent, Q.B., Antipenko, A., Shang, L., Boisson, B., Casanova, J.-L., Abel, L., 2015. Whole-genome sequencing is more powerful than whole-exome sequencing for detecting exome variants. *Proc. Natl. Acad. Sci. U. S. A.* 112, 5473–5478. <https://doi.org/10.1073/pnas.1418631112>
- Bent, A., 1996. Plant Disease Resistance Genes: Function Meets Structure. *Plant Cell* 8, 1757–1771.
- Bergelson, J., Stahl, E., Dudek, S., Kreitman, M., 1998. Genetic Variation Within and Among Populations of *Arabidopsis thaliana*. *Genetics* 148, 1311–1323.
- Bevan, M.W., Uauy, C., Wulff, B.B.H., Zhou, J., Krasileva, K., Clark, M.D., 2017. Genomic innovation for crop improvement. *Nature* 543, 346–354. <https://doi.org/10.1038/nature22011>
- Bieri, S., Mauch, S., Shen, Q.-H., Peart, J., Devoto, A., Casais, C., Ceron, F., Schulze, S., Steinbiß, H.-H., Shirasu, K., Schulze-Lefert, P., 2004. *RARI* Positively Controls Steady State Levels of Barley *MLA* Resistance Proteins and Enables Sufficient *MLA6* Accumulation for Effective Resistance. *Plant Cell* 16, 3480–3495. <https://doi.org/10.1105/tpc.104.026682>

- Biezen, E.A. van der, Jones, J.D.G., 1998. The NB-ARC domain: a novel signalling motif shared by plant resistance gene products and regulators of cell death in animals. *Curr. Biol.* 8, R226–R228. [https://doi.org/10.1016/S0960-9822\(98\)70145-9](https://doi.org/10.1016/S0960-9822(98)70145-9)
- Bogdanove, A.J., Martin, G.B., 2000. *AvrPto*-dependent *Pto*-interacting proteins and *AvrPto*-interacting proteins in tomato. *Proc. Natl. Acad. Sci.* 97, 8836–8840. <https://doi.org/10.1073/pnas.97.16.8836>
- Bomblies, K., Weigel, D., 2007. Hybrid necrosis: autoimmunity as a potential gene-flow barrier in plant species. *Nat. Rev. Genet.* 8, 382–393. <https://doi.org/10.1038/nrg2082>
- Both, M., Csukai, M., Stumpf, M.P.H., Spanu, P.D., 2005. Gene Expression Profiles of *Blumeria graminis* Indicate Dynamic Changes to Primary Metabolism during Development of an Obligate Biotrophic Pathogen. *Plant Cell* 17, 2107–2122. <https://doi.org/10.1105/tpc.105.032631>
- Boyd, L.A., Smith, P.H., Foster, E.M., Brown, J.K.M., 1995. The effects of allelic variation at the *Mla* resistance locus in barley on the early development of *Erysiphe graminis* f.sp. *hordei* and host responses. *Plant J.* 7, 959–968. <https://doi.org/10.1046/j.1365-313X.1995.07060959.x>
- Brown, J.K.M., Rant, J.C., 2013. Fitness costs and trade-offs of disease resistance and their consequences for breeding arable crops. *Plant Pathol.* 62, 83–95. <https://doi.org/10.1111/ppa.12163>
- Brueggeman, R., Rostoks, N., Kudrna, D., Kilian, A., Han, F., Chen, J., Druka, A., Steffenson, B., Kleinhofs, A., 2002. The barley stem rust-resistance gene *Rpg1* is a novel disease-resistance gene with homology to receptor kinases. *Proc. Natl. Acad. Sci.* 99, 9328–9333. <https://doi.org/10.1073/pnas.142284999>
- Büschges, R., Hollricher, K., Panstruga, R., Simons, G., Wolter, M., Frijters, A., van Daelen, R., van der Lee, T., Diergaarde, P., Groenendijk, J., Töpsch, S., Vos, P., Salamini, F., Schulze-Lefert, P., 1997. The Barley *Mlo* Gene: A Novel Control Element of Plant Pathogen Resistance. *Cell* 88, 695–705. [https://doi.org/10.1016/S0092-8674\(00\)81912-1](https://doi.org/10.1016/S0092-8674(00)81912-1)
- Butler, D.G., Cullis, B.R., Gilmour, A.R., Gogel, B.J., 2009. ASReml-R reference manual. Brisb. Qld. Dep. Prim. Ind. Fish.
- Carver, T.L.W., Kunoh, H., Thomas, B.J., Nicholson, R.L., 1999. Release and visualization of the extracellular matrix of conidia of *Blumeria graminis*. *Mycol. Res.* 103, 547–560. <https://doi.org/10.1017/S0953756298007400>
- Chaffin, A.S., Huang, Y.-F., Smith, S., Bekele, W.A., Babiker, E., Gnanesh, B.N., Foresman, B.J., Blanchard, S.G., Jay, J.J., Reid, R.W., Wight, C.P., Chao, S., Oliver, R., Islamovic, E., Kolb, F.L., McCartney, C., Fetch, M., W, J., Beattie, A.D., Bjørnstad, Å., Bonman, J.M., Langdon, T., Howarth, C.J., Brouwer, C.R., Jellen, E.N., Klos, K.E., Poland, J.A., Hsieh, T.-F., Brown, R., Jackson, E., Schlueter, J.A., Tinker, N.A., 2016. A Consensus Map in Cultivated Hexaploid Oat Reveals Conserved Grass Synteny with Substantial

- Chen, W., Kalscheuer, V., Tzschach, A., Menzel, C., Ullmann, R., Schulz, M.H., Erdogan, F., Li, N., Kijas, Z., Arkesteijn, G., Pajares, I.L., Goetz-Sothmann, M., Heinrich, U., Rost, I., Dufke, A., Grasshoff, U., Glaeser, B., Vingron, M., Ropers, H.H., 2008. Mapping translocation breakpoints by next-generation sequencing. *Genome Res.* 18, 1143–1149. <https://doi.org/10.1101/gr.076166.108>
- Chen, W., Liu, T., Gao, L., 2013. Suppression of stripe rust and leaf rust resistances in interspecific crosses of wheat. *Euphytica* 192, 339–346. <https://doi.org/10.1007/s10681-012-0854-2>
- Chen, Y., Singh, S., Rashid, K., Dribnenki, P., Green, A., 2008. Pyramiding of alleles with different rust resistance specificities in *Linum usitatissimum* L. *Mol. Breed.* 21, 419–430. <https://doi.org/10.1007/s11032-007-9142-6>
- Chen, Z., Wang, B., Dong, X., Liu, H., Ren, L., Chen, J., Hauck, A., Song, W., Lai, J., 2014. An ultra-high density bin-map for rapid QTL mapping for tassel and ear architecture in a large F2 maize population. *BMC Genomics* 15. <https://doi.org/10.1186/1471-2164-15-433>
- Chisholm, S.T., Coaker, G., Day, B., Staskawicz, B.J., 2006. Host-Microbe Interactions: Shaping the Evolution of the Plant Immune Response. *Cell* 124, 803–814. <https://doi.org/10.1016/j.cell.2006.02.008>
- Close, T.J., Bhat, P.R., Lonardi, S., Wu, Y., Rostoks, N., Ramsay, L., Druka, A., Stein, N., Svensson, J.T., Wanamaker, S., Bozdag, S., Roose, M.L., Moscou, M.J., Chao, S., Varshney, R.K., Szűcs, P., Sato, K., Hayes, P.M., Matthews, D.E., Kleinhofs, A., Muehlbauer, G.J., DeYoung, J., Marshall, D.F., Madishetty, K., Fenton, R.D., Condamine, P., Graner, A., Waugh, R., 2009. Development and implementation of high-throughput SNP genotyping in barley. *BMC Genomics* 10, 582. <https://doi.org/10.1186/1471-2164-10-582>
- Close, T.J., Wanamaker, S.I., Caldo, R.A., Turner, S.M., Ashlock, D.A., Dickerson, J.A., Wing, R.A., Muehlbauer, G.J., Kleinhofs, A., Wise, R.P., 2004. A New Resource for Cereal Genomics: 22K Barley GeneChip Comes of Age. *Plant Physiol.* 134, 960–968. <https://doi.org/10.1104/pp.103.034462>
- Colmsee, C., Beier, S., Himmelbach, A., Schmutzer, T., Stein, N., Scholz, U., Mascher, M., 2015. BARLEX – the Barley Draft Genome Explorer. *Mol. Plant* 8, 964–966. <https://doi.org/10.1016/j.molp.2015.03.009>
- Corrion, A., Day, B., 2001. Pathogen Resistance Signalling in Plants, in: ELS. John Wiley & Sons, Ltd. <https://doi.org/10.1002/9780470015902.a0020119.pub2>
- Czembor J. H., Czembor H. J., 2001. Powdery Mildew Resistance in Barley Landraces from Morocco. *J. Phytopathol.* 148, 277–288. <https://doi.org/10.1046/j.1439-0434.2000.00507.x>

- Czembor, J.H., 2002. Resistance to powdery mildew in selections from Moroccan barley landraces. *Euphytica* 125, 397–409. <https://doi.org/10.1023/A:1016061508160>
- Dangl, J.L., McDowell, J.M., 2006. Two modes of pathogen recognition by plants. *Proc. Natl. Acad. Sci.* 103, 8575–8576. <https://doi.org/10.1073/pnas.0603183103>
- Davey, J.W., Hohenlohe, P.A., Etter, P.D., Boone, J.Q., Catchen, J.M., Blaxter, M.L., 2011. Genome-wide genetic marker discovery and genotyping using next-generation sequencing. *Nat. Rev. Genet.* 12, 499. <https://doi.org/10.1038/nrg3012>
- Dawson, I.K., Russell, J., Powell, W., Steffenson, B., Thomas, W.T.B., Waugh, R., 2015. Barley: a translational model for adaptation to climate change. *New Phytol.* 206, 913–931. <https://doi.org/10.1111/nph.13266>
- de Vree, P.J.P., de Wit, E., Yilmaz, M., van de Heijning, M., Klous, P., Verstegen, M.J.A.M., Wan, Y., Teunissen, H., Krijger, P.H.L., Geeven, G., Eijk, P.P., Sie, D., Ylstra, B., Hulsman, L.O.M., van Dooren, M.F., van Zutven, L.J.C.M., van den Ouweland, A., Verbeek, S., van Dijk, K.W., Cornelissen, M., Das, A.T., Berkhout, B., Sikkema-Raddatz, B., van den Berg, E., van der Vlies, P., Weening, D., den Dunnen, J.T., Matusiak, M., Lamkanfi, M., Ligtenberg, M.J.L., ter Brugge, P., Jonkers, J., Foekens, J.A., Martens, J.W., van der Luijt, R., van Amstel, H.K.P., van Min, M., Splinter, E., de Laat, W., 2014. Targeted sequencing by proximity ligation for comprehensive variant detection and local haplotyping. *Nat. Biotechnol.* 32, 1019–1025. <https://doi.org/10.1038/nbt.2959>
- Deschamps, S., Campbell, M.A., 2010. Utilization of next-generation sequencing platforms in plant genomics and genetic variant discovery. *Mol. Breed.* 25, 553–570. <https://doi.org/10.1007/s11032-009-9357-9>
- Dhanasekaran, N., Reddy, E.P., 1998. Signaling by dual specificity kinases. *Oncogene* 17, 1447–1455. <https://doi.org/10.1038/sj.onc.1202251>
- Dilbirligi, M., Erayman, M., Gill, K.S., 2005. Analysis of recombination and gene distribution in the 2L1.0 region of wheat (*Triticum aestivum* L.) and barley (*Hordeum vulgare* L.). *Genomics* 86, 47–54. <https://doi.org/10.1016/j.ygeno.2005.03.008>
- Dinka, S.J., Campbell, M.A., Demers, T., Raizada, M.N., 2007. Predicting the Size of the Progeny Mapping Population Required to Positionally Clone a Gene. *Genetics* 176, 2035–2054. <https://doi.org/10.1534/genetics.107.074377>
- Dixon, M.S., Golstein, C., Thomas, C.M., Biezen, E.A. van der, Jones, J.D.G., 2000. Genetic complexity of pathogen perception by plants: The example of *Rcr3*, a tomato gene required specifically by *Cf-2*. *Proc. Natl. Acad. Sci.* 97, 8807–8814. <https://doi.org/10.1073/pnas.97.16.8807>
- Dixon, M.S., Jones, D.A., Keddie, J.S., Thomas, C.M., Harrison, K., Jones, J.D.G., 1996. The Tomato *Cf-2* Disease Resistance Locus Comprises Two Functional Genes Encoding Leucine-Rich Repeat Proteins. *Cell* 84, 451–459. [https://doi.org/10.1016/S0092-8674\(00\)81290-8](https://doi.org/10.1016/S0092-8674(00)81290-8)

- Doležel, J., Kubaláková, M., Paux, E., Bartoš, J., Feuillet, C., 2007. Chromosome-based genomics in the cereals. *Chromosome Res.* 15, 51–66. <https://doi.org/10.1007/s10577-006-1106-x>
- Douchkov, D., Baum, T., Ihlow, A., Schweizer, P., Seiffert, U., 2014. Microphenomics for Interactions of Barley with Fungal Pathogens, in: *Genomics of Plant Genetic Resources*. Springer, Dordrecht, pp. 123–148. https://doi.org/10.1007/978-94-007-7575-6_5
- Douchkov, D., Nowara, D., Zierold, U., Schweizer, P., 2005. A High-Throughput Gene-Silencing System for the Functional Assessment of Defense-Related Genes in Barley Epidermal Cells. *Mol. Plant. Microbe Interact.* 18, 755–761. <https://doi.org/10.1094/MPMI-18-0755>
- Dufayard, J.-F., Bettembourg, M., Fischer, I., Droc, G., Guiderdoni, E., Périn, C., Chantret, N., Diévert, A., 2017. New Insights on Leucine-Rich Repeats Receptor-Like Kinase Orthologous Relationships in Angiosperms. *Front. Plant Sci.* 8. <https://doi.org/10.3389/fpls.2017.00381>
- Eckardt, N.A., 2002. Plant Disease Susceptibility Genes? *Plant Cell* 14, 1983–1986. <https://doi.org/10.1105/tpc.140910>
- Ellinger, D., Naumann, M., Falter, C., Zwikowics, C., Jamrow, T., Manisseri, C., Somerville, S.C., Voigt, C.A., 2013. Elevated Early Callose Deposition Results in Complete Penetration Resistance to Powdery Mildew in *Arabidopsis*. *Plant Physiol.* 161, 1433–1444. <https://doi.org/10.1104/pp.112.211011>
- Ellis, J., Dodds, P., Pryor, T., 2000. Structure, function and evolution of plant disease resistance genes. *Curr. Opin. Plant Biol.* 3, 278–284. [https://doi.org/10.1016/S1369-5266\(00\)00080-7](https://doi.org/10.1016/S1369-5266(00)00080-7)
- Elshire, R.J., Glaubitz, J.C., Sun, Q., Poland, J.A., Kawamoto, K., Buckler, E.S., Mitchell, S.E., 2011a. A robust, simple genotyping-by-sequencing (GBS) approach for high diversity species. *PloS One* 6, e19379. <https://doi.org/10.1371/journal.pone.0019379>
- Elshire, R.J., Glaubitz, J.C., Sun, Q., Poland, J.A., Kawamoto, K., Buckler, E.S., Mitchell, S.E., 2011b. A robust, simple genotyping-by-sequencing (GBS) approach for high diversity species. *PloS One* 6, e19379. <https://doi.org/10.1371/journal.pone.0019379>
- Flagel, L.E., Wendel, J.F., 2009. Gene duplication and evolutionary novelty in plants. *New Phytol.* 183, 557–564. <https://doi.org/10.1111/j.1469-8137.2009.02923.x>
- Flor, H.H., 1971. Current Status of the Gene-For-Gene Concept. *Annu. Rev. Phytopathol.* 9, 275–296. <https://doi.org/10.1146/annurev.py.09.090171.001423>
- Freialdenhoven, A., Peterhansel, C., Kurth, J., Kreuzaler, F., Schulze-Lefert, P., 1996. Identification of Genes Required for the Function of Non-Race-Specific *mlo* Resistance to Powdery Mildew in Barley. *Plant Cell* 8, 5–14. <https://doi.org/10.1105/tpc.8.1.5>

- Friesen, T.L., Faris, J.D., 2004. Molecular mapping of resistance to *Pyrenophora tritici-repentis* race 5 and sensitivity to *Ptr ToxB* in wheat. *Theor. Appl. Genet.* 109, 464–471. <https://doi.org/10.1007/s00122-004-1678-9>
- Fukuoka, S., Saka, N., Mizukami, Y., Koga, H., Yamanouchi, U., Yoshioka, Y., Hayashi, N., Ebana, K., Mizobuchi, R., Yano, M., 2015. Gene pyramiding enhances durable blast disease resistance in rice. *Sci. Rep.* 5, 7773. <https://doi.org/10.1038/srep07773>
- Gassmann, W., Hinsch, M.E., Staskawicz, B.J., 1999. The *Arabidopsis RPS4* bacterial-resistance gene is a member of the TIR-NBS-LRR family of disease-resistance genes. *Plant J.* 20, 265–277. <https://doi.org/10.1046/j.1365-313X.1999.00600.x>
- Giese, H., Holm-Jensen, A.G., Jensen, H.P., Jensen, J., 1993. Localization of the *Laevigatum* powdery mildew resistance gene to barley chromosome 2 by the use of RFLP markers. *Theor. Appl. Genet.* 85, 897–900. <https://doi.org/10.1007/BF00225035>
- Gilbert, L.A., Larson, M.H., Morsut, L., Liu, Z., Brar, G.A., Torres, S.E., Stern-Ginossar, N., Brandman, O., Whitehead, E.H., Doudna, J.A., Lim, W.A., Weissman, J.S., Qi, L.S., 2013. CRISPR-Mediated Modular RNA-Guided Regulation of Transcription in Eukaryotes. *Cell* 154, 442–451. <https://doi.org/10.1016/j.cell.2013.06.044>
- Glawe, D.A., 2008. The Powdery Mildews: A Review of the World's Most Familiar (Yet Poorly Known) Plant Pathogens. *Annu. Rev. Phytopathol.* 46, 27–51. <https://doi.org/10.1146/annurev.phyto.46.081407.104740>
- Gómez-Gómez, L., Boller, T., 2000. *FLS2*: An LRR Receptor-like Kinase Involved in the Perception of the Bacterial Elicitor Flagellin in *Arabidopsis*. *Mol. Cell* 5, 1003–1011. [https://doi.org/10.1016/S1097-2765\(00\)80265-8](https://doi.org/10.1016/S1097-2765(00)80265-8)
- Graner, A., Jahoor, A., Schondelmaier, J., Siedler, H., Pillen, K., Fischbeck, G., Wenzel, G., Herrmann, R.G., 1991. Construction of an RFLP map of barley. *Theor. Appl. Genet.* 83, 250–256. <https://doi.org/10.1007/BF00226259>
- Grant, M.R., McDowell, J.M., Sharpe, A.G., Zabala, M. de T., Lydiate, D.J., Dangl, J.L., 1998. Independent deletions of a pathogen-resistance gene in Brassica and *Arabidopsis*. *Proc. Natl. Acad. Sci.* 95, 15843–15848. <https://doi.org/10.1073/pnas.95.26.15843>
- Griffiths, A.J.F., Gelbart, W.M., Miller, J.H., Lewontin, R.C., 1999. Chromosomal Rearrangements. *Modern Genetic Analysis*. W.H. Freeman & Co Ltd, New York.
- Gupta, P.K., Varshney, R. (Eds.), 2013. *Cereal Genomics II*, 2nd ed. Springer Netherlands.
- Hadado, T.T., Rau, D., Bitocchi, E., Papa, R., 2009. Genetic diversity of barley (*Hordeum vulgare* L.) landraces from the central highlands of Ethiopia: comparison between the Belg and Meher growing seasons using morphological traits. *Genet. Resour. Crop Evol.* 56, 1131–1148. <https://doi.org/10.1007/s10722-009-9437-z>

- Hammond-Kosack, K.E., Jones, and J.D.G., 1997. Plant Disease Resistance Genes. *Annu. Rev. Plant Physiol. Plant Mol. Biol.* 48, 575–607. <https://doi.org/10.1146/annurev.arplant.48.1.575>
- Hanemann, A., Schweizer, G.F., Cossu, R., Wicker, T., Röder, M.S., 2009. Fine mapping, physical mapping and development of diagnostic markers for the *Rrs2* scald resistance gene in barley. *Theor. Appl. Genet.* 119, 1507–1522. <https://doi.org/10.1007/s00122-009-1152-9>
- He, J., Zhao, X., Laroche, A., Lu, Z.-X., Liu, H., Li, Z., 2014a. Genotyping-by-sequencing (GBS), an ultimate marker-assisted selection (MAS) tool to accelerate plant breeding. *Front. Plant Sci.* 5. <https://doi.org/10.3389/fpls.2014.00484>
- He, J., Zhao, X., Laroche, A., Lu, Z.-X., Liu, H., Li, Z., 2014b. Genotyping-by-sequencing (GBS), an ultimate marker-assisted selection (MAS) tool to accelerate plant breeding. *Front. Plant Sci.* 5. <https://doi.org/10.3389/fpls.2014.00484>
- Henk, A.D., Warren, R.F., Innes, R.W., 1999. A New Ac-Like Transposon of *Arabidopsis* Is Associated With a Deletion of the RPS5 Disease Resistance Gene. *Genetics* 151, 1581–1589.
- Hernandez, P., Martis, M., Dorado, G., Pfeifer, M., Gálvez, S., Schaaf, S., Jouve, N., Šimková, H., Valárik, M., Doležel, J., Mayer, K.F.X., 2012. Next-generation sequencing and syntenic integration of flow-sorted arms of wheat chromosome 4A exposes the chromosome structure and gene content. *Plant J.* 69, 377–386. <https://doi.org/10.1111/j.1365-313X.2011.04808.x>
- Hilbers, S., Fischbeck, G., Jahoor, A., 1992. Localization of the *Laevigatum* Resistance Gene *MLLa* against Powdery Mildew in the Barley Genome by the Use of RFLP Markers. *Plant Breed.* 109, 335–338. <https://doi.org/10.1111/j.1439-0523.1992.tb00193.x>
- Hoorn, R.A.L. van der, Kamoun, S., 2008. From Guard to Decoy: A New Model for Perception of Plant Pathogen Effectors. *Plant Cell* 20, 2009–2017. <https://doi.org/10.1105/tpc.108.060194>
- Huang, Y.-F., Poland, J.A., Wight, C.P., Jackson, E.W., Tinker, N.A., 2014. Using Genotyping-By-Sequencing (GBS) for Genomic Discovery in Cultivated Oat. *PLoS ONE* 9. <https://doi.org/10.1371/journal.pone.0102448>
- IBSC, 2012. A physical, genetic and functional sequence assembly of the barley genome. *Nature* 491, nature11543. <https://doi.org/10.1038/nature11543>
- Ihlow, A., Schweizer, P., Seiffert, U., 2008. A high-throughput screening system for barley/powdery mildew interactions based on automated analysis of light micrographs. *BMC Plant Biol.* 8, 6. <https://doi.org/10.1186/1471-2229-8-6>
- Inuma, T., Khodaparast, S.A., Takamatsu, S., 2007. Multilocus phylogenetic analyses within *Blumeria graminis*, a powdery mildew fungus of cereals. *Mol. Phylogenet. Evol.* 44, 741–751. <https://doi.org/10.1016/j.ympev.2007.01.007>

- Isidore, E., Scherrer, B., Bellec, A., Budin, K., Faivre-Rampant, P., Waugh, R., Keller, B., Caboche, M., Feuillet, C., Chalhoub, B., 2005. Direct targeting and rapid isolation of BAC clones spanning a defined chromosome region. *Funct. Integr. Genomics* 5, 97–103. <https://doi.org/10.1007/s10142-004-0127-9>
- Johnston, P.A., Niks, R.E., Meiyalaghan, V., Blanchet, E., Pickering, R., 2013. *Rph22*: mapping of a novel leaf rust resistance gene introgressed from the non-host *Hordeum bulbosum* L. into cultivated barley (*Hordeum vulgare* L.). *Theor. Appl. Genet.* 126, 1613–1625. <https://doi.org/10.1007/s00122-013-2078-9>
- Jones, D.A., Jones, J.D.G., 1997. The Role of Leucine-Rich Repeat Proteins in Plant Defences, in: Andrews, J.H., Tommerup, I.C., Callow, J.A. (Eds.), *Advances in Botanical Research*. Academic Press, pp. 89–167. [https://doi.org/10.1016/S0065-2296\(08\)60072-5](https://doi.org/10.1016/S0065-2296(08)60072-5)
- Jones, J.D.G., Dangl, J.L., 2006. The plant immune system. *Nature* 444, nature05286. <https://doi.org/10.1038/nature05286>
- Jørgensen, J.H., 1992. Discovery, characterization and exploitation of *Mlo* powdery mildew resistance in barley, in: *Breeding for Disease Resistance, Developments in Plant Pathology*. Springer, Dordrecht, pp. 141–152. https://doi.org/10.1007/978-94-017-0954-5_12
- Jørgensen, J.H., Wolfe, P.M., 1994. Genetics of Powdery Mildew Resistance in Barley. *Crit. Rev. Plant Sci.* 13, 97–119. <https://doi.org/10.1080/07352689409701910>
- Jost, M., Taketa, S., Mascher, M., Himmelbach, A., Yuo, T., Shahinnia, F., Rutten, T., Druka, A., Schmutzer, T., Steuernagel, B., Beier, S., Taudien, S., Scholz, U., Morgante, M., Waugh, R., Stein, N., 2016. A homolog of *Blade-On-Petiole 1* and 2 (*BOP1/2*) controls internode length and homeotic changes of the barley inflorescence. *Plant Physiol.* pp.00124.2016. <https://doi.org/10.1104/pp.16.00124>
- Jupe, F., Pritchard, L., Etherington, G.J., MacKenzie, K., Cock, P.J., Wright, F., Sharma, S.K., Bolser, D., Bryan, G.J., Jones, J.D., Hein, I., 2012. Identification and localisation of the NB-LRR gene family within the potato genome. *BMC Genomics* 13, 75. <https://doi.org/10.1186/1471-2164-13-75>
- Jupe, F., Witek, K., Verweij, W., Sliwka, J., Pritchard, L., Etherington, G.J., Maclean, D., Cock, P.J., Leggett, R.M., Bryan, G.J., Cardle, L., Hein, I., Jones, J.D.G., 2013. Resistance gene enrichment sequencing (RenSeq) enables reannotation of the NB-LRR gene family from sequenced plant genomes and rapid mapping of resistance loci in segregating populations. *Plant J. Cell Mol. Biol.* 76, 530–544. <https://doi.org/10.1111/tpj.12307>
- Kajava, A.V., 1998. Structural diversity of leucine-rich repeat proteins. *J. Mol. Biol.* 277, 519–527. <https://doi.org/10.1006/jmbi.1998.1643>
- Keane, P.J., 2012. Horizontal or generalized resistance to pathogens in plants, in: *Plant Pathology*. InTech.

- Kersey, P.J., Allen, J.E., Armean, I., Boddu, S., Bolt, B.J., Carvalho-Silva, D., Christensen, M., Davis, P., Falin, L.J., Grabmueller, C., Humphrey, J., Kerhornou, A., Khobova, J., Aranganathan, N.K., Langridge, N., Lowy, E., McDowall, M.D., Maheswari, U., Nuhn, M., Ong, C.K., Overduin, B., Paulini, M., Pedro, H., Perry, E., Spudich, G., Tapanari, E., Walts, B., Williams, G., Tello–Ruiz, M., Stein, J., Wei, S., Ware, D., Bolser, D.M., Howe, K.L., Kulesha, E., Lawson, D., Maslen, G., Staines, D.M., 2016. Ensembl Genomes 2016: more genomes, more complexity. *Nucleic Acids Res.* 44, D574–D580. <https://doi.org/10.1093/nar/gkv1209>
- Kersey, P.J., Lawson, D., Birney, E., Derwent, P.S., Haimel, M., Herrero, J., Keenan, S., Kerhornou, A., Koscielny, G., Kähäri, A., Kinsella, R.J., Kulesha, E., Maheswari, U., Megy, K., Nuhn, M., Proctor, G., Staines, D., Valentin, F., Vilella, A.J., Yates, A., 2010. Ensembl Genomes: Extending Ensembl across the taxonomic space. *Nucleic Acids Res.* 38, D563–D569. <https://doi.org/10.1093/nar/gkp871>
- Kinane, J., Dalvin, S., Bindslev, L., Hall, A., Gurr, S., Oliver, R., 2000. Evidence that the cAMP Pathway Controls Emergence of Both Primary and Appressorial Germ Tubes of Barley Powdery Mildew. *Mol. Plant. Microbe Interact.* 13, 494–502. <https://doi.org/10.1094/MPMI.2000.13.5.494>
- Kinizios, S., Jahoor, A., Fischbeck, G., 1995. Powdery-mildew-resistance genes *Mla29* and *Mla32* in *H. spontaneum* derived winter-barley lines. *Plant Breed.* 114, 265–266. <https://doi.org/10.1111/j.1439-0523.1995.tb00809.x>
- Koller, T., Brunner, S., Herren, G., Hurni, S., Keller, B., 2018. Pyramiding of transgenic *Pm3* alleles in wheat results in improved powdery mildew resistance in the field. *Theor. Appl. Genet.* 131, 861–871. <https://doi.org/10.1007/s00122-017-3043-9>
- Kølster, P., Munk, L., Stølen, O., Løhde, J., 1986. Near-Isogenic Barley Lines with Genes for Resistance to Powdery Mildew. *Crop Sci.* 26, 903–907. <https://doi.org/10.2135/cropsci1986.0011183X002600050014x>
- Koppolu, R., Anwar, N., Sakuma, S., Tagiri, A., Lundqvist, U., Pourkheirandish, M., Rutten, T., Seiler, C., Himmelbach, A., Ariyadasa, R., Youssef, H.M., Stein, N., Sreenivasulu, N., Komatsuda, T., Schnurbusch, T., 2013. Six-rowed spike4 (*Vrs4*) controls spikelet determinacy and row-type in barley. *Proc. Natl. Acad. Sci.* 110, 13198–13203. <https://doi.org/10.1073/pnas.1221950110>
- Koressaar, T., Remm, M., 2007. Enhancements and modifications of primer design program Primer3. *Bioinformatics* 23, 1289–1291. <https://doi.org/10.1093/bioinformatics/btm091>
- Kou, Y., Wang, S., 2010. Broad-spectrum and durability: understanding of quantitative disease resistance. *Curr. Opin. Plant Biol.* 13, 181–185. <https://doi.org/10.1016/j.pbi.2009.12.010>
- Kourelis, J., Hoorn, R.A.L. van der, 2018. Defended to the Nines: 25 Years of Resistance Gene Cloning Identifies Nine Mechanisms for R Protein Function. *Plant Cell* 30, 285–299. <https://doi.org/10.1105/tpc.17.00579>

- Kranz, J., 2012. Epidemics of Plant Diseases: Mathematical Analysis and Modeling. Springer Science & Business Media.
- Kranz, J., Rotem, J. (Eds.), 1988. Experimental Techniques in Plant Disease Epidemiology. Springer-Verlag, Berlin Heidelberg.
- Kumar, S., Knox, R.E., Singh, A.K., DePauw, R.M., Campbell, H.L., Isidro-Sanchez, J., Clarke, F.R., Pozniak, C.J., N'Daye, A., Meyer, B., Sharpe, A., Ruan, Y., Cuthbert, R.D., Somers, D., Fedak, G., 2018. High-density genetic mapping of a major QTL for resistance to multiple races of loose smut in a tetraploid wheat cross. PLOS ONE 13, e0192261. <https://doi.org/10.1371/journal.pone.0192261>
- Lahaye, T., Hartmann, S., Töpsch, S., Freialdenhoven, A., Yano, M., Schulze-Lefert, P., 1998. High-resolution genetic and physical mapping of the *Rar1* locus in barley. Theor. Appl. Genet. 97, 526–534. <https://doi.org/10.1007/s001220050927>
- Lamari, L., Bernier, C.C., 1989. Evaluation of Wheat Lines and Cultivars to tan Spot [*Pyrenophora Tritici-Repentis*] Based on Lesion Type. Can. J. Plant Pathol. 11, 49–56. <https://doi.org/10.1080/07060668909501146>
- Lance, R.C.M., Nilan, R.A., 1980. Screening for low acid-soluble beta -glucan barleys. Barley Genet. Newsl. 10.
- Lellis, A.D., Kasschau, K.D., Whitham, S.A., Carrington, J.C., 2002. Loss-of-Susceptibility Mutants of *Arabidopsis thaliana* Reveal an Essential Role for *eIF(iso)4E* during Potyvirus Infection. Curr. Biol. 12, 1046–1051. [https://doi.org/10.1016/S0960-9822\(02\)00898-9](https://doi.org/10.1016/S0960-9822(02)00898-9)
- Ling, H.-Q., Zhu, Y., Keller, B., 2003. High-resolution mapping of the leaf rust disease resistance gene *Lr1* in wheat and characterization of BAC clones from the *Lr1* locus. Theor. Appl. Genet. 106, 875–882. <https://doi.org/10.1007/s00122-002-1139-2>
- Liu, B.-H., 1998. Statistical genomics: linkage, mapping, and QTL analysis. CRC Press, Boca Raton, Fla.
- Liu, S., Yeh, C.-T., Tang, H.M., Nettleton, D., Schnable, P.S., 2012. Gene Mapping via Bulk Segregant RNA-Seq (BSR-Seq). PLOS ONE 7, e36406. <https://doi.org/10.1371/journal.pone.0036406>
- López-Larrea, C., 2012. Self and Nonself. Springer Science & Business Media.
- Luderer Rianne, Takken Frank L. W., Wit Pierre J. G. M. de, Joosten Matthieu H. A. J., 2002. *Cladosporium fulvum* overcomes Cf-2-mediated resistance by producing truncated AVR2 elicitor proteins. Mol. Microbiol. 45, 875–884. <https://doi.org/10.1046/j.1365-2958.2002.03060.x>
- Macovei, A., Sevilla, N.R., Cantos, C., Jonson, G.B., Slanina, I., Čermák, T., Voytas, D.F., Choi, I.-R., Chadha-Mohanty, P., 2018. Novel alleles of rice *eIF4G* generated by CRISPR/Cas9-targeted mutagenesis confer resistance to Rice tungro spherical virus. Plant Biotechnol. J. 5. <https://doi.org/10.1111/pbi.12927>

- Mains, E.B., Diktz, S.M., 1930. Physiologic forms of Barley mildew, *Erysiphe graminis hordei*. *Phytopathology* 20.
- Marcel, T.C., Aghnoum, R., Durand, J., Varshney, R.K., Nicks, R.E., 2007. Dissection of the Barley 2L1.0 Region Carrying the ‘*Laevigatum*’ Quantitative Resistance Gene to Leaf Rust Using Near-Isogenic Lines (NIL) and subNIL. *Mol. Plant. Microbe Interact.* 20, 1604–1615. <https://doi.org/10.1094/MPMI-20-12-1604>
- Marone, D., Russo, M.A., Laido, G., De Leonardis, A.M., Mastrangelo, A.M., 2013. Plant Nucleotide Binding Site-Leucine-Rich Repeat (NBS-LRR) Genes: Active Guardians in Host Defense Responses. *Int. J. Mol. Sci.* 14, 7302–7326. <https://doi.org/10.3390/ijms14047302>
- Martienssen, R., 1997. Cell death: Fatal induction in plants. *Curr. Biol.* 7, R534–R537. [https://doi.org/10.1016/S0960-9822\(06\)00274-0](https://doi.org/10.1016/S0960-9822(06)00274-0)
- Mascher, M., Gundlach, H., Himmelbach, A., Beier, S., Twardziok, S.O., Wicker, T., Radchuk, V., Dockter, C., Hedley, P.E., Russell, J., Bayer, M., Ramsay, L., Liu, H., Haberer, G., Zhang, X.-Q., Zhang, Q., Barrero, R.A., Li, L., Taudien, S., Groth, M., Felder, M., Hastie, A., Šimková, H., Staňková, H., Vrána, J., Chan, S., ~~mu~~ -Amatriaín, M., Ounit, R., Wanamaker, S., Bolser, D., Colmsee, C., Schmutzer, T., Aliyeva-Schnorr, L., Grasso, S., Tanskanen, J., Chailyan, A., Sampath, D., Heavens, D., Clissold, L., Cao, S., Chapman, B., Dai, F., Han, Y., Li, H., Li, X., Lin, C., McCooke, J.K., Tan, C., Wang, P., Wang, S., Yin, S., Zhou, G., Poland, J.A., Bellgard, M.I., Borisjuk, L., Houben, A., Doležel, J., Ayling, S., Lonardi, S., Kersey, P., Langridge, P., Muehlbauer, G.J., Clark, M.D., Caccamo, M., Schulman, A.H., Mayer, K.F.X., Platzer, M., Close, T.J., Scholz, U., Hansson, M., Zhang, G., Braumann, I., Spannagl, M., Li, C., Waugh, R., Stein, N., 2017. A chromosome conformation capture ordered sequence of the barley genome. *Nature* 544, 427. <https://doi.org/10.1038/nature22043>
- Mascher, M., Jost, M., Kuon, J.-E., Himmelbach, A., Abfal, A., Beier, S., Scholz, U., Graner, A., Stein, N., 2014. Mapping-by-sequencing accelerates forward genetics in barley. *Genome Biol.* 15, R78. <https://doi.org/10.1186/gb-2014-15-6-r78>
- Mascher, M., Muehlbauer, G.J., Rokhsar, D.S., Chapman, J., Schmutz, J., Barry, K., Muñoz-Amatriaín, M., Close, T.J., Wise, R.P., Schulman, A.H., Himmelbach, A., Mayer, K.F.X., Scholz, U., Poland, J.A., Stein, N., Waugh, R., 2013a. Anchoring and ordering NGS contig assemblies by population sequencing (POPSEQ). *Plant J.* 76, 718–727. <https://doi.org/10.1111/tbj.12319>
- Mascher, M., Richmond, T.A., Gerhardt, D.J., Himmelbach, A., Clissold, L., Sampath, D., Ayling, S., Steuernagel, B., Pfeifer, M., D’Ascenzo, M., Akhunov, E.D., Hedley, P.E., Gonzales, A.M., Morrell, P.L., Kilian, B., Blattner, F.R., Scholz, U., Mayer, K.F.X., Flavell, A.J., Muehlbauer, G.J., Waugh, R., Jeddalo, J.A., Stein, N., 2013b. Barley whole exome capture: a tool for genomic research in the genus *Hordeum* and beyond. *Plant J.* 76, 494–505. <https://doi.org/10.1111/tbj.12294>

- Mascher, M., Wu, S., Amand, P.S., Stein, N., Poland, J., 2013c. Application of Genotyping-by-Sequencing on Semiconductor Sequencing Platforms: A Comparison of Genetic and Reference-Based Marker Ordering in Barley. *PLoS ONE* 8, e76925. <https://doi.org/10.1371/journal.pone.0076925>
- Mayer, K.F.X., Taudien, S., Martis, M., Šimková, H., Suchánková, P., Gundlach, H., Wicker, T., Petzold, A., Felder, M., Steuernagel, B., Scholz, U., Graner, A., Platzer, M., Doležel, J., Stein, N., 2009. Gene Content and Virtual Gene Order of Barley Chromosome 1H. *Plant Physiol.* 151, 496–505. <https://doi.org/10.1104/pp.109.142612>
- McCouch, S., Baute, G.J., Bradeen, J., Bramel, P., Bretting, P.K., Buckler, E., Burke, J.M., Charest, D., Cloutier, S., Cole, G., Dempewolf, H., Dingkuhn, M., Feuillet, C., Gepts, P., Grattapaglia, D., Guarino, L., Jackson, S., Knapp, S., Langridge, P., Lawton-Rauh, A., Lijua, Q., Lusty, C., Michael, T., Myles, S., Naito, K., Nelson, R.L., Pontarollo, R., Richards, C.M., Rieseberg, L., Ross-Ibarra, J., Rounsley, S., Hamilton, R.S., Schurr, U., Stein, N., Tomooka, N., Knaap, E. van der, Tassel, D. van, Toll, J., Valls, J., Varshney, R.K., Ward, J., Waugh, R., Wenzl, P., Zamir, D., 2013. Agriculture: Feeding the future. *Nature* 499, 499023a. <https://doi.org/10.1038/499023a>
- McDonald, B.A., Linde, and C., 2002. Pathogen Population Genetics, Evolutionary Potential, and Durable Resistance. *Annu. Rev. Phytopathol.* 40, 349–379. <https://doi.org/10.1146/annurev.phyto.40.120501.101443>
- McGinnis, K.M., 2010. RNAi for functional genomics in plants. *Brief. Funct. Genomics* 9, 111–117. <https://doi.org/10.1093/bfgp/elp052>
- McHale, L., Tan, X., Koehl, P., Michelmore, R.W., 2006. Plant NBS-LRR proteins: adaptable guards. *Genome Biol.* 7, 212. <https://doi.org/10.1186/gb-2006-7-4-212>
- McIntosh, R.A., Brown, G.N., 1997. Anticipatory breeding for resistance to rust diseases in wheat. *Annu. Rev. Phytopathol.* 35, 311–326. <https://doi.org/10.1146/annurev.phyto.35.1.311>
- Meguro, A., Fujita, K., Kunoh, H., Carver, T.L.W., Nicholson, R.L., 2001. Release of the extracellular matrix from conidia of *Blumeria graminis* in relation to germination. *Mycoscience* 42, 201–209. <https://doi.org/10.1007/BF02464138>
- Meyer, H., Lehmann, C.O., 1979. Resistenzeigenschaften im Gersten- und Weizensortiment Gatersleben 22. Prüfung von Sommergersten auf ihr Verhalten gegen zwei neue Rassen von Mehltau (*Erysiphe graminis* Dc f. sp. *hordei* Marchal). *Kult.* 27, 181–188. <https://doi.org/10.1007/BF02014648>
- Meyer, M., Kircher, M., 2010. Illumina Sequencing Library Preparation for Highly Multiplexed Target Capture and Sequencing. *Cold Spring Harb. Protoc.* 2010, pdb.prot5448-pdb.prot5448. <https://doi.org/10.1101/pdb.prot5448>
- Meyers, B.C., Dickerman, A.W., Michelmore, R.W., Sivaramakrishnan, S., Sobral, B.W., Young, N.D., 1999. Plant disease resistance genes encode members of an ancient and diverse

- protein family within the nucleotide-binding superfamily. *Plant J.* 20, 317–332. <https://doi.org/10.1046/j.1365-313X.1999.00606.x>
- Meyers, B.C., Kozik, A., Griego, A., Kuang, H., Michelmore, R.W., 2003. Genome-Wide Analysis of NBS-LRR-Encoding Genes in *Arabidopsis*. *Plant Cell* 15, 809–834. <https://doi.org/10.1105/tpc.009308>
- Mohr, S., Bakal, C., Perrimon, N., 2010. Genomic Screening with RNAi: Results and Challenges, in: Kornberg, R.D., Raetz, C.R.H., Rothman, J.E., Thorner, J.W. (Eds.), *Annual Review of Biochemistry*, Vol 79. Annual Reviews, Palo Alto, pp. 37–64.
- Monosi, B., Wissler, R.J., Pennill, L., Hulbert, S.H., 2004. Full-genome analysis of resistance gene homologues in rice. *Theor. Appl. Genet.* 109, 1434–1447. <https://doi.org/10.1007/s00122-004-1758-x>
- Moscou, M.J., Lauter, N., Caldo, R.A., Nettleton, D., Wise, R.P., 2011. Quantitative and temporal definition of the *Mla* transcriptional regulon during barley–powdery mildew interactions. *Mol. Plant. Microbe Interact.* 24, 694–705.
- Munck, L., Karlsson, K.E., Hagberg, A., Eggum, B.O., 1970. Gene for Improved Nutritional Value in Barley Seed Protein. *Science* 168, 985–987. <https://doi.org/10.1126/science.168.3934.985>
- Muñoz-Amatriaín, M., Lonardi, S., Luo, M., Madishetty, K., Svensson, J.T., Moscou, M.J., Wanamaker, S., Jiang, T., Kleinhofs, A., Muehlbauer, G.J., Wise, R.P., Stein, N., Ma, Y., Rodriguez, E., Kudrna, D., Bhat, P.R., Chao, S., Condamine, P., Heinen, S., Resnik, J., Wing, R., Witt, H.N., Alpert, M., Beccuti, M., Bozdogan, S., Cordero, F., Mirebrahim, H., Ounit, R., Wu, Y., You, F., Zheng, J., Simková, H., Doležel, J., Grimwood, J., Schmutz, J., Duma, D., Altschmied, L., Blake, T., Bregitzer, P., Cooper, L., Dilbirligi, M., Falk, A., Feiz, L., Graner, A., Gustafson, P., Hayes, P.M., Lemaux, P., Mammadov, J., Close, T.J., 2015. Sequencing of 15 622 gene-bearing BACs clarifies the gene-dense regions of the barley genome. *Plant J.* 84, 216–227. <https://doi.org/10.1111/tpj.12959>
- Muñoz-Amatriaín, M., Moscou, M.J., Bhat, P.R., Svensson, J.T., Bartoš, J., Suchánková, P., Šimková, H., Endo, T.R., Fenton, R.D., Lonardi, S., Castillo, A.M., Chao, S., Cistué, L., Cuesta-Marcos, A., Forrest, K.L., Hayden, M.J., Hayes, P.M., Horsley, R.D., Makoto, K., Moody, D., Sato, K., Vallés, M.P., Wulff, B.B.H., Muehlbauer, G.J., Doležel, J., Close*, T.J., 2011. An Improved Consensus Linkage Map of Barley Based on Flow-Sorted Chromosomes and Single Nucleotide Polymorphism Markers. *Plant Genome* 4, 238–249. <https://doi.org/10.3835/plantgenome2011.08.0023>
- Newman, R.K., Newman, C.W., 2008. *Barley for Food and Health: Science, Technology, and Products*. John Wiley & Sons.
- Newton, A.C., Flavell, A.J., George, T.S., Leat, P., Mullholland, B., Ramsay, L., Revoredo-Giha, C., Russell, J., Steffenson, B.J., Swanston, J.S., Thomas, W.T.B., Waugh, R., White, P.J., Bingham, I.J., 2011. Crops that feed the world 4. Barley: a resilient crop? Strengths and

- weaknesses in the context of food security. *Food Secur.* 3, 141. <https://doi.org/10.1007/s12571-011-0126-3>
- Nielsen, K.A., Nicholson, R.L., Carver, T.L.W., Kunoh, H., Oliver, R.P., 2000. First touch: An immediate response to surface recognition in conidia of *Blumeria graminis*. *Physiol. Mol. Plant Pathol.* 56, 63–70. <https://doi.org/10.1006/pmpp.1999.0241>
- Noël, L., Moores, T.L., van Der Biezen, E.A., Parniske, M., Daniels, M.J., Parker, J.E., Jones, J.D., 1999. Pronounced intraspecific haplotype divergence at the *RPP5* complex disease resistance locus of *Arabidopsis*. *Plant Cell* 11, 2099–2112.
- Nürnberger, T., Brunner, F., Kemmerling, B., Piater, L., 2004. Innate immunity in plants and animals: striking similarities and obvious differences. *Immunol. Rev.* 198, 249–266. <https://doi.org/10.1111/j.0105-2896.2004.0119.x>
- Nussbaumer, T., Martis, M.M., Roessner, S.K., Pfeifer, M., Bader, K.C., Sharma, S., Gundlach, H., Spannagl, M., 2013. MIPS PlantsDB: a database framework for comparative plant genome research. *Nucleic Acids Res.* 41, D1144–D1151. <https://doi.org/10.1093/nar/gks1153>
- O’Halloran, D.M., 2015. PrimerView: high-throughput primer design and visualization. *Source Code Biol. Med.* 10, 8. <https://doi.org/10.1186/s13029-015-0038-2>
- Pan, Q., Xu, Y., Li, K., Peng, Y., Zhan, W., Li, W., Li, L., Yan, J., 2017. The Genetic Basis of Plant Architecture in 10 Maize Recombinant Inbred Line Populations1. *Plant Physiol.* 175, 858–873. <https://doi.org/10.1104/pp.17.00709>
- Parlevliet, J.E., 2002. Durability of resistance against fungal, bacterial and viral pathogens; present situation. *Euphytica* 124, 147–156. <https://doi.org/10.1023/A:1015601731446>
- Pellio, B., Streng, S., Bauer, E., Stein, N., Perovic, D., Schiemann, A., Friedt, W., Ordon, F., Graner, A., 2005. High-resolution mapping of the *Rym4/Rym5* locus conferring resistance to the barley yellow mosaic virus complex (BaMMV, BaYMV, BaYMV-2) in barley (*Hordeum vulgare* ssp. *vulgare*L.). *Theor. Appl. Genet.* 110, 283–293. <https://doi.org/10.1007/s00122-004-1832-4>
- Pethybridge, S.J., Nelson, S.C., 2015. Leaf Doctor: A New Portable Application for Quantifying Plant Disease Severity. *Plant Dis.* 99, 1310–1316. <https://doi.org/10.1094/PDIS-03-15-0319-RE>
- Pfeifer, M., Martis, M., Asp, T., Mayer, K.F.X., Lübberstedt, T., Byrne, S., Frei, U., Studer, B., 2013. The Perennial Ryegrass GenomeZipper: Targeted Use of Genome Resources for Comparative Grass Genomics. *Plant Physiol.* 161, 571–582. <https://doi.org/10.1104/pp.112.207282>
- Pieterse, C.M.J., Leon-Reyes, A., Ent, S.V. der, Wees, S.C.M.V., 2009. Networking by small-molecule hormones in plant immunity. *Nat. Chem. Biol.* 5, 308–316. <https://doi.org/10.1038/nchembio.164>

- Piffanelli, P., Zhou, F., Casais, C., Orme, J., Jarosch, B., Schaffrath, U., Collins, N.C., Panstruga, R., Schulze-Lefert, P., 2002. The Barley *MLO* Modulator of Defense and Cell Death Is Responsive to Biotic and Abiotic Stress Stimuli. *Plant Physiol.* 129, 1076–1085. <https://doi.org/10.1104/pp.010954>
- Poland, J.A., Balint-Kurti, P.J., Wisser, R.J., Pratt, R.C., Nelson, R.J., 2009. Shades of gray: the world of quantitative disease resistance. *Trends Plant Sci.* 14, 21–29. <https://doi.org/10.1016/j.tplants.2008.10.006>
- Poland, J.A., Brown, P.J., Sorrells, M.E., Jannink, J.-L., 2012. Development of High-Density Genetic Maps for Barley and Wheat Using a Novel Two-Enzyme Genotyping-by-Sequencing Approach. *PLOS ONE* 7, e32253. <https://doi.org/10.1371/journal.pone.0032253>
- Poursarebani, N., Seidensticker, T., Koppolu, R., Trautewig, C., Gawroński, P., Bini, F., Govind, G., Rutten, T., Sakuma, S., Tagiri, A., Wolde, G.M., Youssef, H.M., Battal, A., Ciannamea, S., Fusca, T., Youssef, H.M., Nussbaumer, T., Pozzi, C., Börner, A., Lundqvist, U., Komatsuda, T., Salvi, S., Tuberosa, R., Uauy, C., Sreenivasulu, N., Rossini, L., Schnurbusch, T., 2015. The Genetic Basis of Composite Spike Form in Barley and “Miracle-Wheat.” *Genetics* genetics.115.176628. <https://doi.org/10.1534/genetics.115.176628>
- Pryce-jones, E., Carver, T., Gurr, S.J., 1999. The roles of cellulase enzymes and mechanical force in host penetration by *Erysiphe graminis* f.sp.*hordei*. *Physiol. Mol. Plant Pathol.* 55, 175–182. <https://doi.org/10.1006/pmpp.1999.0222>
- Putnam, N.H., O’Connell, B.L., Stites, J.C., Rice, B.J., Blanchette, M., Calef, R., Troll, C.J., Fields, A., Hartley, P.D., Sugnet, C.W., Haussler, D., Rokhsar, D.S., Green, R.E., 2016. Chromosome-scale shotgun assembly using an in vitro method for long-range linkage. *Genome Res.* <https://doi.org/10.1101/gr.193474.115>
- Řepková, J., Dreiseitl, A., Lízal, P., Kyjovská, Z., Teturová, K., Psočková, R., Jahoor, A., 2006. Identification of Resistance Genes Against Powdery Mildew in Four Accessions of *Hordeum vulgare* SSP. *Spontaneum*. *Euphytica* 151, 23–30. <https://doi.org/10.1007/s10681-006-9109-4>
- Ricaud, C., 1974. Factors affecting yellow spot development, its control and effect on cane and sugar yields. *Proc. Congr.*
- Romero, L.E., Lozano, I., Garavito, A., Carabali, S.J., Triana, M., Villareal, N., Reyes, L., Duque, M.C., Martinez, C.P., Calvert, L., Lorieux, M., 2014. Major QTLs Control Resistance to Rice Hoja Blanca Virus and Its Vector *Tagosodes orizicolus*. *G3amp58 GenesGenomesGenetics* 4, 133–142. <https://doi.org/10.1534/g3.113.009373>
- Ruperao, P., Edwards, D., 2015. Bioinformatics: identification of markers from next-generation sequence data. *Methods Mol. Biol.* Clifton NJ 1245, 29–47. https://doi.org/10.1007/978-1-4939-1966-6_3

- Saisho, D., Myoraku, E., Kawasaki, S., Sato, K., Takeda, K., 2007. Construction and Characterization of a Bacterial Artificial Chromosome (BAC) Library from the Japanese Malting Barley variety 'Haruna Nijo.' *Breed. Sci.* 57, 29–38. <https://doi.org/10.1270/jsbbs.57.29>
- Saisho, D., Takeda, K., 2011. Barley: Emergence as a New Research Material of Crop Science. *Plant Cell Physiol.* 52, 724–727. <https://doi.org/10.1093/pcp/pcr049>
- Sambrook, J., Fritsch, E.F., Maniatis, T., 1989. *Molecular cloning: a laboratory manual*. Mol. Cloning Lab. Man.
- Saraste, M., Sibbald, P.R., Wittinghofer, A., 1990. The P-loop — a common motif in ATP- and GTP-binding proteins. *Trends Biochem. Sci.* 15, 430–434. [https://doi.org/10.1016/0968-0004\(90\)90281-F](https://doi.org/10.1016/0968-0004(90)90281-F)
- Schiff, C.L., Wilson, I.W., Somerville, S.C., 2001. Polygenic powdery mildew disease resistance in *Arabidopsis thaliana*: quantitative trait analysis of the accession Warschau-1. *Plant Pathol.* 50, 690–701. <https://doi.org/10.1046/j.1365-3059.2001.00611.x>
- Schönfeld, M., Ragni, A., Fischbeck, G., Jahoor, A., 1996. RFLP mapping of three new loci for resistance genes to powdery mildew (*Erysiphe graminis* f. sp. *hordei*) in barley. *Theor. Appl. Genet.* 93, 48–56. <https://doi.org/10.1007/BF00225726>
- Schulte, D., Ariyadasa, R., Shi, B., Fleury, D., Saski, C., Atkins, M., deJong, P., Wu, C.-C., Graner, A., Langridge, P., Stein, N., 2011. BAC library resources for map-based cloning and physical map construction in barley (*Hordeum vulgare* L.). *BMC Genomics* 12, 247. <https://doi.org/10.1186/1471-2164-12-247>
- Schulze-Lefert, P., Vogel, J., 2000. Closing the ranks to attack by powdery mildew. *Trends Plant Sci.* 5, 343–348. [https://doi.org/10.1016/S1360-1385\(00\)01683-6](https://doi.org/10.1016/S1360-1385(00)01683-6)
- Schweizer, P., Pokorny, J., Abderhalden, O., Dudler, R., 1999. A Transient Assay System for the Functional Assessment of Defense-Related Genes in Wheat. *Mol. Plant. Microbe Interact.* 12, 647–654. <https://doi.org/10.1094/MPMI.1999.12.8.647>
- Schweizer, P., Stein, N., 2011. Large-Scale Data Integration Reveals Colocalization of Gene Functional Groups with Meta-QTL for Multiple Disease Resistance in Barley. *Mol. Plant. Microbe Interact.* 24, 1492–1501. <https://doi.org/10.1094/MPMI-05-11-0107>
- Schwessinger, B., Zipfel, C., 2008. News from the frontline: recent insights into PAMP-triggered immunity in plants. *Curr. Opin. Plant Biol., Biotic Interactions* 11, 389–395. <https://doi.org/10.1016/j.pbi.2008.06.001>
- Seah, S., Yaghoobi, J., Rossi, M., Gleason, C.A., Williamson, V.M., 2004. The nematode-resistance gene, *Mi-1*, is associated with an inverted chromosomal segment in susceptible compared to resistant tomato. *Theor. Appl. Genet.* 108, 1635–1642. <https://doi.org/10.1007/s00122-004-1594-z>

- Seeholzer, S., Tsuchimatsu, T., Jordan, T., Bieri, S., Pajonk, S., Yang, W., Jahoor, A., Shimizu, K.K., Keller, B., Schulze-Lefert, P., 2010. Diversity at the *Mla* Powdery Mildew Resistance Locus from Cultivated Barley Reveals Sites of Positive Selection. *Mol. Plant. Microbe Interact.* 23, 497–509. <https://doi.org/10.1094/MPMI-23-4-0497>
- Seiffert, U., Schweizer, P. (Eds.), 2005. *Bioinformatics Using Computational Intelligence Paradigms, Studies in Fuzziness and Soft Computing.* Springer-Verlag, Berlin Heidelberg.
- Sekhwil, M., Li, P., Lam, I., Wang, X., Cloutier, S., You, F., 2015. Disease Resistance Gene Analogs (RGAs) in Plants. *Int. J. Mol. Sci.* 16, 19248–19290. <https://doi.org/10.3390/ijms160819248>
- Sharma, Shiveta, Sharma, Shailendra, Kopisch-Obuch, F.J., Keil, T., Laubach, E., Stein, N., Graner, A., Jung, C., 2011. QTL analysis of root-lesion nematode resistance in barley: 1. *Pratylenchus neglectus*. *Theor. Appl. Genet.* 122, 1321–1330. <https://doi.org/10.1007/s00122-011-1533-8>
- Shi, B.J., Sutton, T., Collins, N.C., Pallotta, M., Langridge, P., 2010. Construction of a barley bacterial artificial chromosome library suitable for cloning genes for boron tolerance, sodium exclusion and high grain zinc content. *Plant Breed.* 129, 291–296. <https://doi.org/10.1111/j.1439-0523.2009.01762.x>
- Shin, J.S., Chao, S., Corpuz, L., Blake, T., 1990. A partial map of the barley genome incorporating restriction fragment length polymorphism, polymerase chain reaction, isozyme, and morphological marker loci. *Genome* 33, 803–810. <https://doi.org/10.1139/g90-121>
- Silvar, C., Perovic, D., Nussbaumer, T., Spannagl, M., Usadel, B., Casas, A., Igartua, E., Ordon, F., 2013. Towards Positional Isolation of Three Quantitative Trait Loci Conferring Resistance to Powdery Mildew in Two Spanish Barley Landraces. *PLoS ONE* 8, e67336. <https://doi.org/10.1371/journal.pone.0067336>
- Silvar, C., Perovic, D., Scholz, U., Casas, A.M., Igartua, E., Ordon, F., 2012. Fine mapping and comparative genomics integration of two quantitative trait loci controlling resistance to powdery mildew in a Spanish barley landrace. *Theor. Appl. Genet.* 124, 49–62. <https://doi.org/10.1007/s00122-011-1686-5>
- Simmonds, N.W., 1991. Genetics of Horizontal Resistance to Diseases of Crops. *Biol. Rev.* 66, 189–241. <https://doi.org/10.1111/j.1469-185X.1991.tb01140.x>
- Singh, R.P., Hodson, D.P., Huerta-Espino, J., Jin, Y., Njau, P., Wanyera, R., Herrera-Foessel, S.A., Ward, R.W., 2008. Will Stem Rust Destroy the World's Wheat Crop?, in: *Advances in Agronomy.* Academic Press, pp. 271–309. [https://doi.org/10.1016/S0065-2113\(08\)00205-8](https://doi.org/10.1016/S0065-2113(08)00205-8)
- Śliwka, J., Jakuczun, H., Chmielarz, M., Hara-Skrzypiec, A., Tomczyńska, I., Kilian, A., Zimnoch-Guzowska, E., 2012. Late blight resistance gene from *Solanum ruiz-ceballosii* is

- located on potato chromosome X and linked to violet flower colour. *BMC Genet.* 13, 11. <https://doi.org/10.1186/1471-2156-13-11>
- Spindel, J., Wright, M., Chen, C., Cobb, J., Gage, J., Harrington, S., Lorieux, M., Ahmadi, N., McCouch, S., 2013. Bridging the genotyping gap: using genotyping by sequencing (GBS) to add high-density SNP markers and new value to traditional bi-parental mapping and breeding populations. *Theor. Appl. Genet.* 126, 2699–2716. <https://doi.org/10.1007/s00122-013-2166-x>
- Stahl, E.A., Dwyer, G., Mauricio, R., Kreitman, M., Bergelson, J., 1999. Dynamics of disease resistance polymorphism at the *Rpm1* locus of *Arabidopsis*. *Nature* 400, 667–671. <https://doi.org/10.1038/23260>
- St.Clair, D.A., 2010. Quantitative Disease Resistance and Quantitative Resistance Loci in Breeding. *Annu. Rev. Phytopathol.* 48, 247–268. <https://doi.org/10.1146/annurev-phyto-080508-081904>
- Stein, N., Graner, A., 2004. Map-Based Gene Isolation in Cereal Genomes, in: *Cereal Genomics*. Springer, Dordrecht, pp. 331–360. https://doi.org/10.1007/1-4020-2359-6_11
- Stein, N., Herren, G., Keller, B., 2001. A new DNA extraction method for high-throughput marker analysis in a large-genome species such as *Triticum aestivum*. *Plant Breed.* 120, 354–356. <https://doi.org/10.1046/j.1439-0523.2001.00615.x>
- Stein, N., Prasad, M., Scholz, U., Thiel, T., Zhang, H., Wolf, M., Kota, R., Varshney, R.K., Perovic, D., Grosse, I., Graner, A., 2007. A 1,000-loci transcript map of the barley genome: new anchoring points for integrative grass genomics. *Theor. Appl. Genet.* 114, 823–839. <https://doi.org/10.1007/s00122-006-0480-2>
- Steuernagel, B., Periyannan, S.K., Hernández-Pinzón, I., Witek, K., Rouse, M.N., Yu, G., Hatta, A., Ayliffe, M., Bariana, H., Jones, J.D.G., Lagudah, E.S., Wulff, B.B.H., 2016. Rapid cloning of disease-resistance genes in plants using mutagenesis and sequence capture. *Nat. Biotechnol.* 34, nbt.3543. <https://doi.org/10.1038/nbt.3543>
- Steuernagel, B., Witek, K., Jones, J.D.G., Wulff, B.B.H., 2017. MutRenSeq: A Method for Rapid Cloning of Plant Disease Resistance Genes, in: *Wheat Rust Diseases, Methods in Molecular Biology*. Humana Press, New York, NY, pp. 215–229. https://doi.org/10.1007/978-1-4939-7249-4_19
- Stirnweis, D., Milani, S.D., Brunner, S., Herren, G., Buchmann, G., Peditto, D., Jordan, T., Keller, B., 2014. Suppression among alleles encoding nucleotide-binding–leucine-rich repeat resistance proteins interferes with resistance in F₁ hybrid and allele-pyramided wheat plants. *Plant J.* 79, 893–903. <https://doi.org/10.1111/tbj.12592>
- Surana, P., Xu, R., Fuerst, G., Chapman, A.V.E., Nettleton, D., Wise, R.P., 2017. Interchromosomal Transfer of Immune Regulation During Infection of Barley with the Powdery Mildew Pathogen. *G3 Genes Genomes Genet.* 7, 3317–3329. <https://doi.org/10.1534/g3.117.300125>

- Szűcs, P., Blake, V.C., Bhat, P.R., Chao, S., Close, T.J., Cuesta-Marcos, A., Muehlbauer, G.J., Ramsay, L., Waugh, R., Hayes, P.M., 2009. An Integrated Resource for Barley Linkage Map and Malting Quality QTL Alignment. *Plant Genome* 2, 134–140. <https://doi.org/10.3835/plantgenome2008.01.0005>
- Takken, F.L., Goverse, A., 2012. How to build a pathogen detector: structural basis of NB-LRR function. *Curr. Opin. Plant Biol., Biotic interactions* 15, 375–384. <https://doi.org/10.1016/j.pbi.2012.05.001>
- Takken, F.L.W., Joosten, M.H.A.J., 2000. Plant Resistance Genes: Their Structure, Function and Evolution. *Eur. J. Plant Pathol.* 106, 699–713. <https://doi.org/10.1023/A:1026571130477>
- Tanksley, S.D., Ganal, M.W., Martin, G.B., 1995. Chromosome landing: a paradigm for map-based gene cloning in plants with large genomes. *Trends Genet.* 11, 63–68. [https://doi.org/10.1016/S0168-9525\(00\)88999-4](https://doi.org/10.1016/S0168-9525(00)88999-4)
- Tena, G., Boudsocq, M., Sheen, J., 2011. Protein kinase signaling networks in plant innate immunity. *Curr. Opin. Plant Biol.* 14, 519–529. <https://doi.org/10.1016/j.pbi.2011.05.006>
- Thiel, T., Kota, R., Grosse, I., Stein, N., Graner, A., 2004. SNP2CAPS: a SNP and INDEL analysis tool for CAPS marker development. *Nucleic Acids Res.* 32, e5–e5. <https://doi.org/10.1093/nar/gnh006>
- Thind, A.K., Wicker, T., Šimková, H., Fossati, D., Moullet, O., Brabant, C., Vrána, J., Doležel, J., Krattinger, S.G., 2017. Rapid cloning of genes in hexaploid wheat using cultivar-specific long-range chromosome assembly. *Nat. Biotechnol.* 35, nbt.3877. <https://doi.org/10.1038/nbt.3877>
- Tian, D., Araki, H., Stahl, E., Bergelson, J., Kreitman, M., 2002. Signature of balancing selection in *Arabidopsis*. *Proc. Natl. Acad. Sci.* 99, 11525–11530. <https://doi.org/10.1073/pnas.172203599>
- Ullrich, S.E., 2010a. *Barley: Production, Improvement, and Uses*. John Wiley & Sons.
- Ullrich, S.E., 2010b. Significance, Adaptation, Production, and Trade of Barley, in: Ullrich, S.E. (Ed.), *Barley*. Wiley-Blackwell, pp. 3–13. <https://doi.org/10.1002/9780470958636.ch1>
- van de Wouw, M., van Hintum, T., Kik, C., van Treuren, R., Visser, B., 2010. Genetic diversity trends in twentieth century crop cultivars: a meta analysis. *TAG Theor. Appl. Genet. Theor. Angew. Genet.* 120, 1241–1252. <https://doi.org/10.1007/s00122-009-1252-6>
- Van der Biezen, E.A., Jones, J.D., 1998. Plant disease-resistance proteins and the gene-for-gene concept. *Trends Biochem. Sci.* 23, 454–456.
- Van Ooijen, J.W., 2006. JoinMap® 4.0: software for the calculation of genetic linkage maps in experimental population. Kyazma BV.

- Varshney, R.K., Hoisington, D.A., Tyagi, A.K., 2006. Advances in cereal genomics and applications in crop breeding. *Trends Biotechnol.* 24, 490–499. <https://doi.org/10.1016/j.tibtech.2006.08.006>
- Varshney, R.K., Marcel, T.C., Ramsay, L., Russell, J., Röder, M.S., Stein, N., Waugh, R., Langridge, P., Niks, R.E., Graner, A., 2007. A high density barley microsatellite consensus map with 775 SSR loci. *Theor. Appl. Genet.* 114, 1091–1103. <https://doi.org/10.1007/s00122-007-0503-7>
- Varshney, R.K., Tuberosa, R. (Eds.), 2007. *Genomics-Assisted Crop Improvement: Vol 1: Genomics Approaches and Platforms*. Springer Netherlands.
- Villa, T.C.C., Maxted, N., Scholten, M., Ford-Lloyd, B., 2005. Defining and identifying crop landraces. *Plant Genet. Resour.* 3, 373–384. <https://doi.org/10.1079/PGR200591>
- von Korff, M., Wang, H., Léon, J., Pillen, K., 2005a. AB-QTL analysis in spring barley. I. Detection of resistance genes against powdery mildew, leaf rust and scald introgressed from wild barley. *Theor. Appl. Genet.* 111, 583–590. <https://doi.org/10.1007/s00122-005-2049-x>
- von Korff, M., Wang, H., Léon, J., Pillen, K., 2005b. AB-QTL analysis in spring barley. I. Detection of resistance genes against powdery mildew, leaf rust and scald introgressed from wild barley. *Theor. Appl. Genet.* 111, 583–590. <https://doi.org/10.1007/s00122-005-2049-x>
- Voorrips, R.E., 2002. MapChart: Software for the Graphical Presentation of Linkage Maps and QTLs. *J. Hered.* 93, 77–78. <https://doi.org/10.1093/jhered/93.1.77>
- Vrána, J., Kubaláková, M., Simková, H., Cíhalíková, J., Lysák, M.A., Dolezel, J., 2000. Flow sorting of mitotic chromosomes in common wheat (*Triticum aestivum* L.). *Genetics* 156, 2033–2041.
- Wang, B., Zhu, Y., Zhu, J., Liu, Z., Liu, H., Dong, X., Guo, J., Li, W., Chen, J., Gao, C., Zheng, X., E, L., Lai, J., Zhao, H., Song, W., 2018. Identification and Fine-Mapping of a Major Maize Leaf Width QTL in a Re-sequenced Large Recombinant Inbred Lines Population. *Front. Plant Sci.* 9. <https://doi.org/10.3389/fpls.2018.00101>
- Wang, R., Sun, L., Bao, L., Zhang, J., Jiang, Y., Yao, J., Song, L., Feng, J., Liu, S., Liu, Z., 2013. Bulk segregant RNA-seq reveals expression and positional candidate genes and allele-specific expression for disease resistance against enteric septicemia of catfish. *BMC Genomics* 14, 929. <https://doi.org/10.1186/1471-2164-14-929>
- Wang, Y., Cheng, X., Shan, Q., Zhang, Y., Liu, J., Gao, C., Qiu, J.-L., 2014. Simultaneous editing of three homoeoalleles in hexaploid bread wheat confers heritable resistance to powdery mildew. *Nat. Biotechnol.* 32, 947–951. <https://doi.org/10.1038/nbt.2969>
- Warr, A., Robert, C., Hume, D., Archibald, A., Deeb, N., Watson, M., 2015. Exome Sequencing: Current and Future Perspectives. *G3 GenesGenomesGenetics* 5, 1543–1550. <https://doi.org/10.1534/g3.115.018564>

- Warren, R.F., Henk, A., Mowery, P., Holub, E., Innes, R.W., 1998. A mutation within the leucine-rich repeat domain of the *Arabidopsis* disease resistance gene *RPS5* partially suppresses multiple bacterial and downy mildew resistance genes. *Plant Cell* 10, 1439–1452.
- Wei, F., Gobelmann-Werner, K., Morroll, S.M., Kurth, J., Mao, L., Wing, R., Leister, D., Schulze-Lefert, P., Wise, R.P., 1999. The *Mla* (Powdery Mildew) Resistance Cluster Is Associated With Three NBS-LRR Gene Families and Suppressed Recombination Within a 240-kb DNA Interval on Chromosome 5S (1HS) of Barley. *Genetics* 153, 1929–1948.
- Weiss, E., Zohary, D., 2011. The Neolithic Southwest Asian Founder Crops: Their Biology and Archaeobotany. *Curr. Anthropol.* 52, S237–S254. <https://doi.org/10.1086/658367>
- Wenzl, P., Li, H., Carling, J., Zhou, M., Raman, H., Paul, E., Hearnden, P., Maier, C., Xia, L., Caig, V., Ovesná, J., Cakir, M., Poulsen, D., Wang, J., Raman, R., Smith, K.P., Muehlbauer, G.J., Chalmers, K.J., Kleinhofs, A., Huttner, E., Kilian, A., 2006. A high-density consensus map of barley linking DArT markers to SSR, RFLP and STS loci and agricultural traits. *BMC Genomics* 7, 206. <https://doi.org/10.1186/1471-2164-7-206>
- Wiberg, A., 1974. Sources of resistance to powdery mildew in barley. *Hereditas* 78, 1–40. <https://doi.org/10.1111/j.1601-5223.1974.tb01426.x>
- Winfield, M.O., Wilkinson, P.A., Allen, A.M., Barker, G.L.A., Coghill, J.A., BurrIDGE, A., Hall, A., Brenchley, R.C., D'Amore, R., Hall, N., Bevan, M.W., Richmond, T., Gerhardt, D.J., Jeddelloh, J.A., Edwards, K.J., 2012. Targeted re-sequencing of the allohexaploid wheat exome. *Plant Biotechnol. J.* 10, 733–742. <https://doi.org/10.1111/j.1467-7652.2012.00713.x>
- Witek, K., Jupe, F., Witek, A.I., Baker, D., Clark, M.D., Jones, J.D.G., 2016. Accelerated cloning of a potato late blight-resistance gene using RenSeq and SMRT sequencing. *Nat. Biotechnol.* 34, 656–660. <https://doi.org/10.1038/nbt.3540>
- Wolter, M., Hollricher, K., Salamini, F., Schulze-Lefert, P., 1993. The *mlo* resistance alleles to powdery mildew infection in barley trigger a developmentally controlled defence mimic phenotype. *Mol. Gen. Genet.* MGG 239, 122–128.
- Wolters, A.-M.A., Caro, M., Dong, S., Finkers, R., Gao, J., Visser, R.G.F., Wang, X., Du, Y., Bai, Y., 2015. Detection of an inversion in the Ty-2 region between *S. lycopersicum* and *S. habrochaites* by a combination of de novo genome assembly and BAC cloning. *TAG Theor. Appl. Genet. Theor. Angew. Genet.* 128, 1987–1997. <https://doi.org/10.1007/s00122-015-2561-6>
- Yamaguchi, K., Yamada, K., Kawasaki, T., 2013. Receptor-like cytoplasmic kinases are pivotal components in pattern recognition receptor-mediated signaling in plant immunity. *Plant Signal. Behav.* 8. <https://doi.org/10.4161/psb.25662>
- Yamanaka, N., Watanabe, S., Toda, K., Hayashi, M., Fuchigami, H., Takahashi, R., Harada, K., 2005. Fine mapping of the *FTI* locus for soybean flowering time using a residual

- heterozygous line derived from a recombinant inbred line. *Theor. Appl. Genet.* 110, 634–639. <https://doi.org/10.1007/s00122-004-1886-3>
- Yang, P., Lüpken, T., Habekuss, A., Hensel, G., Steuernagel, B., Kilian, B., Ariyadasa, R., Himmelbach, A., Kumlehn, J., Scholz, U., Ordon, F., Stein, N., 2014. *PROTEIN DISULFIDE ISOMERASE LIKE 5-1* is a susceptibility factor to plant viruses. *Proc. Natl. Acad. Sci.* 111, 2104–2109. <https://doi.org/10.1073/pnas.1320362111>
- Ye, Y., Ding, Y., Jiang, Q., Wang, F., Sun, J., Zhu, C., 2017. The role of receptor-like protein kinases (RLKs) in abiotic stress response in plants. *Plant Cell Rep.* 36, 235–242. <https://doi.org/10.1007/s00299-016-2084-x>
- Yeo, F.K.S., Wang, Y., Vozabova, T., Huneau, C., Leroy, P., Chalhoub, B., Qi, X.Q., Niks, R.E., Marcel, T.C., 2016. Haplotype divergence and multiple candidate genes at *Rphq2*, a partial resistance QTL of barley to *Puccinia hordei*. *Theor. Appl. Genet.* 129, 289–304. <https://doi.org/10.1007/s00122-015-2627-5>
- Yitbarek, S., Berhane, L., Fikadu, A., Van Leur, J. a. G., Grando, S., Ceccarelli, S., 1998. Variation in Ethiopian barley landrace populations for resistance to barley leaf scald and netblotch. *Plant Breed.* 117, 419–423. <https://doi.org/10.1111/j.1439-0523.1998.tb01966.x>
- Youssef, H.M., Eggert, K., Koppolu, R., Alqudah, A.M., Poursarebani, N., Fazeli, A., Sakuma, S., Tagiri, A., Rutten, T., Govind, G., Lundqvist, U., Graner, A., Komatsuda, T., Sreenivasulu, N., Schnurbusch, T., 2016. *VRS2* regulates hormone-mediated inflorescence patterning in barley. *Nat. Genet.* 49, ng.3717. <https://doi.org/10.1038/ng.3717>
- Yu, S., Yang, C., Fan, Y., Zhuang, J., Li, X., 2008. Genetic dissection of a thousand-grain weight quantitative trait locus on rice chromosome 1. *Chin. Sci. Bull.* 53, 2326–2332. <https://doi.org/10.1007/s11434-008-0281-x>
- Yu, Y., Tomkins, J.P., Waugh, R., Frisch, D.A., Kudrna, D., Kleinhofs, A., Brueggeman, R.S., Muehlbauer, G.J., Wise, R.P., Wing, R.A., 2000. A bacterial artificial chromosome library for barley (*Hordeum vulgare* L.) and the identification of clones containing putative resistance genes. *Theor. Appl. Genet.* 101, 1093–1099. <https://doi.org/10.1007/s001220051584>
- Zeng, X., Long, H., Wang, Z., Zhao, S., Tang, Y., Huang, Z., Wang, Y., Xu, Q., Mao, L., Deng, G., Yao, X., Li, X., Bai, L., Yuan, H., Pan, Z., Liu, R., Chen, X., WangMu, Q., Chen, M., Yu, L., Liang, J., DunZhu, D., Zheng, Y., Yu, S., LuoBu, Z., Guang, X., Li, J., Deng, C., Hu, W., Chen, C., TaBa, X., Gao, L., Lv, X., Abu, Y.B., Fang, X., Nevo, E., Yu, M., Wang, J., Tashi, N., 2015. The draft genome of Tibetan hulless barley reveals adaptive patterns to the high stressful Tibetan Plateau. *Proc. Natl. Acad. Sci.* 112, 1095–1100. <https://doi.org/10.1073/pnas.1423628112>
- Zhang, Q.F., Webster, R.K., Allard, R.W., 1987. Geographical distribution and associations between resistance to four races of *Rhynchosporium secalis*. *Phytopathol. USA.*

- Zhang, X.S., Choi, J.H., Heinz, J., Chetty, C.S., 2006. Domain-Specific Positive Selection Contributes to the Evolution of *Arabidopsis* Leucine-Rich Repeat Receptor-Like Kinase (LRR RLK) Genes. *J. Mol. Evol.* 63, 612–621. <https://doi.org/10.1007/s00239-005-0187-z>
- Zhao, Z., Tavoosidana, G., Sjölander, M., Göndör, A., Mariano, P., Wang, S., Kanduri, C., Lezcano, M., Sandhu, K.S., Singh, U., Pant, V., Tiwari, V., Kurukuti, S., Ohlsson, R., 2006. Circular chromosome conformation capture (4C) uncovers extensive networks of epigenetically regulated intra- and interchromosomal interactions. *Nat. Genet.* 38, 1341–1347. <https://doi.org/10.1038/ng1891>
- Zipfel, C., 2014. Plant pattern-recognition receptors. *Trends Immunol.* 35, 345–351. <https://doi.org/10.1016/j.it.2014.05.004>
- Zipfel, C., Felix, G., 2005. Plants and animals: a different taste for microbes? *Curr. Opin. Plant Biol., Biotic interactions* 8, 353–360. <https://doi.org/10.1016/j.pbi.2005.05.004>
- Zohary, D., Hopf, M., Weiss, E., 2012. *Domestication of Plants in the Old World: The origin and spread of domesticated plants in Southwest Asia, Europe, and the Mediterranean Basin*, Fourth Edition. ed. Oxford University Press, Oxford, New York.

8 Appendix Tables

Appendix 1: List of the identified resistant barley accessions, available in Gatersleben genebank, to seven modern, highly virulent powdery mildew isolates.

	Resistant accessions ¹	Powdery mildew isolates						
		78P ²	D12-12 ²	CH4.8 ²	35 ³	69 ³	148 ³	289 ³
1	Res_11	2.5	24.1	2.5	38.0	47.4	38.0	47.4
2	Res_40	2.5	3.6	2.5	2.5	2.5	2.5	2.5
3	Res_42	2.5	2.5	2.5	2.5	2.5	2.5	2.5
4	Res_54	2.5	2.5	2.5	32.4	32.4	32.4	32.4
5	Res_72	2.5	2.5	2.5	2.5	15.5	2.5	2.5
6	Res_77	2.5	2.5	2.5	2.5	2.5	2.5	2.5
7	Res_79	2.5	2.5	9.0	9.0	15.5	12.3	9.0
8	Res_89	2.5	4.1	5.8	5.8	9.0	12.3	2.5
9	Res_108	2.5	2.5	2.5	2.5	2.5	2.5	2.5
10	Res_33	3.3	3.3	2.5	32.4	66.1	38.0	26.8
11	Res_28	3.6	3.6	2.5	9.0	21.1	12.3	15.5
12	Res_55	4.1	2.5	15.5	47.4	66.1	47.4	38.0
13	Res_58	4.1	4.9	2.5	38.0	32.4	32.4	26.8
14	Res_50	4.9	7.1	2.5	2.5	9.0	2.5	11.4
15	Res_70	5.1	2.5	2.5	32.4	32.4	26.8	26.8
16	Res_16	5.8	13.7	12.3	51.1	38.0	47.4	38.0
17	Res_18	8.0	8.2	2.5	26.8	32.4	21.1	26.8
18	Res_38	8.0	11.9	15.5	47.4	56.8	38.0	66.1
19	Res_84	9.0	6.6	5.8	38.0	38.0	56.8	38.0
20	Res_85	9.8	14.3	5.8	38.0	47.4	47.4	38.0
21	Res_12	13.4	19.7	21.1	47.4	38.0	32.4	47.4
22	Res_15	13.6	13.3	5.8	47.4	38.0	47.4	38.0
23	Res_17	16.7	5.8	2.5	56.8	47.4	56.8	56.8
24	Res_86	17.4	10.4	2.5	2.5	32.4	2.5	2.5
25	Res_48	17.7	30.0	2.5	56.8	51.1	47.4	38.0

Appendix 1; continued

		Powdery mildew isolates						
	Resistant accessions¹	78P²	D12-12²	CH4.8²	35³	69³	148³	289³
28	Res_35	20.7	12.4	9.0	32.4	47.4	26.8	32.4
29	Res_41	21.3	21.2	2.5	2.5	5.8	5.8	2.5
30	Res_103	21.5	23.3	21.1	2.5	2.5	2.5	2.5
31	Res_67	21.6	13.2	2.5	5.8	2.5	12.3	2.5
32	Res_73	20.1	13.0	2.5	2.5	2.5	2.5	2.5
33	Res_9	28.5	11.8	15.5	47.4	47.4	47.4	38.0
34	Res_14	30.4	26.3	15.5	38.0	47.4	32.4	38.0
35	Res_27	38.2	29.3	2.5	38.0	38.0	47.4	56.8
	Golden Promise	50.0	50.0	47.3	55.3	47.4	42.4	56.8
	Ingrid	57.7	53.1	54.5	56.8	56.8	66.1	32.4
	Morex	67.1	66.2	73.9	59.4	57.4	68.0	67.4

¹The accessions were previously re-named according to number of tested barley accessions. The accession with the ID of Res_73 is corresponded to 'HOR2573 which highlighted in gray.

² European isolates

³ Israeli isolates

Appendix 2: Summary of QTL found for *Bgh* resistance in F2 generation of ‘HOR2573 x Morex’ population.

Population	Chr	Markers_interval ¹	Interval size(bp) ²	LOD ³	R ² *	Add ⁴	Dom ⁵
F2	1H	ge00236s01- ge00382s01	480,448,403-511,924,174	3.3	0.02	-10.8	-6.2
	2H	ge00372s01- ge00260s01	750,535,187_758,850,944	23.1	0.27	-32.5	-29.2

¹ 95% confidence interval flanked by DNA-markers.

²The physical coordinates of the 95% confidence interval flanked by markers on barley reference genome.

³LOD significant Threshold value: 3

⁴ additive effect

⁵ dominant effect

* R² percentage of phenotypic variance explained by the QTL

Appendix 3: List of the gene located in the confidence interval of the detected major single QTL flanked by M238 and M252

Gene ID	Chr.	Physical pos ¹ . start	Physical pos. end	Conf. ²	Gene Size (bp)	Annotation ³
HORVU2Hr1G126170	2H	762,834,084	762,844,599	HC	10,516	undescribed protein
HORVU2Hr1G126180	2H	762,856,615	762,863,667	HC	7,053	undescribed protein
HORVU2Hr1G126190	2H	762,884,974	762,885,653	LC	680	undescribed protein
HORVU2Hr1G126200	2H	762,888,691	762,892,551	HC	3,861	LRR-LRK family protein
HORVU2Hr1G126210	2H	762,894,418	762,896,103	LC	1,686	undescribed protein
HORVU2Hr1G126220	2H	762,932,507	762,932,706	HC	200	non-specific serine/threonine protein kinase
HORVU2Hr1G126230	2H	762,948,938	762,953,829	HC	4,892	RING/U-box superfamily protein
HORVU2Hr1G126240	2H	762,985,247	762,985,748	HC	502	undescribed protein
HORVU2Hr1G126250	2H	762,988,918	762,992,772	HC	3,855	LRR-LRK family protein
HORVU2Hr1G126260	2H	762,993,731	762,994,590	LC	860	undescribed protein
HORVU2Hr1G126270	2H	762,993,731	763,014,651	LC	20,921	undescribed protein
HORVU2Hr1G126280	2H	762,997,087	763,012,501	LC	15,415	undescribed protein
HORVU2Hr1G126290	2H	763,009,236	763,015,651	HC	2,536	undescribed protein
HORVU2Hr1G126300	2H	763,028,813	763,029,821	LC	1,009	undescribed protein
HORVU2Hr1G126310	2H	763,030,237	763,030,558	LC	322	undescribed protein
HORVU2Hr1G126320	2H	763,068,669	763,069,446	LC	778	undescribed protein
HORVU2Hr1G126330	2H	763,068,669	763,069,446	LC	778	undescribed protein
HORVU2Hr1G126340	2H	763,070,723	763,071,609	LC	887	undescribed protein
HORVU2Hr1G126350	2H	763,099,080	763,099,933	HC	854	SCAR homolog 2
HORVU2Hr1G126360	2H	763,127,149	763,129,662	LC	2,514	undescribed protein
HORVU2Hr1G126370	2H	763,149,795	763,150,358	HC	564	undescribed protein
HORVU2Hr1G126380	2H	763,199,723	763,217,682	HC	17,960	NBS-LRR family protein
HORVU2Hr1G126390	2H	763,203,996	763,204,284	HC	289	undescribed protein
HORVU2Hr1G126400	2H	763,204,441	763,204,837	LC	397	retrotransposon protein, putative, unclassified
HORVU2Hr1G126410	2H	763,206,913	763,207,301	LC	389	undescribed protein

Appendix 3; continued

Gene ID	Chr.	Physical pos.¹. start	Physical pos. end	Conf.²	Gene Size (bp)	Annotation³
HORVU2Hr1G126420	2H	763,207,414	763,207,619	LC	206	undescribed protein
HORVU2Hr1G126430	2H	763,319,071	763,322,424	LC	3,354	undescribed protein
HORVU2Hr1G126440	2H	763,333,005	763,348,847	HC	15,843	NBS-LRR family protein
HORVU2Hr1G126450	2H	763,362,551	763,362,787	LC	237	retrotransposon protein, putative, unclassified
HORVU2Hr1G126460	2H	763,401,509	763,401,661	LC	153	undescribed protein
HORVU2Hr1G126470	2H	763,467,610	763,469,844	HC	2,235	LRR-LRK family protein
HORVU2Hr1G126480	2H	763,470,476	763,470,621	LC	146	undescribed protein
HORVU2Hr1G126490	2H	763,538,813	763,543,592	HC	4,780	protein kinase superfamily protein
HORVU2Hr1G126500	2H	763,541,059	763,543,493	LC	2,435	undescribed protein
HORVU2Hr1G126510	2H	763,550,972	763,558,662	HC	7,011	NBS-LRR family protein
HORVU2Hr1G126520	2H	763,551,445	763,551,751	LC	307	undescribed protein
HORVU2Hr1G126530	2H	763,559,144	763,561,388	LC	2,245	undescribed protein
HORVU2Hr1G126540	2H	763,693,944	763,695,606	HC	1,663	homology with Amidase superfamily
HORVU2Hr1G126550	2H	763,746,573	763,747,639	HC	1,067	Zn-dependent hydrolase of beta-lactamase
HORVU2Hr1G126560	2H	763,754,880	763,755,894	LC	1,015	unknown function
HORVU2Hr1G126570	2H	763,821,584	763,823,933	HC	2,350	PATATIN-like protein 4
HORVU2Hr1G126580	2H	763,877,006	763,877,263	HC	258	protein FAR1-related sequence 3
HORVU2Hr1G126590	2H	763,878,464	763,878,987	LC	524	undescribed protein
HORVU2Hr1G126600	2H	763,885,160	763,888,302	HC	3,143	protein SYS1 homolog
HORVU2Hr1G126610	2	763,960,551	763,972,812	HC	12,262	transportin 1
HORVU2Hr1G126620	2	763,960,649	763,961,361	LC	713	undescribed protein
HORVU2Hr1G126630	2	764,036,292	764,037,329	LC	1,038	transposon protein, putative, Pong sub-class
HORVU2Hr1G126640	2	764,045,393	764,045,814	HC	422	translocon at the outer membrane of chloroplasts 64-V
HORVU2Hr1G126650	2	764,051,631	764,052,511	HC	881	amidase 1
HORVU2Hr1G126660	2	764,066,166	764,068,524	HC	2,359	PATATIN-like protein 4

Appendix 3; continued

Gene ID	Chr.	Physical pos ¹ . start	Physical pos. end	Conf. ²	Gene Size (bp)	Annotation ³
HORVU2Hr1G126670	2	764,069,607	764,070,999	LC	1,393	transposon protein, putative, CACTA, En/Spm sub-class
HORVU2Hr1G126680	2	764,088,260	764,089,173	LC	914	undescribed protein
HORVU2Hr1G126690	2	764,279,329	764,290,102	HC	10,774	acyl-CoA N-acyltransferase with RING/FYVE/PHD-type zinc finger protein
HORVU2Hr1G126700	2	764,279,385	764,282,382	LC	2,998	undescribed protein
HORVU2Hr1G126710	2	764,332,459	764,333,183	LC	725	NA
HORVU2Hr1G126720	2	764,378,805	764,380,707	HC	1,903	chitinase 12
HORVU2Hr1G126730	2	764,420,452	764,424,390	HC	3,939	C2 calcium/lipid-binding plant phosphoribosyltransferase family protein
HORVU2Hr1G126740	2	764,571,007	764,574,276	HC	3,270	chitinase family protein
HORVU2Hr1G126750	2	764,585,667	764,594,323	HC	8657	DNA-directed RNA polymerase II subunit 1
HORVU2Hr1G126760	2	764,637,921	764,638,247	HC	327	chitinase 12
HORVU2Hr1G126770	2	764,659,682	764,662,501	LC	2,820	undescribed protein
HORVU2Hr1G126780	2	764,740,554	764,743,362	LC	2,809	undescribed protein
HORVU2Hr1G126790	2	764,845,211	764,846,307	LC	1,097	undescribed protein
HORVU2Hr1G126800	2	764,857,492	764,859,404	HC	1,913	FAR1-related sequence 5
HORVU2Hr1G126810	2	765,050,410	765,159,289	HC	108,880	receptor kinase 1
HORVU2Hr1G126820	2	765,053,233	765,053,802	LC	570	undescribed protein
HORVU2Hr1G126830	2	765,053,377	765,054,343	LC	967	undescribed protein
HORVU2Hr1G126840	2	765,057,966	765,058,706	LC	741	undescribed protein
HORVU2Hr1G126850	2	765,066,649	765,068,201	LC	1,553	transposon protein, putative, CACTA, En/Spm sub-class
HORVU2Hr1G126860	2	765,073,279	765,074,638	LC	1,360	Retrotransposon protein, putative, Ty1-copia subclass
HORVU2Hr1G126870	2	765,156,820	765,157,404	HC	585	autophagy-related protein 7
HORVU2Hr1G126880	2	765,246,329	765,246,896	LC	568	undescribed protein

Appendix 3; continued

Gene ID	Chr.	Physical pos¹. start	Physical pos. end	Conf.²	Gene Size (bp)	Annotation³
HORVU2Hr1G126890	2	765,434,709	765,435,276	LC	568	undescribed protein
HORVU2Hr1G126900	2	765,486,881	765,487,987	LC	1,107	undescribed protein
HORVU2Hr1G126910	2	765,518,641	765,518,952	LC	312	undescribed protein
HORVU2Hr1G126920	2	765,523,123	765,523,341	LC	219	retrotransposon protein, putative, unclassified
HORVU2Hr1G126930	2	765,605,271	765,608,372	HC	3,102	CsAtPR5
HORVU2Hr1G126940	2	765,627,839	765,634,298	HC	6,460	phosphatidylinositol-4-phosphate 5-kinase family protein
HORVU2Hr1G126950	2	765,634,629	765,637,443	HC	2,815	eamA-like transporter family protein
HORVU2Hr1G126960	2	765,665,646	765,666,966	HC	1,321	CsAtPR5, putative, expressed
HORVU2Hr1G126970	2	765,717,517	765,717,848	LC	332	undescribed protein
HORVU2Hr1G126980	2	765,723,631	765,724,784	HC	1,154	undescribed protein
HORVU2Hr1G126990	2	765,727,790	765,728,039	LC	250	undescribed protein
HORVU2Hr1G127000	2	765,727,924	765,728,196	LC	273	undescribed protein
HORVU2Hr1G127010	2	765,728,706	765,729,641	LC	936	retrotransposon protein, putative, unclassified
HORVU2Hr1G127020	2	765,729,737	765,730,087	HC	351	undescribed protein
HORVU2Hr1G127030	2	765,730,088	765,730,234	HC	147	serine/threonine-protein kinase SMG1
HORVU2Hr1G127040	2	765,730,322	765,730,750	HC	429	undescribed protein
HORVU2Hr1G127050	2	765,746,141	765,746,407	LC	267	undescribed protein
HORVU2Hr1G127060	2	765,749,699	765,752,266	HC	2,568	eamA-like transporter family protein
HORVU2Hr1G127070	2	765,752,637	765,758,046	HC	5410	phosphatidylinositol-4-phosphate 5-kinase family protein
HORVU2Hr1G127080	2	765,766,187	765,767,095	LC	909	undescribed protein
HORVU2Hr1G127090	2	765,910,275	765,917,856	HC	7,582	tubulin folding cofactor B
HORVU2Hr1G127100	2	765,910,275	765,919,163	HC	8,889	LRR-LRK family protein
HORVU2Hr1G127110	2	765,919,366	765,920,959	LC	1,594	undescribed protein
HORVU2Hr1G127120	2	765,936,571	765,937,404	HC	834	tubulin folding cofactor B
HORVU2Hr1G127130	2	765,943,371	765,945,953	HC	2,583	undescribed protein

Appendix 3; continued

Gene ID	Chr.	Physical pos¹. start	Physical pos. end	Conf.²	Gene Size (bp)	Annotation³
HORVU2Hr1G127140	2	765,970,232	766,051,910	HC	81,679	rRNA N-glycosidase
HORVU2Hr1G127150	2	766,023,361	766,023,581	LC	221	undescribed protein
HORVU2Hr1G127160	2	766,024,144	766,026,591	HC	2,448	undescribed protein
HORVU2Hr1G127170	2	766,073,646	766,074,774	LC	1,129	undescribed protein
HORVU2Hr1G127180	2	766,077,529	766,078,615	LC	1,087	undescribed protein
HORVU2Hr1G127190	2	766,081,548	766,084,908	HC	3,361	RING/FYVE/PHD zinc finger superfamily protein
HORVU2Hr1G127200	2	766,084,135	766,084,268	LC	134	undescribed protein
HORVU2Hr1G127210	2	766,098,911	766,100,937	HC	2,027	undescribed protein
HORVU2Hr1G127220	2	766,141,777	766,145,430	HC	3,654	S-adenosyl-L-methionine-dependent methyltransferases superfamily protein
HORVU2Hr1G127230	2	766,285,098	766,286,125	HC	1,028	undescribed protein
HORVU2Hr1G127240	2	766,302,071	766,302,457	LC	387	undescribed protein

¹ Physical position based on the barley reference genome (Mascher et al., 2017)

² Confidence of gene: High-confidence (HC) genes and low-confidence (LC) genes

³ The function of the genes were predicted using automated gene annotation of the barley reference genome

Appendix 4: Summary of BAC clones spanning the *MIL-H* interval.

BAC clone¹	BAC_contig²	AGP_chr³	AGP_pos⁴	Length⁵	Cluster⁶	BAC_bin⁷
HVVMRXALLMA0276H13	HVVMRXALLMA0276H13_C1	2H	762,784,896	169,423	241	15
	HVVMRXALLMA0276H13_C2	2H	762,954,419	545	241	15
	HVVMRXALLMA0276H13_C3	2H	762,955,064	597	241	15
	HVVMRXALLMA0276H13_C5	2H	762,955,761	761	241	15
	HVVMRXALLMA0276H13_C6	2H	762,956,622	1,413	241	15
	HVVMRXALLHA0265L21	HVVMRXALLHA0265L21_C3	2H	762,958,135	1,371	241
HVVMRXALLHA0265L21_C8		2H	762,959,606	5,266	241	16
HVVMRXALLHA0265L21_C11		2H	762,964,972	2,510	241	16
HVVMRXALLHA0265L21_C12		2H	762,967,582	750	241	16
HVVMRXALLHA0265L21_C13		2H	762,968,432	1,842	241	16
HVVMRXALLHA0265L21_C15		2H	762,970,374	1,578	241	16
HVVMRXALLMA0301J16	HVVMRXALLMA0301J16_C1	2H	762,972,052	3,816	241	16
	HVVMRXALLMA0301J16_C2	2H	762,975,968	1,211	241	16
	HVVMRXALLMA0301J16_C3	2H	762,977,279	999	241	16
	HVVMRXALLMA0301J16_C4	2H	762,978,378	1,115	241	16
	HVVMRXALLMA0301J16_C5	2H	762,979,593	2,032	241	16

Appendix 4; continued

BAC clone¹	BAC_contig²	AGP_chr³	AGP_pos⁴	Length⁵	Cluster⁶	BAC_bin⁷
	HVVMRXALLMA0301J16_C6	2H	762,981,725	4,658	241	16
	HVVMRXALLMA0301J16_C7	2H	762,986,483	29,983	241	16
	HVVMRXALLMA0301J16_C8	2H	763,016,566	5,485	241	16
	HVVMRXALLMA0301J16_C9	2H	763,022,151	2,245	241	16
	HVVMRXALLMA0301J16_C10	2H	763,024,496	3,376	241	16
	HVVMRXALLMA0301J16_C11	2H	763,027,972	3,186	241	16
	HVVMRXALLMA0301J16_C11	2H	763,031,258	48,388	241	16
	HVVMRXALLMA0301J16_C12	2H	763,079,746	512	241	16
	HVVMRXALLMA0301J16_C13	2H	763,080,358	522	241	16
	HVVMRXALLMA0301J16_C14	2H	763,080,980	529	241	16
	HVVMRXALLMA0301J16_C15	2H	763,081,609	677	241	16
	HVVMRXALLMA0301J16_C16	2H	763,082,386	696	241	16
	HVVMRXALLMA0301J16_C17	2H	763,083,182	696	241	16
	HVVMRXALLMA0301J16_C18	2H	763,083,978	697	241	16
	HVVMRXALLMA0301J16_C19	2H	763,084,775	728	241	16
	HVVMRXALLMA0301J16_C20	2H	763,085,603	748	241	16

Appendix 4; continued

BAC clone¹	BAC_contig²	AGP_chr³	AGP_pos⁴	Length⁵	Cluster⁶	BAC_bin⁷
	HVVMRXALLMA0301J16_C21	2H	763,086,451	779	241	16
	HVVMRXALLMA0301J16_C22	2H	763,087,330	827	241	16
	HVVMRXALLMA0301J16_C23	2H	763,088,257	882	241	16
	HVVMRXALLMA0301J16_C24	2H	763,089,239	930	241	16
	HVVMRXALLMA0301J16_C25	2H	763,090,269	997	241	16
	HVVMRXALLMA0301J16_C26	2H	763,091,366	998	241	16
	HVVMRXALLMA0301J16_C27	2H	763,092,464	1,052	241	16
	HVVMRXALLMA0301J16_C28	2H	763,093,616	1,165	241	16
	HVVMRXALLMA0301J16_C29	2H	763,094,881	1,174	241	16
	HVVMRXALLMA0301J16_C30	2H	763,096,155	1,252	241	16
	HVVMRXALLMA0301J16_C31	2H	763,097,507	1,271	241	16
	HVVMRXALLMA0301J16_C32	2H	763,098,878	1,363	241	16
	HVVMRXALLMA0301J16_C33	2H	763,100,341	1,416	241	16
	HVVMRXALLMA0301J16_C34	2H	763,101,857	1,476	241	16
	HVVMRXALLMA0301J16_C35	2H	763,103,433	1,526	241	16
	HVVMRXALLMA0301J16_C36	2H	763,105,059	1,594	241	16

Appendix 4; continued

BAC clone ¹	BAC_contig ²	AGP_chr ³	AGP_pos ⁴	Length ⁵	Cluster ⁶	BAC_bin ⁷
	HVVMRXALLMA0301J16_C37	2H	763,106,753	1,695	241	16
	HVVMRXALLMA0301J16_C38	2H	763,108,548	2,017	241	16
	HVVMRXALLMA0301J16_C39	2H	763,110,665	2,030	241	16
	HVVMRXALLMA0301J16_C41	2H	763,112,795	3,428	241	16
	HVVMRXALLMA0301J16_C42	2H	763,116,323	4,045	241	16
HVVMRX83KHA0131O13	HVVMRX83KHA0131O13_C2	2H	763,120,468	4,102	241	17
	HVVMRX83KHA0131O13_C2	2H	763,124,670	13,057	241	17
	HVVMRX83KHA0131O13_C2	2H	763,137,827	9,509	241	17
	HVVMRX83KHA0131O13_C8	2H	763,147,436	959	241	17
	HVVMRX83KHA0131O13_C9	2H	763,148,495	887	241	17
HVVMRXALLHA0246H10	HVVMRXALLHA0246H10_C4	2H	763,149,482	744	241	17
	HVVMRXALLHA0246H10_C8	2H	763,150,326	3,943	241	17
	HVVMRXALLHA0246H10_C9	2H	763,154,369	718	241	17
	HVVMRXALLHA0246H10_C13	2H	763,155,187	2,240	241	17
	HVVMRXALLHA0246H10_C14	2H	763,157,527	2,214	241	17
	HVVMRXALLHA0246H10_C15	2H	763,159,841	3,782	241	17

Appendix 4; continued

BAC clone ¹	BAC_contig ²	AGP_chr ³	AGP_pos ⁴	Length ⁵	Cluster ⁶	BAC_bin ⁷
HVVMRXALLHC0076A01	HVVMRXALLHC0076A01_C1	2H	763,163,723	905	241	18
	HVVMRXALLHC0076A01_C1	2H	763,164,728	34,177	241	18
	HVVMRXALLHC0076A01_C2	2H	763,199,005	84,261	241	18
	HVVMRXALLHC0076A01_C4	2H	763,283,366	683	241	18
	HVVMRXALLHC0076A01_C7	2H	763,284,149	864	241	18
	HVVMRXALLHC0076A01_C9	2H	763,285,113	664	241	18
HVVMRXALLMA0320H13	HVVMRXALLMA0320H13_C1	2H	763,285,877	651	241	19
	HVVMRXALLMA0320H13_C2	2H	763,286,628	1,949	241	19
	HVVMRXALLMA0320H13_C2	2H	763,288,677	3,930	241	19
	HVVMRXALLMA0320H13_C3	2H	763,292,707	4,527	241	19
	HVVMRXALLMA0320H13_C3	2H	763,297,334	1,561	241	19
	HVVMRXALLMA0320H13_C3	2H	763,298,995	909	241	19
	HVVMRXALLMA0320H13_C4	2H	763,300,004	573	241	19
	HVVMRXALLMA0320H13_C6	2H	763,300,677	3,374	241	19
	HVVMRXALLEA0216D09	HVVMRXALLEA0216D09_C1	2H	763,304,151	595	241
HVVMRXALLEA0216D09_C2		2H	763,304,846	3,444	241	20

Appendix 4; continued

BAC clone ¹	BAC_contig ²	AGP_chr ³	AGP_pos ⁴	Length ⁵	Cluster ⁶	BAC_bin ⁷
	HVVMRXALLEA0216D09_C4	2H	763,449,200	4,428	241	20
	HVVMRXALLEA0216D09_C6	2H	763,453,728	1,850	241	20
HVVMRXALLHA0399O24	HVVMRXALLHA0399O24_C1	2H	763,455,678	1,756	241	20
	HVVMRXALLHA0399O24_C6	2H	763,457,534	744	241	20
	HVVMRXALLHA0399O24_C12	2H	763,462,327	514	241	20
	HVVMRXALLHA0399O24_C12	2H	763,462,941	3,246	241	20
HVVMRX83KHA0124C21	HVVMRX83KHA0124C21_C3	2H	763,466,287	4,829	241	21
	HVVMRX83KHA0124C21_C5	2H	763,471,216	9,206	241	21
	HVVMRX83KHA0124C21_C6	2H	763,480,522	1,102	241	21
	HVVMRX83KHA0124C21_C6	2H	763,481,724	12,813	241	21
	HVVMRX83KHA0124C21_C7	2H	763,494,637	2,257	241	21
	HVVMRX83KHA0124C21_C8	2H	763,496,994	1,473	241	21
HVVMRXALLMA0013I07	HVVMRXALLMA0013I07_C1	2H	763,498,567	2,188	241	21
	HVVMRXALLMA0013I07_C2	2H	763,500,855	1,065	241	21
	HVVMRXALLMA0013I07_C4	2H	763,502,020	1,098	241	21
	HVVMRXALLMA0013I07_C6	2H	763,503,218	1,813	241	21

Appendix 4; continued

BAC clone ¹	BAC_contig ²	AGP_chr ³	AGP_pos ⁴	Length ⁵	Cluster ⁶	BAC_bin ⁷
	HVVMRXALLMA0013I07_C7	2H	763,505,929	751	241	21
	HVVMRXALLMA0013I07_C9	2H	763,506,780	69,930	241	21
	HVVMRXALLMA0013I07_C10	2H	763,576,810	2,606	241	21
	HVVMRXALLMA0013I07_C13	2H	763,579,516	532	241	21
	HVVMRXALLMA0013I07_C17	2H	763,580,148	1,388	241	21
HVVMRXALLEA0301J21	HVVMRXALLEA0301J21_C1	2H	763,581,636	2,546	241	22
	HVVMRXALLEA0301J21_C2	2H	763,584,282	1,321	241	22
	HVVMRXALLEA0301J21_C2	2H	763,585,703	31,078	241	22
	HVVMRXALLEA0301J21_C5	2H	763,616,881	1,169	241	22
	HVVMRXALLEA0301J21_C5	2H	763,618,150	2,526	241	22
	HVVMRXALLEA0301J21_C6	2H	763,620,776	925	241	22
HVVMRXALLHA0802F14	HVVMRXALLHA0802F14_C1	2H	763,621,801	972	241	23
	HVVMRXALLHA0802F14_C1	2H	763,622,873	855	241	23
	HVVMRXALLHA0802F14_C6	2H	763,623,828	550	241	23
	HVVMRXALLHA0802F14_C7	2H	763,624,478	2,556	241	23
	HVVMRXALLHA0802F14_C7	2H	763,627,134	1,359	241	23

Appendix 4; continued

BAC clone ¹	BAC_contig ²	AGP_chr ³	AGP_pos ⁴	Length ⁵	Cluster ⁶	BAC_bin ⁷
	HVVMRXALLHA0802F14_C9	2H	763,629,285	3,968	241	23
	HVVMRXALLHA0802F14_C10	2H	763,633,353	1,176	241	23
	HVVMRXALLHA0802F14_C11	2H	763,634,629	4,905	241	23
	HVVMRXALLHA0802F14_C13	2H	763,639,634	4,212	241	23
HVVMRXALLHA0351I05	HVVMRXALLHA0351I05_C9	2H	763,643,946	1,194	241	24
	HVVMRXALLHA0351I05_C12	2H	763,645,240	1,559	241	24
	HVVMRXALLHA0351I05_C13	2H	763,646,899	520	241	24
	HVVMRXALLHA0351I05_C14	2H	763,647,519	2,018	241	24
	HVVMRXALLHA0351I05_C15	2H	763,649,637	1,403	241	24
HVVMRXALLMA0105H07	HVVMRXALLMA0105H07_C1	2H	763,651,140	15,554	241	24
	HVVMRXALLMA0105H07_C7	2H	763,666,794	15,320	241	24
	HVVMRXALLMA0105H07_C8	2H	763,682,214	513	241	24
	HVVMRXALLMA0105H07_C9	2H	763,682,827	555	241	24
	HVVMRXALLMA0105H07_C10	2H	763,683,482	558	241	24
	HVVMRXALLMA0105H07_C11	2H	763,684,140	569	241	24
	HVVMRXALLMA0105H07_C12	2H	763,684,809	575	241	24

Appendix 4; continued

BAC clone ¹	BAC_contig ²	AGP_chr ³	AGP_pos ⁴	Length ⁵	Cluster ⁶	BAC_bin ⁷
	HVVMRXALLMA0105H07_C17	2H	763,685,484	612	241	24
	HVVMRXALLMA0105H07_C18	2H	763,686,196	624	241	24
	HVVMRXALLMA0105H07_C19	2H	763,686,920	629	241	24
	HVVMRXALLMA0105H07_C23	2H	763,687,649	889	241	24
	HVVMRXALLMA0105H07_C26	2H	763,688,638	964	241	24
	HVVMRXALLMA0105H07_C28	2H	763,689,702	1,043	241	24
	HVVMRXALLMA0105H07_C29	2H	763,690,845	1,110	241	24
	HVVMRXALLMA0105H07_C31	2H	763,692,055	1,263	241	24
	HVVMRXALLMA0105H07_C42	2H	763,693,418	2,059	241	24
	HVVMRXALLMA0105H07_C46	2H	763,695,577	3,517	241	24
HVVMRX83KHA0013M14	HVVMRX83KHA0013M14_C1	2H	763,699,194	55,210	241	25

¹ID of the bacterial artificial chromosome (BAC) clones spanning the target interval, bold texts indicate those BAC clones that are located on the minimum tiling path (MTP) ²Assembled sequence contig of aforementioned BAC, prefix of the BAC_contig is the BAC ID while the suffix ‘_C<NUMBER>’ is the ID of the contig ³AGP stands for ‘A Golden Path’ and is used to describe assemblies with an ordered list of all of its components. The _chr part indicates the assigned pseudomolecule chromosome. ⁴AGP stands for ‘A Golden Path’ and is used to describe assemblies with an ordered list of all of its components. The _pos part indicates the physical position in basepairs on the pseudomolecule chromosome. ⁵The length in basepairs for the BAC_contig. ⁶ID of the BAC cluster. A BAC cluster consists of overlapping BAC clones, connected by direct (sequence homology) or indirect means (e.g. BAC end contigs). ⁷Number that shows the order of the BAC as indicated by the Hi-C (chromosome conformation capture) map inside a single cluster.

9 Erklärungen

1. Hiermit erkläre ich, dass diese Arbeit weder in gleicher noch in ähnlicher Form bereits anderen Prüfungsbehörden vorgelegen hat.

Weiter erkläre ich, dass ich mich an keiner anderen Hochschule um einen Doktorgrad beworben habe.

Göttingen, den

.....

(Unterschrift)

2. Hiermit erkläre ich eidesstattlich, dass diese Dissertation selbständig und ohne unerlaubte Hilfe angefertigt wurde.

Göttingen, den

.....

(Unterschrift)